MOLECULAR MECHANISMS OF MYOCARDIAL FIBROSIS DEVELOPMENT

by

Nicole L. Rosin

Submitted in partial fulfilment of the requirements
for the degree of Doctor of Philosophy

at

Dalhousie University
Halifax, Nova Scotia
April 2014

DEDICATION PAGE

For my family

Something here does not make sense. Let's go and poke it with a stick. – The Doctor

TABLE OF CONTENTS

LIST OF TABLES ..... **ix**

LIST OF FIGURES ..... **x**

ABSTRACT ..... **xii**

LIST OF ABBREVIATIONS USED ..... **xiii**

ACKNOWLEDGMENTS ..... **xvi**

CHAPTER 1: INTRODUCTION **1**

1.1 Heart Failure **1**

1.1.1 Role Of Myocardial Fibrosis In Heart Failure 1

1.1.2 Mechanics Of Diastolic Dysfunction 3

1.2 Age-Related Myocardial Fibrosis **3**

1.2.1 Clinical Implications 3

1.2.2 Etiology 4

1.2.3 Cellular Contribution To Age-Related Fibrosis 6

1.2.4 Fibrotic Signaling 7

1.3 Regulation of Collagen **9**

1.3.1 Collagen Biosynthesis 9

1.3.2 Collagen Post-Translational Processing (Crosslinking) 10

1.3.3 ECM Degradation 11

1.3.4 Age-Related Myocardial Fibrosis And Lysyl Oxidase 12

1.4 Role of AngiotensinII in Myocardial Fibrosis **15**

1.4.1 AngII-Induced Myocardial Fibrosis 15

1.4.2 The Role Of Hypertension 17
1.4.3 Cellular Involvement 19
1.4.4 Fibrotic Signaling In AngII-Induced Myocardial Fibrosis 20
CHAPTER 2: HYPOTHESIS, RATIONALE AND OBJECTIVES 22
2.1 Study 1: Collagen regulation in age-related fibrosis 22
2.2 Study 2: Blood Pressure Dependence of AngII-induced Myocardial Fibrosis 22
2.3 Study 3: Role And Regulation Of CTGF In AngII-Induced Myocardial Fibrosis 23
2.4 Study 4: The Effects Of Interrupting Collagen Homeostasis On AngII-Induced Myocardial Fibrosis In Aged Mice 23
CHAPTER 3: MATERIALS AND METHODS 24
3.1 Animals 24
3.2 GFP Chimeric Animals 24
3.3 Drug Infusion 24
3.4 Blood Pressure Measurements 25
3.5 Echocardiography 25
3.6 Tissue Harvest 26
3.7 Cell Isolation and Culture 26
3.7.1 Fibroblasts (Cardiac and skin) 26
3.7.2 Peripheral Blood Mononuclear Cells And Bone Marrow Cells 27
3.7.3 Fibrocytes 27
3.7.4 Cardiomyocytes 28
3.7.5 Endothelial Cells 28
3.7.6 In Vitro Treatments 28
3.8 Histological Analysis 29

3.9 Immunohistochemistry 29

3.10 Immunofluorescence Staining And Confocal Microscopy 30

3.11 Enzyme Linked Immunosorbent Assay 31

3.11.1 ELISA For CTGF 31

3.11.2 ELISA For Aldosterone 31

3.12 Immunoblotting 32

3.13 Flow Cytometry 32

3.14 Hydroxyproline Assay 33

3.14.1 Serum Preparation 33

3.14.2 Tissue Preparation 33

3.15 Relative Real-Time Quantitative Polymerase Chain Reaction (qPCR) 34

3.16 Proliferation Assays 36

3.16.1 MTT 36

3.16.2 Cell-Titer Blue Assay 36

3.16.3 BrdU 36

3.16.4 Ki67 37

3.17 Scratch Assay 37

3.18 MMP2 And MMP9 Gel Zymography 38

3.19 Statistical Analysis 38

CHAPTER 4: DISRUPTION OF COLLAGEN HOMEOSTASIS CAN REVERSE AGE-RELATED MYOCARDIAL FIBROSIS 40

4.1 Introduction 41

4.2 Results 43

4.2.1 Physiological Measurements 43

4.2.2 Significant Myocardial Fibrosis Develops With Age 43

4.2.3 Mechanisms Involved In The Observed Collagen Increase 43
4.2.4 Age-Related Fibrosis Is Associated With A Significant Up-Regulation Of Pro-Fibrotic Pathways Including TGFβ 45
4.2.5 Age-Related Fibrosis Is Reversible By Disrupting Collagen Homeostasis 46
4.2.6 LOX Inhibition Also Affects Collagen Homeostasis Beyond Collagen Crosslinking 47
4.2.7 Functional Effects Of BAPN Exposure 48
4.3 Discussion 59
CHAPTER 5: BLOOD PRESSURE DEPENDANCE OF ANGIOTENSINII INDUCED MYOCARDIAL FIBROSIS 63
5.1 Introduction 64
5.2 Results 65
5.2.1 Model Establishment 65
5.2.2 Myocardial Fibrosis 66
5.2.3 Cellular Infiltration 66
5.2.4 Myocardial Pro-Fibrotic Cytokine Environment 67
5.2.5 Myocardial Chemokine Expression Associated With Fibrocyte Migration 67
5.2.6 Effects Of Hydralazine At The Cellular Level 68
5.3 Discussion 78
CHAPTER 6: THE ROLE AND REGULATION OF CTGF IN ANGII-INDUCED MYOCARDIAL FIBROSIS 84
6.1 Introduction 85
6.2 Results 87

6.2.1 Bone-Marrow Derived Progenitors Are Mobilized From The Bone Marrow And Infiltrate Into The Myocardium After AngII Exposure 87
6.2.2 CTGF Is The First Pro-Fibrotic Cytokine Seen In The Myocardium After AngII Exposure 88
6.2.3 Myocardial Resident Cells Produce CTGF In Response To AngII 89
6.2.4 Fibrocytes Isolated And Cultured In Vitro From AngII Exposed Myocardium Also Contribute To CTGF Expression 90
6.2.5 Fibrocytes Proliferate In Response To CTGF 91
6.2.6 Fibrocytes Differentiate To ECM Producing Cells Under The Influence Of CTGF . 91
6.3 Discussion 104
6.3.1 Bone Marrow-Derived Progenitor Cells Mobilize And Migrate To The Myocardium 104
6.3.2 Fibrotic Mediators: Interaction Between CTGF And TGFβ 104
6.3.3 CTGF Regulation Of Fibrocyte Proliferation And ECM Production 107
6.3.4 Mechanism Of Action Of CTGF 109
CHAPTER 7: INTERRUPTION OF COLLAGEN HOMEOSTASIS ALTERS THE FIBROTIC RESPONSE TO ANGII EXPOSURE 111
7.1 Introduction 112
7.2 Results 114
7.2.1 Cellular Infiltration After AngII Exposure 114
7.2.2 AngII Exposure Results In Increased Myocardial Fibrosis 114
7.2.3 Regulation Of Collagen Homeostasis 115
7.2.4 Cellular Response To Signaling 117
7.3 Discussion 122

CHAPTER 8: DISCUSSION 124

8.1 Summary Of Findings And Comparison To Literature 124

8.2 Future Directions 134

REFERENCES 136

APPENDIX A: COPYRIGHT PERMISSION 150

LIST OF TABLES

Table 3.1 Forward And Reverse Primers Used For qPCR …….. 35

Table 3.2 Antibody Concentrations And Supplier Information ……... 39

Table 4.1 Echocardiography Data ……..…….. 50

LIST OF FIGURES

Figure 1.1 The Relationship Between LOX And TGFβ Regulation …….. 14

Figure 4.1 Age-Related Fibrosis Development ……...…… 51

Figure 4.2 Collagen Crosslinking …… 52

Figure 4.3 MMP Activity …… 53

Figure 4.4 Fibrotic Growth Factors And Aging …….. 54

Figure 4.5 LOX Inhibition And Collagen Processing ……. 55

Figure 4.6 Functional Effects Of LOX Inhibition ……... 57

Figure 4.7 *In Vitro* Effects of LOX Inhibition …… 58

Figure 5.1 Establishing The Model ……. 70

Figure 5.2 Myocardial Fibrosis ……... 71

Figure 5.3 Cellular Infiltration …… 72

Figure 5.4 Immunohistochemical Staining ……. 73

Figure 5.5 Pro-Fibrotic Microenvironment ……. 74

Figure 5.6 Chemokine Expression …….. 75

Figure 5.7 Transcription Factor Expression …… 76

Figure 5.8 Cellular Effects of Hydralazine ……. 77

Figure 6.1 Fibrocyte Infiltration ……. 93

Figure 6.2 Fibrocyte Mobilization …….. 95

Figure 6.3 CTGF And TGFβ Production …… 96

Figure 6.4 Cardiomyocytes Produce CTGF …… 98

Figure 6.5 Microvascular Endothelial Cells Produce CTGF …….. 99

Figure 6.6 Isolated Fibrocytes Produce CTGF ……... 100

Figure 6.7 Fibrocytes Proliferate In Response to CTGF …… 101

Figure 6.8 Fibrocytes Differentiate And Produce ECM In Response to CTGF …. 102

Figure 6.9 CTGF Does Not Affect The Mobility Of Isolated Fibrocytes …….. 103

Figure 7.1 Fibrosis And Cellular Infiltration …….. 118

Figure 7.2 Collagen And Fibrotic Factor Expression ……. 119

Figure 7.3 Collagen Degradation ……. 120

Figure 7.4 Cellular Response To AngII Exposure ……... 121

ABSTRACT

The prevention of heart failure in our aging population has become a healthcare priority. As part of the normal aging process patients have been shown to develop age-related myocardial fibrosis, which is characterized by excess deposition and a lack of clearance of extracellular matrix (ECM) proteins, contributing to the development of heart failure. The increase in ECM proteins is caused by an imbalance between the following: (1) collagen biosynthesis by fibroblasts, (2) post-synthetic collagen processing (cross-linking) which stabilizes collagen, and (3) collagen degradation.

The focus of this thesis lays mainly on collagen biosynthesis and processing, and how interrupting these can affect the overall balance of collagen in the myocardium. The two main objectives of this thesis lay in 1 – characterizing the role of a key pro-fibrotic signal in the TGFβ pathway, connective tissue growth factor (CTGF), in hypertension induced myocardial fibrosis development, and 2 – investigating the role of lysyl oxidase (LOX), an enzyme involved in the crosslinking of collagen that has been implicated in age-related myocardial fibrosis development.

This thesis provides novel evidence that CTGF regulation is an important step in the early stages of myocardial fibrosis development through regulating new collagen synthesis and that CTGF is produced as a downstream mediator of TGFβ after AngII exposure not directly through AngII-AT_1R signaling. Additionally, novel evidence is presented that LOX inhibition reduces age-related myocardial fibrosis and that the decrease in collagen protein content observed after LOX inhibition is associated with a significant decrease in new pro-collagen 1 mRNA synthesis. This suggests that LOX inhibition also inhibits new collagen synthesis by an unknown mechanism. Overall, these studies have contributed new mechanistic knowledge about myocardial fibrosis development and explored potential therapeutic strategies aimed at interrupting collagen homeostasis, which are key to understanding myocardial fibrosis development.

LIST OF ABBREVIATIONS USED

A	Late Mitral Inflow Velocity
AngII	AngiotensinII
ANOVA	Analysis of Variance
AT_1R	AngiotensinII Receptor Type 1
AT_2R	AngiotensinII Receptor Type 2
BAPN	β-Aminopropionitrile
BM	Bone Marrow
BSA	Bovine Serum Albumin
COL1A1	Collagen type 1, A1 subunit
CTGF	Connective Tissue Growth Factor
d	day
E	Early Mitral Inflow Velocity
ECM	Extracellular Matrix
EF	Ejection Fraction
ELISA	Enzyme Linked Immunosorbent Assay
FBS	Fetal Bovine Serum
FGF	Fibroblast Growth Factor
FS	Percentage Fractional Shortening
GFP	Green Fluorescent Protein
Gy	Gray
H&E	Hematoxylin and Eosin
HIF1α	Hypoxia Inducible Factor 1 alpha

hr	Hour
HW/BW	Heart Weight to Body Weight Ratio
IL1β	Interleukin 1 beta
IL6	Interleukin 6
ISd	Septal Wall Thickness in Diastole
ISs	Septal Wall Thickness in systole
LOX	Lysyl Oxidase
LVIDd	Left Ventricular Interior Diameter in Diastole
LVIDs	Left Ventricular Interior Diameter in Systole
LVPWd	Left Ventricular Posterior Wall Thickness in Diastole
LVPWs	Left Ventricular Posterior Wall Thickness in Systole
min	Minute
MMP	Matrix Metalloproteinase
PBMC	Peripheral Blood Mononuclear Cell
PBS	Phosphate Buffered Saline
PDGF	Platelet Derived Growth Factor
RAAS	Renin Angiotensin Aldosterone System
SMA	Smooth Muscle Actin
TGFβ	Transforming Growth Factor beta 1
TGFβR	TGFβ Receptor
TIMP	Tissue Inhibitor of MMPs
TNFα	Tumour Necrosis Factor alpha
qPCR	Quantitative Real-Time Polymerase Chain Reaction

SEM	Standard Error of the Mean
wk	Week
yr	Year

ACKNOWLEDGMENTS

"If I have seen further it is by standing on the shoulders of giants." – Isaac Newton.

I have always appreciated this quote and am grateful that in every new venture that I have had, there have been such giants. Not only is the path forward visible thanks to the hard work of those that came before me, but being surrounded by intelligent and thoughtful people on a daily basis clears the fog and allows me to see the ground on which I am currently standing.

I would like to thank my supervisors Drs. JF Légaré and Tim Lee for your guidance and for allowing me to grow as a researcher during my time in the lab. I appreciate that you have pushed me not to give up and also allowed me to move on from failed ideas. To my fellow grad room prisoners and the members of the transplant lab, especially Mryanda, Alison, Mike and Alec - thank-you for being both distracting and distractible. It has been fun, and I may have learned some things along the way. To Tanya Myers, thank-you for all of the technical assistance and training over the years (since I am not allowed to write what I want to, I will leave it at that). You have all become good friends and I will remember the times we shared, in and out of the lab far longer than I will remember the science that I did here. I also need to thank Dennis for helping me to stay sane at the end of this process. I am excited to see what real life will be like.

Finally, I owe so much to my family, both financially and otherwise. It is from my parents that I learned to work hard, and just as importantly to make the time to enjoy life as it happens. I also appreciate those calls from Bryan saying that he was proud of me, even if those calls seem to come from Vancouver in the wee hours of the morning!

CHAPTER 1: INTRODUCTION

1.1 Heart Failure

1.1.1 Role Of Myocardial Fibrosis In Heart Failure

Myocardial fibrosis is a common pathological feature of cardiovascular disease. It occurs due to the accumulation of extracellular matrix (ECM) proteins as a result of post-infarct tissue ischemia. Alternately, it can occur from non-ischemic causes such as in response to pressure overload as a result of hypertension[1]. The focus of this thesis will be on the latter of these two causes of myocardial fibrosis.

Fibrosis is characterized by an over-abundant deposition of ECM molecules as well as a deficit in ECM degradation [2, 3]. Previous studies have established that there is a correlation between fibrosis, as measured by amount of interstitial collagen, with diastolic dysfunction (assessed using Doppler echocardiography to measure reduced relaxation of the left ventricle [4]). The excess ECM protein results in a loss of contractility and increased stiffness, ultimately leading to organ dysfunction and end-stage heart failure [2, 5]. Our current understanding of the molecular mechanisms culminating in increased matrix deposition is incomplete, warranting further investigation into the pathways involved.

The ECM proteins produced by fibroblasts and myofibroblasts (the activated/differentiated contractile phenotype of fibroblasts) in the healthy myocardial tissue consist primarily (85%) of collagen type I found in thick tensile fibers and collagen type III (11%) found in elastic tissue surrounding vessels[6, 7]. Other constituents of the ECM include collagen type IV, type V laminin, fibronectin and elastin[6]. The primary

role of collagens I and III are structural support of cardiomyocytes during contraction[1, 7]. Specifically in diastole, collagen provides scaffolding and prevents overstretching, myocyte slippage and maintains tissue structure[1].

There is evidence for a direct causative effect of a net increase in ECM proteins on impaired diastolic function. Reducing collagen by disrupting cross-linking, which allows for collagen degradation through the use of a lysyl-oxidase inhibitor, AGE-breaker or by knocking out the pro-collagen 1alpha2 gene decreases both the amount of collagen and the diastolic stiffness in rodent models[8-10]. Intra-arteriolar administration of collagenase into the myocardium results in a degradation of small and medium collagen fibrils and increased the total LV volume[11]. On the other hand, transgenic mice expressing collagenase resistant collagen type I had increased reactive fibrosis and remodeling with a decrease in function[1]. Taken together the evidence confirms that accumulation of collagen contributes to passive stiffness of the ventricle and diastolic dysfunction.

In addition to the increased production of collagen, there is also an increase in elastin, proteoglycans, and basement membrane observed in hypertensive disease models[2]. At the same time, structural alterations also occur. With sustained hypertrophy, collagen fibers encircle the circumference of the muscle fibers and interrupt the ability of muscle fibers to stretch during diastole, contributing to diastolic stiffness and dysfunction[7]. The deregulation of matrix proteins also interrupts cardiomyocyte excitation-contraction coupling, due to blocking myocyte-myocyte interaction and myocyte-endomysium adhesion[2].

1.1.2 Mechanics Of Diastolic Dysfunction

The term diastolic dysfunction implies that systolic function, or the ability of the heart to contract and thereby expel blood from the left ventricle, is maintained, while failure occurs due to the inability of the left ventricle to relax (both passively and actively) thereby reducing the internal volume when fully expanded[12]. This consequently decreases the volume of oxygenated blood available to be expelled during systole and ultimately contributes to heart failure.

A more specific measure of diastolic function than ejection fraction (EF), the E/A ratio (filling velocity due to passive relaxation/velocity due to atrial pressure) also decreases with patient age[13]. Stiffness of ventricular muscle when calculated using stretch strain curves also increases with mouse age and correlates with an increase in interstitial collagen[14]. In addition to increased collagen reducing passive relaxation, there are also changes in collagen structure, reducing active relaxation from energy stored in coiled collagen during contraction[6]. As collagen accumulates, it isolates myocytes from one another, resulting in changes in myocyte orientation, loss of force transmission[6] and electrical coupling between myocytes[1]. Excessive collagen also cuts cardiomyocytes off from the microvasculature resulting in local hypoxia and the potential necrosis of isolated myocytes[1].

1.2 Age-Related Myocardial Fibrosis

1.2.1 Clinical Implications

Of particular clinical importance are the compounding effects of age on myocardial fibrosis development. Heart failure is the highest reported cause of hospitalization in elderly patients[15]. The percentage of patients that are hospitalized

with heart failure increases with age; at 80yr and older approximately 80-85% of patients will be diagnosed with cardiovascular disease compared to approximately 40% at 40-59yr [16]. Mortality is approximately 50% within 5yr of diagnosis with heart failure[16]. The most common cause of heart failure is left ventricular (LV) dysfunction, which is generally broken into two categories based on the % of blood volume exchanged each cycle (ejection fraction); heart failure with reduced ejection fraction (HFrEF) and heart failure with preserved ejection fraction (HFpEF). Both of which are approximately equal in prevalence (proportion of the population affected) and incidence (new diagnoses per year). HFrEF is defined as heart failure that occurs with an EF $\leq$ 40% and is most often due to the occurrence of a myocardial infarction. This thesis will primarily focus on myocardial fibrosis that is thought to contribute to the development of diastolic dysfunction with a reduced diastolic volume, which affects the majority of patients presenting with HFpEF (EF $\geq$ 40) [16, 17].

Current treatments for HFrEF target risk factors such as hypertension and include the use of angiotensin receptor blockers (ARB) or angiotensin converting enzyme inhibitors (ACEi) [16]. However, effective medical therapies for myocardial fibrosis and HFpEF (diastolic dysfunction) remain elusive. Considering the aging population in North America and the effects of age on cardiovascular risk factors, the effects of aging should be taken into account when attempting to understand the underlying mechanisms of fibrosis development.

1.2.2 Etiology

Previous studies have established that age-related myocardial fibrosis is characterized by significant increases in myocardial collagen content that continually

accumulates over time [18-22]. During aging, collagen accumulation also results in thickening of the abundant collagen fibers [6]. Perivascular fibrosis also increases, evident by an increase in the quantity and thickness of collagen fibers surrounding the small coronary arteries. This perivascular fibrosis permeates from the perivascular area into the surrounding region and contributes to the overall increase in interstitial fibrosis with age [6, 7].

Age-related fibrosis has not been attributed to one direct source of 'injury', but results from a response to many contributing factors. Chronic stress on the myocardium over time, elevated incidence of hypertension and coronary disease with age as well as cellular senescence contribute to the development of myocardial fibrosis in the elderly[12]. Unfortunately, studies using anti-hypertensive agents (ARBs or ACE inhibitors) in clinical trials for elderly patients with HFpEF have demonstrated either no change or only moderate reduction of myocardial fibrosis and improvement in diastolic function[23-25]. However, anti-hypertensive agents used in animal models of age-related fibrosis elicit a reduction in fibrosis and functional improvement [26-28]. It follows that hypertension at least contributes to fibrosis development in the setting of age-related fibrosis although other confounding risk factors are present in patients.

Prior focus on age-related fibrosis has largely been on morphological and structural changes within the myocardium. Emphasis has not been on the specific molecular and cellular mechanisms involved in fibrosis development in age-dependant models and how these compare to younger individuals.

1.2.3 Cellular Contribution To Age-Related Fibrosis

Cardiac myofibroblasts are thought to be the predominant cellular mediator of myocardial fibrosis [29-33]. Myofibroblasts express α-smooth muscle actin (SMA), migrate to sites of fibrosis and actively contribute to fibrotic tissue accumulation through the production of pro-fibrotic cytokines and collagen synthesis [1, 34, 35].

There are many potential sources of fibroblasts from which the myofibroblast population is derived: proliferation and migration of interstitial or perivascular fibroblasts; differentiation from pericytes; bone marrow-derived fibrocytes; or endothelial mesenchymal transition[36, 37]. Undifferentiated cardiac fibroblasts are mesenchymal cells that lack a specific identifying marker and are therefore generally identified by their morphological appearance: flat, spindle shaped, and having multiple processes. They represent one of the most common populations of cells in the myocardium [34]. In response to fibrotic stimuli such as transforming growth factor-β 1 (TGFβ), cardiac fibroblasts become activated myofibroblasts that are believed to be the primary producers of ECM.

Recent studies have provided evidence that cellular aging contributes to decreased healing responses and worsens fibrosis after injury. Increased age of bone marrow derived cells (such as fibrocytes) and myocardial resident cells (cardiomyocytes, fibroblasts and endothelial cells) act synergistically. Sopko *et al.* 2011 observed that there were fewer bone marrow derived cells after transverse aortic constriction as a model of pressure overload in aged animals compared to young counterparts. They also correlated a decrease in hypertrophy and an increase in overall fibrosis in the myocardium when either mice were old with young bone marrow or young mice had been transplanted with

old bone marrow [38]. Thus, supporting both that bone marrow derived cells are playing a direct role in fibrosis development and that age has a pro-fibrotic impact on bone marrow-derived and myocardial resident cell function. However, they did not address the mechanisms responsible for the differences seen between young and old bone marrow or in young and old mice.

1.2.4 Fibrotic Signaling

A limited number of studies have been published relating to the development of myocardial fibrosis in aging models. At baseline, aged animals have elevated blood pressure and show increased myocardial collagen content compared to young animals[39]. Molecular changes that have been associated with aged myocardium and with direct effects on fibrosis development include increases in AT_1R and AT_2R [40, 41]. When aged spontaneously hypertensive rats were treated for an extended period with an ARB or ACE inhibitor much of the hypertrophy and fibrosis was ameliorated. However, when an age-matched group was treated with a sufficient dose of hydralazine to achieve an equal blood pressure reduction between groups, animals developed LV hypertrophy, myocardial hypertrophy and fibrosis compared to young animals, although at a reduced level from the untreated aged group[26]. Taken together, this suggests that age-related fibrosis is not solely dependent on elevated blood pressure, but also on direct AngII signaling.

The reported expression of TGFβ mRNA during aging is inconsistent; some studies report slight increases and others show no change in expression, although this was not assessed using qPCR[40, 42]. TGF-β is chemotactic for fibroblasts, stimulates fibroblast proliferation, and increases the synthesis of a number of ECM proteins

including collagen [19, 43-46]. However, age-related changes in isolated myocardial fibroblasts suggest that they have a reduced ability to respond to TGFβ via the TGFβ receptors (TGFβRI and TGFβR2) and the SMAD pathway [39, 47, 48]. On the other hand, the involvement of TGFβ signaling in the development of age-related fibrosis is supported by the reduction of fibrosis in aged mice with only one functional TGFβ allele. The constitutive levels of connective tissue growth factor (CTGF), a downstream mediator of the fibrotic signaling of TGFβ and other fibrotic mediators in senescent myocardium have not to our knowledge been reported at this time.

Bujak *et al* showed using an ischemia reperfusion (IR) model that, in areas of myocardial infarct injury, older mice had increased expression of a variety of chemokines (CCL2, MIP1α, MIP2), pro-inflammatory cytokines (tumor necrosis factor-α; TNFα, interleukins; IL1β, IL6, monocyte colony stimulating factor; MCSF), and mesenchymal proteins (α-smooth muscle actin; SMA, collagen osteopontin) as well as decreased myofibroblast accumulation when compared to young mice. They also found a striking decrease in the stimulatory ability of TGFβ via the SMAD pathway to stimulate fibroblast activity in old mice compared to their young counterparts. Although old mice started at baseline with higher collagen content in the heart, potentially due to increased signaling and myofibroblast activity, they developed more hypertrophy and a much 'looser' scar after IR containing less collagen, suggesting that the responsiveness of older cells to injury was inhibited at advanced age [39]. However, the regulation of downstream mediators of TGFβ such as CTGF or other fibrotic factors was not examined.

1.3 Regulation of Collagen

1.3.1 Collagen Biosynthesis

The most abundant protein present in the ECM is collagen. Collagen is produced predominantly by fibroblasts and secreted into the extracellular space for processing. The collagen family is comprised of at least 28 members that contain the common feature of one or more triple-helical domains [49]. Most relevant to myocardial fibrosis are the fibril-forming collagens that are the most abundant in the myocardium, namely types I and III [34]. The two subunits of type I collagen, α1 (1) and α2 (1) are coded for by two genes, which are transcribed by only a limited number of cell types; fibroblasts, osteoblasts and odontoblasts. Of these, only fibroblasts are present within the myocardial tissue. There are a variety of response elements located on the promoter and first intron of each of the type I collagen subunits that provide enhancer and inhibitory functions. TGFβ, TNFα and IFNγ response elements have all been identified and include nuclear factor-1, IF1, IF2 (both negative regulators), SP1, AP1, NFκB and SMAD binding elements amongst others[50].

It remains unclear if an increase in mRNA is partially responsible for the increase in collagen and other ECM proteins observed in age-related myocardial fibrosis. Some reports have suggested that mRNA expression of Col1A1, Col3A, and fibronectin are elevated in age-related fibrosis [4]. This is in contrast to others who suggest the mRNA expression of these collagen subunits are not increased and may in fact decrease within the myocardium during aging [13, 42, 48]. Given the conflicting reports on ECM mRNA regulation and the clear evidence demonstrating increased myocardial collagen of aging

animals, the increase in protein is often attributed to post-translational regulation enhancing ECM stability.

1.3.2 Collagen Post-Translational Processing (Crosslinking)

Collagen is extensively processed post-translationally. Briefly, fibrillar collagen type 1 is a trimer composed of two type 1α1 and one type 1α2 chains. The chains are cleaved when the pro-peptide is translated into the rough endoplasmic reticulum. A number of proline and lysine residues are hydroxylated (by prolyl 3-hydroxylase or lysyl 4-hydroxylase respectively), which are necessary for hydrogen bonding after the three monomers spontaneously form triple helical microfibrils. Some hydroxylysine residues are glycosylated prior to trimer secretion into the extracellular space, where both C and N-terminal specific proteinases cleave the ends of the pro-collagen. Fibrils spontaneously form from these processed microfibrils[51].

The mechanical strength of the fibril-forming collagens are dependent on cross-links, which include the enzymatically driven lysyl oxidation and non-enzymatic glycation [49]. Non-enzymatic crosslinking and advanced glycation end-products (AGEs) increase during aging, due partially to the accumulation over time of reactions between collagen and carbohydrates such as glucose [52, 53]. AGEs contribute to fibrosis development in two ways; 1- they perpetuate collagen cross-linking, increasing stiffness and 2- are recognized by receptors, such as RAGE (receptor of AGEs)[53]. RAGE is expressed on macrophages and endothelial cells and its activation increases the expression of TGFβ, CTGF, PDGF and the production of ROS resulting in protein turnover, inflammation and fibrosis[52-54]. Therapeutic reduction of glycation and therefore AGE formation, or breaking established glycation cross-links reduces stiffness

and increases heart function in the setting of age-related fibrosis [9, 55]. Whether the cause of improvement in function is reduction in crosslinks or the decreasing the number of AGEs remains unclear.

Enzymatic crosslinking is initiated by lysyl oxidase (LOX), which is an extracellular copper-dependent enzyme. LOX oxidizes the amino group on lysine or hydroxylysine, allowing the formation of reactive aldehydes (Schiff bases) leading to spontaneous non-reducible bonds forming with native lysine or hydroxyproline residues on other collagen molecules[56]. Collagen cross-linking is believed to be responsible for making collagen more resistant to degradation by collagenases and adding to its physical strength [56, 57]. Furthermore, some investigators have suggested that LOX expression may be increased in the myocardium of aging animals, supporting a role for collagen crosslinking by LOX in age-related myocardial fibrosis [56]. However, conclusive evidence that collagen crosslinking contributes to age-related myocardial fibrosis *in vivo* is lacking.

1.3.3 ECM Degradation

Collagen homeostasis within the myocardium is maintained by matrix metalloproteinases (MMPs) that enzymatically digest ECM proteins and regulate the release of bound molecules from the ECM. MMPs are regulated at the level of transcription, pro-MMP protein activation, and by the activity of tissue inhibitors of MMPs (TIMPs)[58]. MMP2 and MMP9 have been extensively studied in the context of myocardial fibrosis and also release ECM-bound, latent TGFβ [59]. In models of myocardial fibrosis, MMP2 overexpression led to increased fibrosis and knocking down MMP2 or MMP9 resulted in reduced fibrosis [60-62].

In fact, increased angiotensinII (AngII) signaling in aged myocardium, through increased presence of the AngII receptors, increases MMP9 production by fibroblasts[63]. In a spontaneous hypertensive heart failure rat model and in Dahl salt sensitive rats, MMP2 and 9 are increased compared to wild type rats, and this increase is enhanced with age in both strains[64, 65]. Likewise there is increase in MMP2 and 9 activity, measured by gelatin zymography with age[64]. Overall, the increased activity of MMPs 2 and 9 that occur during aging may be acting to counter the increased collagen production observed in aging in order to maintain collagen homeostasis. Ultimately, increased degradation of collagen is not sufficient to maintain homeostasis during aging and a net increase in collagen protein within the myocardium is observed.

1.3.4 Age-Related Myocardial Fibrosis And Lysyl Oxidase

LOX activity can have significant effects on collagen homeostasis through cross-linking and consequently inhibiting degradation of collagen proteins. This is supported by evidence that LOX expression is significantly increased in both patients and animal models of myocardial fibrosis [66-68]. Investigators have suggested that the regulation of collagen crosslinking may represent a potential therapeutic target for myocardial fibrosis [56]. Currently available LOX inhibitors are known to form direct irreversible links with the LOX enzyme, with the limitation of significant *in vivo* toxicity including extensive damage to connective tissue [56]. Nevertheless, *in vivo* experiments have been conducted with the LOX inhibitors β-aminoproprionitrile (BAPN) and D-Penicillamine. Using BAPN, Kato et al demonstrated that left ventricular diastolic stiffness could be improved by LOX inhibition [10]. One of the earliest published uses of BAPN was in a hypertension model of fibrosis that showed partial prevention of myocardial fibrosis

development and associated mechanical stiffness of the cardiac muscle, but the exact underlying mechanisms for these findings were not explored [69]. To the best of our knowledge, BAPN has never been used as a treatment in the context of age-related myocardial fibrosis.

In patients with myocardial fibrosis investigators have been able to show significant increases in myocardial LOX expression, which was associated with increased pro-fibrotic cytokine expression, particularly TGF-β [66, 67]. Furthermore, pharmacological inhibition of TGF−βRIII (with P144) in a spontaneously hypertensive rat model resulted in reduced LOX expression and decreased collagen deposition and cross-linking, all suggesting a close regulation between LOX activity, TGF-β signaling, and ECM regulation [68]. In support of TGF-β regulation of LOX in age-related fibrosis, others have shown that TGF-β can increase LOX production [70]. Taken together, these studies support a prominent role for TGF-β signaling in the development and maintenance of age-related myocardial fibrosis, but the relationship to LOX in the context of aging has yet to be fully characterized.

Myocardial fibroblasts express LOX in addition to TGFβ and ECM proteins, placing these cells at the center of our understanding of fibrosis. Figure 1.1 illustrates the complex relationship between LOX, ECM processing, and regulation by TGFβ. Furthermore, fibroblasts produce additional ECM proteins such as MMPs and TIMPs, which can regulate fibroblast function and are directly linked to LOX activity, indicating complex regulatory feedback mechanisms [34].

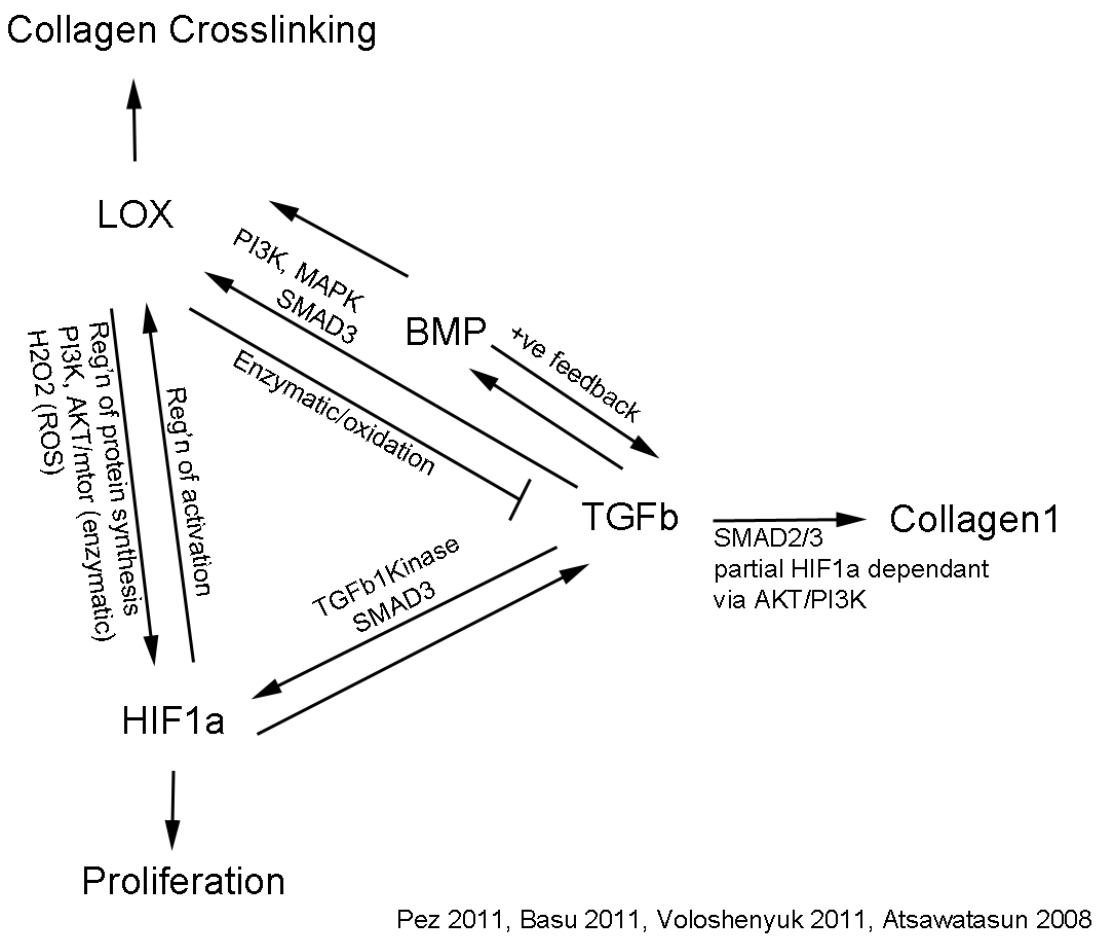

Figure 1.1 The Relationship Between LOX And TGFβ Regulation

The diagram illustrates the regulatory feedback mechanisms involved in LOX and TGFβ expression and activity that may play a role in maintaining collagen homeostasis. Direct regulation between LOX and TGFβ occur, as does regulation through intermediates such as HIF1α. LOX enzymatically inhibits TBFβ activity, while TGFβ increases LOX mRNA expression both directly and through activating bone morphogenic protein (BMP). LOX also regulates HIF1α protein synthesis through direct enzymatic activity and activation of reactive oxygen species, and HIF1α regulates the activation of LOX. HIF1α also increases TGFβ expression, while TGFβ increases HIF1α mRNA expression.

1.4 Role of AngiotensinII in Myocardial Fibrosis

1.4.1 AngII-Induced Myocardial Fibrosis

Experimental models for myocardial fibrosis allow for manipulation of the complex *in vivo* setting. In order to understand and determine the causative initiating signals of myocardial fibrosis development we used a rodent model of AngII-initiated hypertension-induced myocardial fibrosis. Other experimental models of hypertension leading to myocardial fibrosis include: increasing components of the Renin-Angiotensin-Aldosterone System (RAAS; by exogenous administration of AngII, aldosterone or genetic manipulation); and surgical interference (by renal artery banding, 2 kidney-1 clip). All show similar progression of fibrosis development to direct pressure overload, such as with aortic banding[6].

AngII has been implicated in the development of fibrosis in the myocardium, as well as in other organs [19, 71]. AngII is a hormone member of the RAAS and is involved in blood pressure regulation[20]. Specifically, AngII binds to angiotensin specific receptors, AT_1R and AT_2R, of which AT_1R is more extensively expressed in adult tissue [72]. Briefly, the classical RAAS functions as follows to regulate blood pressure: 1- Renin is primarily produced in the kidney, but is found locally in the myocardium; 2- Renin cleaves angiotensinogen, mainly produced in the liver, but also produced locally in the myocardium, to angiotensin I (AngI) and inhibits angiotensinogen production; 3- ACE is produced by endothelial cells of the vasculature, where it remains membrane bound. ACE cleaves AngI to AngII, as well as activating the bradykinin system; 4- AngII directly functions to regulate blood pressure through activation of AT_1R increasing renal vasoconstriction, tubular sodium reabsorption, systemic

vasoconstriction, release of aldosterone and angiotensinogen as well as central nervous system stimulation of blood pressure, such as by modulating thirst and salt appetite[73]. The elevation of AngII serum levels has been correlated with the development of hypertension and cardiac hypertrophy, conditions that lead to cardiac fibrosis and also contribute to fibrosis of other tissues [74, 75].

There is also mounting evidence that AngII contributes to myocardial fibrosis beyond its hypertensive effects. In older rats there is an increase in AT_1R mRNA expression in the myocardium compared to younger rats (24m vs 2m)[76]. Direct signaling of cardiomyocytes through AT_1R results in increased TGFβ expression through AP1 signaling and increased NOX expression[77]. Constitutive activation of AT_1R through gain-of-function mutation in mice increases myocardial fibrosis[78]. Myocardial fibroblasts also express AT_1R, which facilitates signaling through PKC resulting in up-regulation of ECM regulatory proteins such as MMP9, TGFβ, CTGF, etc[37, 63, 79]. AngII exposure results in increases of nitric oxide synthase, NAPDH oxidase, mitochondrial catalase, all of which contribute to an increase in reactive oxygen species (ROS) generation[4, 80]. ROS generation ultimately results in mitogen activated protein kinase (MAPK) activation and down stream signaling, leading to increased MCP1 and TGFβ expression, further contributing to fibrosis development[81, 82].

The other AngII receptor (AT_2R) is expressed at the highest level shortly before birth[73], and is normally expressed in adult tissue at only low levels[76]. When mice have AT_2R knocked out, they develop normally with no obvious developmental deficiencies. However, AT_2R-/- mice show reduced regulation of drinking and intensified blood pressure increase after AngII infusion compared to wild type,

suggesting that AT_2R mediated vasodilation is acting synergistically with central nervous system regulation of hemodynamics[83]. Use of a specific AT_2R agonist attenuates TNFα stimulation of pro-inflammatory molecules (TNFα, MCP1 and IL6), suggesting that signaling through AT_2R is primarily anti-inflammatory[84]. Overall, there is mounting evidence that AT_2R signaling acts as a counterbalance to AT_1R induction of pro-inflammatory and pro-fibrotic pathways.

Multiple studies on the clinical use of ARBs and ACE inhibitors (reviewed in detail by Probstfield *et al*) support the role of AngII and RAAS in cardiovascular disease progression and fibrosis[85]. At the tissue level, increased levels of AngII elicit an increase in endothelial dysfunction (NO synthase), inflammatory markers (TNFα, IL6), pro-fibrotic markers (TGFβ, CTGF), proliferation (PDGF, TGFβ) and adhesion molecules (vCAM, iCAM), which together facilitate the recruitment of monocytes and fibrocytes into the interstitium [81, 85]. In addition, the constitutive expression of AT_1R in mice results in hypertension, fibrosis and eventual heart failure[78]. Taken together, these observations have led to the development of exogenous administration of AngII to rodents through a subcutaneous osmotic pump to result in hypertension, which has become a well-established model for the study of cardiac fibrosis[20, 86, 87].

1.4.2 The Role Of Hypertension

Numerous clinical studies have provided evidence for a link between hypertension and fibrosis development [2, 19, 20, 88]. The incidence of hypertension increases with age, and has been associated as a risk factor for age-related fibrosis development[89]. Pathologically, high blood pressure results in remodeling,

characterized by left ventricular hypertrophy, myocyte hypertrophy, myocyte apoptosis and the appearance of fibrotic tissue[90].

Mechanically, pressure overload caused by hypertension physically stretches the cardiomyocytes, increasing the expression of contractile protein (β-myosin heavy chain, α-actin), fibroblast proliferation and ECM production[20, 91]. Cardiomyocyte hypertrophy also induces humoral signaling including increased AngII production and perpetuates mechanical stress [92]. Cellular hypertrophy of cardiomyocytes has also been linked to changes in expression of calcium exchangers. There is a resultant prolongation of calcium transient within the cells increasing time to relax and contract, but with an overall maintenance of calcium homeostasis during early stages of hypertrophy (although this is not the case during late stages of heart failure)[93]. There is also evidence of interruption in coordination of excitation-relaxation coupling due to myocardial fibrosis[90]. Cellular hypertrophy is accompanied by autophagy and apoptosis of cardiomyocytes[91]. In combination, these effects reduce the contractile ability of viable cardiomyocytes and myocardial tissue[94]. Taken together these result in further stress on the myocardium and perpetuate the development of fibrosis.

Fibroblasts also produce collagen in response to direct mechanical load due to signaling through changes in the cellular cytoskeleton, integrins and stretch-activated channels[1]. Current therapies for hypertension primarily target the RAAS, such as ACEi and ARBs, however these do not fully inhibit the development of myocardial fibrosis [23-25]. These data highlight the fact that controversy remains about AngII-induced myocardial fibrosis development and whether the physical effects of hypertension, or

associated increases in AngII signaling, are the primary trigger resulting in myocardial fibrosis.

1.4.3 Cellular Involvement

Recent evidence published by our laboratory has shown that a significant number of the cells that are recruited to the myocardium as soon as one day after AngII exposure are hematopoietic progenitor cells, termed fibrocytes [87]. This novel observation was supported by recent publications highlighting the importance of fibrocytes in myocardial fibrosis development [95, 96]. Fibrocytes possess both hematopoietic progenitor markers (CD34, CD45 or CD133) and mesenchymal markers (collagen type I, fibronectin or vimentin)[97, 98]. While the identification of fibrocytes in heart tissue is new, evidence for the involvement of fibrocytes in other fibrotic disorders has previously been described in models of lung, kidney, liver and skin fibrosis [99-102].

Fibrocytes are thought to have a direct contribution to fibrosis development after being recruited into injured tissue, at which point they differentiate into a myofibroblast phenotype, which are then responsible for ECM deposition. They start to express increased levels of SMA and fibronectin, and to synthesize new collagen [103]. Myofibroblasts derived from fibrocytes can also increase the cross-linking of deposited collagen, as determined by their ability to increase contraction of collagen matrix *in vitro* [97].

In the AngII exposure model, fibrocytes are recruited to the myocardium prior to ECM deposition [87]. Fibrocytes express numerous chemokine receptors including CCR2 and CXCR4, which recognize CCL2 and CXCL12 respectively, which are involved in fibrocyte migration both *in vitro* and to *in vivo* sites of fibrotic injury [97,

104, 105]. In fact, a number of studies have recently provided support for the causal role of fibrocytes in fibrosis development by blocking chemokine signaling. Haudek *et al* showed reduced cellular infiltration and collagen deposition in mice lacking the ability to produce the chemokine CCL2[96]. However, recent work from our group has provided new evidence that inhibition of CCR2, the receptor for CCL2 allows migration to occur, suggesting that later reduction in fibrosis is due to non-chemotactic effects of CCL2 within the myocardium [106].

1.4.4 Fibrotic Signaling In AngII-Induced Myocardial Fibrosis

Age-related myocardial fibrosis does not appear to be associated with the inflammatory cell infiltration that is observed in the AngII-induced model. However, there are similarities in the downstream fibrotic signaling in both the local cardiac AngII signaling pathway and the hypertensive effects of AngII on the myocardium in both of these processes[81, 107]. In order to focus on the role and regulation of fibrotic factors that may be driving the development of myocardial fibrosis we therefore used the AngII-induced model, which allows for artificial control over the initiation of a known fibrotic stimulus.

Downstream signaling of AngII results in increased pro-fibrotic cytokine production, including TGFβ, CTGF, platelet derived growth factor (PDGF) and fibroblast growth factor (FGF) produced by fibroblasts as well as inflammatory cells. These growth factors provide signals needed for fibroblasts to differentiate into active myofibroblasts[4]. The current rhetoric concerning pro-fibrotic signaling suggests that one of the first molecules to respond in the fibrotic pathway after AngII exposure is TGFβ[45, 107-109]. TGF-β has been shown to be chemotactic for fibroblasts, stimulates

fibroblast proliferation, and increases the synthesis of a number of ECM proteins [19, 43-46]. This is supported by evidence that ECM synthesis can be limited by TGF-β neutralizing antibody or truncated TGF-β type II receptors [110].

Once activated, TGF-β binds to TGFβRII, which causes dimerization with TGFβRI and the phosphorylation of cytoplasmic SMAD2/3. The pSMAD2/3 complex is translocated to the nucleus and acts as a transcription factor influencing the up-regulation of a variety of pro-fibrotic factors, including CTGF [33, 46, 111]. Specifically, pSMAD2/3 interacts with the TGFβ response element found in the upstream regulatory region of the CTGF sequence, resulting in increased transcription of CTGF mRNA [112, 113]. CTGF belongs to a highly conserved family of growth factors that have been shown to exert a wide range of biological activities downstream of TGF-β: ECM deposition, wound repair, angiogenesis, migration, differentiation, and cell survival/proliferation [114-117].

Although this pathway has been supported by *in vivo* studies using SMAD3 knockout mice, which do not produce CTGF when treated with TGFβ, one must keep in mind that CTGF has other regulatory response elements in addition to the TGFβRE, raising the possibility that a TGFβ/SMAD independent mechanism may be involved in its regulation in response to AngII exposure[118]. Given the complexity in TGF-β regulation and its importance in regulating inflammatory responses, many investigators are now looking at manipulation of downstream mediators of TGF-β, such as SMAD proteins and CTGF as therapeutic options.

CHAPTER 2: HYPOTHESIS, RATIONALE AND OBJECTIVES

2.1 Study 1: Collagen regulation in age-related fibrosis

Rationale: There is a limited amount of knowledge regarding the cause of age-related myocardial fibrosis. The involvement of the TGFβ signaling pathway in fibrosis development has been speculated, but the causative mechanism remains unknown. In addition, there is little known about specific effects of reducing collagen crosslinking in the setting of age-related myocardial fibrosis. The possibility of modulating collagen homeostasis as a possible therapeutic avenue led to the development of the first objective of this thesis.

Objective: To determine if the disruption of collagen homeostasis can decrease age-related myocardial fibrosis and to characterize associated molecular changes in the extracellular environment. (Chapter 4, Manuscript 1)

2.2 Study 2: Blood Pressure Dependence of AngII-induced Myocardial Fibrosis

Rationale: Ambiguity regarding the underlying mechanism of AngII-induced myocardial fibrosis, specifically whether the main cause is the noted increase in blood pressure or direct signaling through the AngII receptors led to the second objective of the current thesis.

Objective: To determine the causative mechanism of AngII-induced myocardial fibrosis using hydralazine, a non-RAAS based anti-hypertensive agent (Chapter 5, Manuscript 2).

2.3 Study 3: Role And Regulation Of CTGF In AngII-Induced Myocardial Fibrosis

Rationale: Despite what is currently understood about the effects of CTGF *in vitro* on fibroblasts and their production of ECM proteins, there has not yet been a causal link established between CTGF and myocardial fibrosis development. This has led to the third objective of this thesis.

Objective: To determine the role that CTGF plays in AngII-induced myocardial fibrosis and how CTGF expression is regulated during the development of myocardial fibrosis (Chapter 6, Manuscript 3).

2.4 Study 4: The Effects Of Interrupting Collagen Homeostasis On AngII-Induced Myocardial Fibrosis In Aged Mice

Rationale: Increases in fibrosis and fibrotic signaling occur during aging. It is not clear if the accumulation of collagen and associated changes in signaling or cellular aging are the primary contributors to the development of age-related myocardial fibrosis. This has led to the fourth objective of this thesis.

Objective: To determine if interrupting collagen homeostasis and fibrotic signaling prior to inducing myocardial fibrosis in aged mice will alter the fibrotic response to AngII. (Chapter 7, Manuscript 4).

CHAPTER 3: MATERIALS AND METHODS

3.1 Animals

All work was approved by Dalhousie University's *Committee on Laboratory Animals* in accordance with the Canadian Council on Animal Care guidelines. Male C57BL/6 (Stock No. 000664) and CAG-EGFP (Stock No. 006567) transgenic mice were purchased from the Jackson Laboratory (Bar Harbour, ME) and were housed within the Carleton Animal Care Facility at Dalhousie University. Mice were acquired at 8wk, 12wk or 40wk and provided with food and water *ad libitum* for 1wk prior to experimentation.

3.2 GFP Chimeric Animals

Chimeric animals were generated by transplanting bone marrow constitutively expressing GFP into lethally irradiated mice, as previously described[37, 119]. Bone marrow cells were harvested from 8wk old CAG-EGFP transgenic mice with a C57Bl/6 background that ubiquitously express enhanced GFP under control of the CAG promoter. Recipient mice were irradiated with two doses of 5.5Gy and unfractionated GFP+ BM cells ($1x10^6$ cells) were injected via tail vein. Engraftment was evaluated 8wk after transplant by collecting peripheral blood cells and evaluating the frequency of GFP+ cells relative to the total peripheral nucleated cells. Only animals with engraftment greater than 60% GFP+ were used for further experimentation.

3.3 Drug Infusion

Animals had mini osmotic pumps implanted under general anesthesia as previously reported[37]. Animals were anesthetized with isoflurane (Baxter Healthcare

Corp., New Providence, NJ) in oxygen at which point a 1-2 cm mid-scapular skin incision was made between the shoulder blades and a mini osmotic pump (Alzet, Palo Alto, CA) was inserted subcutaneously. Animals were randomly assigned to receive AngII (3 or 7 day pumps 2.0μg/kg/min[37], Sigma Aldrich), hydralazine (6.9 μg/kg/min), BAPN (2 x 7 day pumps at 104.2μg/kg/min[120], Sigma) or a vehicle control of saline. Incisions were closed using surgical staples. The pumps remained in for 6 or 12hr, 1, 3 or 7d during which the animals were provided food and water *ad libitum* and observed for signs of morbidity (respiratory distress, weight loss and lethargy).

3.4 Blood Pressure Measurements

Blood pressure measurements were taken via the Coda2 noninvasive cuff system (Kent Scientific, Torrington, CT). Animals were allowed to acclimate to the apparatus the day prior to measurements being collected. A minimum of 5 consecutive measurements were recorded for each animal and all measurements were conducted at the same time of the day. Experience in our laboratory and findings from others have shown that blood pressure measurements taken at the completion of the experiment reflect changes due to AngII infusion that have been stable over several days, supporting our approach to measure blood pressure at 7 d [121, 122].

3.5 Echocardiography

A trained sonographer, blinded to the experimental groups, carried out the transthoracic echocardiograms using a Vivid 7 ultrasound device (GE Healthcare Canada, Mississauga, ON). Mice were anesthetized with isoflurane, body temperature was maintained on a heating pad and electrocardiograms were monitored during the procedure. Two-dimensional M-mode measurements in short axis view at the mid-

papillary level included; left ventricular interior diameter in diastole (LVIDd), systole (LVIDs), septal wall thickness in diastole (ISd), systole (ISs), left ventricular posterior wall thickness in diastole (LVPWd) and systole (LVPWs). The percentage fractional shortening (FS) was calculated and the Teichholz method was used to calculate ejection fraction (EF) based on changes in the left ventricular interior diameter [123]. Pulse wave tissue Doppler was used to determine the early and late mitral inflow velocities (E and A respectively) and the E/A ratio was calculated.

3.6 Tissue Harvest

Animals were then anesthetized with isoflurane and sacrificed via exsanguination. Hearts from experimental animals were harvested and weighed then divided into three sections along the vertical axis. The base section of the heart was processed for histological examination with the other two pieces snap frozen immediately for molecular analysis. Blood was collected using cardiac puncture after anesthetization, allowed to coagulate then centrifuged for serum isolation. Serum was then aliquoted and stored at -80^{o}C.

3.7 Cell Isolation and Culture

3.7.1 Fibroblasts (Cardiac and skin)

Cardiac fibroblasts were isolated from mice at either 8wk or 40wk. Hearts were harvested under sterile conditions and used for cell isolation as previously described[37]. Alternately skin fibroblasts were isolated from ear clippings. Briefly, hearts or ear clippings were mechanically and enzymatically digested in a collagenase solution (50 mM collagenase II, Cedarlane, Burlington, ON) in RPMI 1640 media (Gibco, Burlington,

ON) at 37°C with agitation for 30min. Cell isolates were washed in complete RPMI containing 10% heat-inactivated FBS, 2mM L-glutamine, 100mg/mL streptomycin and 100U/mL Penicillin. Cells were then plated in T25 flasks coated with 0.1% gelatin, incubated for 3d at 37°C and 5% CO_2, at which point all non-adherent cellular debris was removed and media was replenished.

3.7.2 Peripheral Blood Mononuclear Cells And Bone Marrow Cells

Peripheral blood mononuclear cells (PBMCs) and bone marrow (BM) cells were isolated from naïve or 3d AngII exposed mice. Briefly, blood was collected in heparin containing syringes via cardiac puncture and centrifuged. The PBMC containing layer was isolated, washed and residual red blood cells were lysed using ammonium chloride solution. BM cells were removed from the tibias and femurs by flushing with 10mL of Dulbecco's phosphate buffered saline (dPBS; Invitrogen) after removal of the bone ends.

3.7.3 Fibrocytes

Hearts from mice infused with AngII for 3d were harvested under sterile conditions and used for cell isolation as previously described[37]. Briefly, hearts were mechanically and enzymatically digested in a collagenase solution (50mg/mL collagenase II, Cedarlane, Burlington, ON) in RPMI 1640 media (Gibco, Burlington, ON) at 37°C with agitation for 45min. Cell isolates were washed in complete RPMI containing 10% heat-inactivated fetal bovine serum (FBS; Sigma), 2mM L-glutamine, 100mg/mL streptomycin and 100U/mL Penicillin. Cells were then plated in T25 flasks coated with 0.1% gelatin, incubated for 3d at 37°C and 5% CO_2, at which point all non-adherent cellular debris was removed and media was replenished.

3.7.4 Cardiomyocytes

Neonatal cardiomyocytes were isolated from day old C57Bl/6 pups as reported previously[124]. In short, pups were decapitated, hearts were excised and mechanically and enzymatically digested in 0.25% trypsin-EDTA for 20min. Cell isolates were washed in complete DMEM media containing 20% FBS, 2mM L-glutamine, 100μM non-essential amino acids, 100mg/mL streptomycin and 100U/mL Penicillin and allowed to differentially adhere to a T75 flask for 2hr. Cardiomyocytes were then collected from the suspension and plated on 0.1% gelatin coated 6-well plates.

3.7.5 Endothelial Cells

The brain microvascular endothelial cell line, B.End3 (ATCC, Manssas, VA) was cultured according to the supplier's instructions using DMEM containing 10% heat-inactivated FBS, 2mM L-glutamine, 100mg/mL streptomycin and 100U/mL Penicillin.

3.7.6 In Vitro Treatments

Isolated fibroblasts, fibrocytes, neonatal cardiomyocytes and endothelial cells were serum starved overnight prior to being treated with a) AngII (100nM), b) AngII + anti-TGFβ neutralizing antibody (15ug/mL; R&D Systems, Minneapolis, MN)[125, 126], c) hydralazine (40nM) d) sterile filtered full-length recombinant human CTGF produced in E.Coli (125ng/mL[127]; CRC022B Cell Sciences, Canton, MA, USA), e) recombinant human TGFβ expressed in mammalian A293 cells (10ng/mL[128]; Abcam), f) BAPN (200μM[129]), g) dPBS as vehicle control or various combinations as outlined in figure legends.

3.8 Histological Analysis

Hearts were processed for histological assay by: a) fixing with 10% formalin in PBS for 24hr or b) protecting with optimal cutting temperature media (OCT)/sucrose mixture followed by snap freezing. Formalin fixed tissues were paraffin embedded and serially sectioned on a microtome (5μm). Basic myocardial histology and cellular infiltration were examined using heart cross-sections stained with hematoxylin and eosin (H&E). Images of entire myocardial cross-sections were compiled from 5x objective images taken with an Axiocam HRC colour camera. Cellular infiltration was semi-quantified by using an overlaid grid over whole myocardial cross-sections. Grids that contained any mononuclear cellular infiltration were tallied as well as total grids encompassed by the heart and these values used to calculate the % area affected by infiltration, as previously reported[130].

Collagen was detected using Sirius red stain and tissue counterstained with fast green stain. Collagen was then quantified using a technique modified from Underwood *et al*[131]. In short, images of entire myocardial cross-sections were compiled from 5x objective images taken with an Axiocam HRC colour camera. Image analysis software (Photoshop CS5, Adobe Systems Inc, San Jose, CA) was used to quantify the amount of tissue positive for Sirius red by selecting and counting red pixels. This was compared to total area of the myocardial cross-section in pixels. Sections from individual animals were averaged and experimental groups compared to control animals.

3.9 Immunohistochemistry

Immunohistochemistry for αSMA, CTGF and Ki-67 was performed on paraffin embedded tissues, which were cut in 5um sections on a microtome, de-paraffinized and

heat-treated for antigen retrieval prior to staining. Briefly, endogenous peroxidases were quenched with 3% hydrogen peroxide; endogenous biotin was blocked (DAKO Biotin Blocking System, DakoCytomation, Mississauga, ON); and non-specific staining was blocked with normal goat serum. Sections were incubated with primary antibody overnight at 4^{o}C, followed by a host-specific biotin-conjugated secondary antibody. The antibody complexes were then conjugated to an avidin-biotin complex (Vectastain ABC kit; Vector, Burlington, CA) and developed using 3,3' diaminobenzidine as the chromogen (DAB; DakoCytomation). See Table 3.2 for antibody concentrations and supplier information. Light microscopy was performed; pictures were captured and analyzed in Adobe Photoshop 5.0.

3.10 Immunofluorescence Staining And Confocal Microscopy

Isolated cells were plated on glass coverslips overnight, fixed in 4% paraformaldehyde. Tissue sections were fixed in 4% paraformaldehyde (PFA; EMD Millipore, Gibbstown, NJ), cryoprotected in OCT-sucrose solution prior to freezing and sectioning at 10um on a cryostat. Cells or tissues were blocked against non-specific antibody binding with 10% normal goat serum and stained for CD45, collagen type 1, cardiac troponin I (CTnI), GFP, αSMA or CD133 overnight at 4^{o}C. Antibodies were detected using incubation for 1h at room temperature with anti-host specific Alexa Flour 488, 555 or 647 fluorescently labeled secondary antibodies raised in goat and nuclei were counterstained with Hoescht stain (Sigma Aldrich) or ToPro3 (Invitrogen) for imaging using confocal microscopy. See Table 3.2 for antibody concentrations and supplier information.

Images were captured with a Zeiss Axiovert 200 inverted microscope with a Hamamatsu ORCA-R2 digital camera with an AttoArc 2 HBO 100W lamp. Confocal images were captured on a Zeiss LSM 510 META microscope and single z-plane slices are shown.

3.11 Enzyme Linked Immunosorbent Assay

Aliquoted serum samples were thawed, avoiding repeated freeze-thaw cycles and the manufacturer's protocols for ELISAs were used:

3.11.1 ELISA For CTGF

Serum CTGF concentrations were measured using a commercially available ELISA kit (UCSN Life Sciences, China) following the manufacturer's protocol. Samples were run in duplicate, both at a 1:5 dilution with diluent buffer and undiluted along with a serial dilution of known standard and negative controls. Chromogenic substrate was incubated for 20min and the plate was read at 450nm immediately after stop solution was added. Values that fell within the range of the standard curve were calculated, averaged and compared between groups.

3.11.2 ELISA For Aldosterone

Serum aldosterone levels were assessed using a standard ELISA kit (Cayman Chemical Company, Ann Arbor, MI) as per the manufacturer's instructions. Briefly, serum samples were diluted 1:4 and plated out in triplicate, along with recommended controls. The plate was covered and incubated for 18 hrs at 4°C. The plate was then developed for 1.5 hrs while shaking and was read at 420 nm. The total concentrations for each sample were calculated, averaged and compared between groups.

3.12 Immunoblotting

Western blotting was performed on samples isolated from snap frozen heart sections. Sections were homogenized in RIPA buffer (150mM NaCl, 50mM Tris-HCL base, 0.1% SDS, 0.1% Triton X-100, 0.5% deoxycholic acid) with the addition of protease inhibitors (complete protease inhibitor tablet excluding metalloproteinases; Roche). Samples were denatured by boiling with Laemmli sample buffer. Protein was separated on a 12% SDS-PAGE gel and transferred to Immobilon PVDF membrane (Millipore, Bedford, MA). Membranes were incubated with 5% skim milk in buffer (except for pSMAD2 for which 2% BSA in buffer was used as block) for 1hr before incubation with anti-CTGF, SMAD2/3, pSMAD2, LOX, βtubulin (loading control) or βactin (loading control) antibody overnight at 4^{o}C. Blots were developed using horseradish peroxidase-linked goat anti-rabbit IgG and an Amersham ECL prime kit (GE Life Sciences, Buckinghamshire, UK). See Table 3.2 for antibody concentrations and supplier information.

3.13 Flow Cytometry

Cell surface expression of CD45 and cytosolic expression of vimentin and CTnI was determined using flow cytometry. Briefly, isolated PBMCs and BM cells were incubated with a monoclonal rat anti-CD45 antibody followed by FITC-conjugated goat anti-rat IgG_{2b} secondary antibody. Cells were then permeabilized using a commercial kit (BD Biosciences) and incubated with PerCP conjugated monoclonal mouse vimentin antibody. Isolated neonatal cardiomyocytes were incubated with polyclonal rabbit anti-CTnI followed by an Alexa-488 conjugated goat anti-rabbit IgG secondary antibody. Following antibody incubations cells were fixed in 1% formalin solution for storage prior

to analysis. Cells were analyzed with a BD FACScalibur flow cytometer (BD Biosciences, Mississauga, ON, Canada) within 5d of labeling. Findings were confirmed using isotype controls (CD45: rat IgG_{2b} eBiosciences, San Diego, CA, USA; vimentin-PerCP: IgG_1-PerCP Santa Cruz; and CTnI: rabbit IgG, Sigma Aldrich). A secondary-only control was used to confirm the absence of nonspecific binding of the secondary antibody. See Table 3.2 for antibody concentrations and supplier information.

3.14 Hydroxyproline Assay

Prepared supernatant (as outlined below) was transferred to a clear, flat-bottomed 96-well plate and allowed to evaporate until dry at 60°C prior to the hydroxyproline assay protocol being carried out according to the manufacturers protocol (Sigma). In short, Chloromine T in oxidation buffer was added to samples and incubated at RT for 5min followed by DMAB with perchloric acid incubation for 90min at 60°C. The plate was then read on an Infinite 200Pro plate reader (Tecan, Switzerland) at 560nm.

3.14.1 Serum Preparation

Equal volumes of mouse serum and concentrated HCl were incubated at 120°C for 3hr. Activated charcoal (5mg) was added to each sample and centrifuged.

3.14.2 Tissue Preparation

Approximately 10mg of flash frozen ventricular tissue was homogenized in 100µL of 1M NaCl and incubated overnight at 4°C. Samples were then centrifuged and supernatant was transferred to a new cryovial. Concentrated HCl was added and incubated at 120°C for 3hr followed by centrifugation.

3.15 Relative Real-Time Quantitative Polymerase Chain Reaction (qPCR)

Total RNA was isolated from snap frozen heart sections using TRIzol (Invitrogen, Carlsbad, CA) according to the manufacturer's protocol. First strand cDNA was synthesized from RNA using iScript cDNA Synthesis Kit (Biorad, Hercules, CA). The qPCR was completed using iQ SYBR Green Supermix (Biorad) and the iQ Multicolour Real-Time PCR Detection System thermocycler (Biorad) was used for detection. Primers were designed using PrimerBlast, which searches for possible non-specific products during design. Efficiency curves and no-template control samples were run with samples during each thermal cycle. Melt curves were run after cycling to ensure target specificity. Primers were designed against mRNA sequences are listed in Table 3.1.

Gene Symbol	Forward Primer	Reverse Primer
CTGF	TCAACCTCAGACACTGGTTTCG	TAGAGCAGGTCTGTCTGCAAGC
TGFβ	GGTCTCCCAAGGAAAGGTAGG	CTCTTGAGTCCCTCGCATCC
PDGFB	GCATCTGCCTGAAGTGTGTACC	TTAAGGACTTGACCCTGCTTCC
FGF	CCAGCGGCATCACCTCGCTT	GGGTCGCTCTTCTCGCGGAC
MMP2	AGGACAAGTGGTCCGCGTAAAG	CCACTTCCGGTCATCATCGTAGT
TIMP1	CGGATCAGGTCCTCGTGGGCT	GCCTGGATTCCGTGGCAGGC
COL1A1	CAACAGTCGCTTCACCTACAGC	GTGGAGGGAGTTTACACGAAGC
CCL2	CCAGCCAACTCTCACTGAAGC	AGCTCTCCAGCCTACTCATTGG
CXCL12	GTAGAATGGAGCCAGACCATCC	ATTCGATCAGAGCCCATAGAGC
IL1β	TCCTCGGCCAAGACAGGTCGCT	CCCCCACACGTTGACAGCTAGGT
HIF1α	AACAGTCCCTCTGTAGTTGTGG	TAGCGACAAAGTGCATAAAACC
LOX	TACTCCAGACTCTGTGCGCT	GGACTCAGATCCCACGAAGG
18S	TCAACTTTCGATGGTAGTCGCCGT	TCCTTGGATGTGGTAGCCGTTTCT

Table 3.1 Forward And Reverse Primers Used For qPCR

Expression was normalized to the 18S ribosomal gene using the Pfaffl method[132].

3.16 Proliferation Assays

3.16.1 MTT

An MTT assay for assessment of relative cellular proliferation was carried out according to the manufacturer's instructions (Invitrogen). In brief, cells were plated in 96-well tissue culture plates and allowed to adhere overnight prior to stimulation. Cells were stimulated for 24hr at which point MTT reagent was added for 4hr, followed by SDS-HCL solution for 18hr to stop the reaction. Samples were mixed and absorbance was then read at 570nm.

3.16.2 Cell-Titer Blue Assay

A modified resazurin based metabolic activity assay (similar to Alamar Blue) for assessment of relative cellular proliferation was carried out according to the manufacturer's instructions (Promega, Madison, WI). In brief, cells were plated in 96-well black-sided, clear-bottomed culture plates and allowed to adhere overnight then serum deprived overnight prior to stimulation. Cells were stimulated for 48hr at which point resazurin reagent was added and incubated at 37^{o}C for 4hr. Plates were then read and resorufin production was determined by measure fluorescence at excitation 560, emission 590nm.

3.16.3 BrdU

A BrdU assay for the assessment of relative proliferation was completed according to the manufacturer's protocol (Millipore, Billerica MA). In brief, primary fibroblasts were plated on 96-well culture plates, allowed to adhere overnight and serum starved for 24 hrs prior to treatment. The cells were then treated with either saline as a

control, AngII (100 nM), hydralazine (40 nM) or AngII+hydralazine for 6 hrs, at which point the BrdU reagent was added to the culture plate. After 24 hrs from the time of treatment, the plates were fixed, dried and stored at 4^{o}C until analysis. Plates were then incubated with primary anti-BrdU antibody, washed, incubated with secondary biotin-conjugated anti-goat antibody, washed, incubated with substrate, stopped and read at 490nm.

3.16.4 Ki67

Relative proliferation was also assessed by immuno-fluorescent staining of Ki67 proliferation marker in cells plated on gelatin-coated coverslips. Cells were allowed to reach 50% confluency, then stimulated for 24hr at which point cells were fixed using 4% para-formaldehyde for 10min at room temperature. Non-specific binding was blocked using secondary host serum then coverslips were incubated overnight at 4^{o}C with anti-Ki67 antibody. Bound antibody was detected using anti-host specific Cy3 fluorescently labeled secondary antibodies (Invitrogen) and nuclei were stained with hoescht dye. Images were captured with a Zeiss Axiovert 200 inverted microscope with a Hamamatsu ORCA-R2 digital camera with an AttoArc 2 HBO 100W lamp. Relative proliferation was assessed by counting the number of Ki67 positive nuclei relative to the total number of nuclei in 5 random fields of view at 20x magnification.

3.17 Scratch Assay

Fibrocytes were isolated as previously described and cultured to 80% confluency on 6-well plates. A sterile pipette tip was used to remove cells from a strip in the middle of the well. Images were captured at 10x immediately (0hr) or after 16hr of culture with CTGF or with PBS as control. Leading edges of the cell fronts were demarcated and the

distance between was semi-quantified using a pixel count method. The relative distance was then calculated as a fraction of distance recovered by cells compared to control.

3.18 MMP2 And MMP9 Gel Zymography

Zymogram gels (10% polyacrylamide with gelatin) were purchased from BioRad. Protein samples were isolated from whole myocardium using RIPA buffer, as above, with protease inhibitors excluding metalloproteinase inhibitors. There were 5μg of sample loaded per well and gels were incubated in digestion buffer containing calcium chloride for 48hr prior to Coomasie staining. Images were captured using the AlphaImager system (Protein Simple, Santa Clara, CA). ImageJ was used to assess densitometry and activity reported as relative change from 8wk.

3.19 Statistical Analysis

Data are represented as means ± SEM. One-way ANOVA tests were completed using the Bonferroni post-hoc test to compare multiple experimental groups and to compare experimental groups to the saline control. T-tests were used for comparison if there were only 2 groups. All qPCR results were evaluated based on the one-sample T-test to compare changes in relative expression to a theoretical mean of 1.000. All statistical calculations were computed using GraphPad Prism4 software and significance was determined if $p<0.05$.

Primary Antibodies	WB Concentration (μg/mL) or dilution			Host	Supplier	Cat No.
	IHC/IF	WB	FC			
αSMA	2			Mouse	Sigma	A5228
β-Actin		0.5		Rabbit	Sigma	A2066
β-Tubulin		1		Mouse	Sigma	T8328
CD45			2.5	Rat	Cedarlane	CL9446AP
CD45	1:50			Rat	BD	550539
CD133	5			Rabbit	Abcam	ab19898
Col1	5			Rabbit	Rockland	600-401-103
CTGF	2.5	5		Rabbit	Abcam	ab6992
CTnI	20			Rabbit	Abcam	ab19651
GFP	1:200			Rabbit	Abcam	ab290
Ki-67	1:1000			Rat	Dako	M7249
LOX		1		Rabbit	Millipore	ABT112
SMAD2/3		1:1000		Rabbit	Cell Signaling	3102
pSMAD2		1:1000		Rabbit	Cell Signaling	3104
PerCP-Vimentin			40	Mouse	Santa Cruz	sc-32322
Secondary Antibodies						
Biotin anti-mouse	1:500			Goat	Vector (From MOM kit)	BMK2202
Biotin anti-rabbit	1:500			Goat	Vector	BA-1000
Alexa488 anti-rabbit	1:500			Goat	Invitrogen	A11008
Cy3 anti-rat	1:500			Goat	Jackson	112-165-072
Cy3 anti-mouse	1:500			Goat	Jackson	115-165-003
Cy3 anti-rabbit	1:500			Goat	Jackson	111-165-003
FITC anti-Rat			1:100	Goat	Cedarlane	CLCC40001
Peroxidase anti-mouse		1:2000-5000		Goat	Vector	PI-2000
Peroxidase anti-rabbit		1:2000-5000		Goat	Vector	PI-1000

Table 3.2 Antibody Concentrations And Supplier Information

Concentrations of antibodies used for immunohistochemistry (IHC), immunofluorescence (IF), western blot (WB) and flow cytometry (FC) are provided. The supplier and catalogue numbers are also listed.

CHAPTER 4: DISRUPTION OF COLLAGEN HOMEOSTASIS CAN REVERSE AGE-RELATED MYOCARDIAL FIBROSIS

This work appears in part in the publication:

Rosin N.L., Sopel M, Falkenham A., Lee T.D.G., Légaré J.F. Disruption of collagen homeostasis can reverse age-related myocardial fibrosis. Submitted to *Cardiovascular Research* Feb 3, 2014

Contribution:

NR – designed the study, carried out experimentation, collected and analyzed data, and prepared the manuscript

MS, AF – assisted with experimentation and data collection

TL, JFL – assisted with study design and critical review of the manuscript

4.1 Introduction

Myocardial fibrosis is a common pathological feature of many cardiovascular disorders and is characterized by an over-abundant deposition and/or deficit in degradation of ECM molecules[2]. The excess ECM protein results in loss of myocardial contractility and increased stiffness[2]. The functional result of myocardial fibrosis is diastolic dysfunction and ultimately diastolic heart failure, where affected patients have preserved ejection fraction, associated with significant adverse health outcomes[12].

Of particular clinical importance is the relationship of age with the development of myocardial fibrosis. Several investigators have shown that the aging myocardium is associated with progressive and significant ECM deposition termed age-related fibrosis[18]. Prior work in this area has shown a correlation between the degree of fibrosis, as measured by amount of interstitial collagen, with diastolic dysfunction during aging[4, 13]. Diastolic heart failure is reported to be the highest cause of hospitalization in elderly patients[15]. However, the mechanisms responsible for the development of age-related myocardial fibrosis have yet to be fully characterized. There is convincing evidence to conclude that the increased collagen in the myocardium of aging animals represents an imbalance between one or more of the following: (1) collagen biosynthesis by fibroblasts, (2) post-synthetic collagen processing (cross-linking) which makes collagen less prone to degradation, and (3) collagen degradation. However, only a limited number of studies have been published to date investigating the fundamental cause of the imbalance.

A key mechanism in collagen processing is the cross-linking of collagen fibers in the extracellular environment[12]. The enzyme responsible for the initiation of collagen

crosslinking is LOX. LOX expression and activity have been previously reported to increase with age[56]. It has been postulated that an increase in collagen crosslinking directly contributes to the increase in tissue stiffness within the myocardium[14] that occurs during aging, but clear evidence regarding this process is currently lacking.

TGFβ has been suggested as the main cytokine involved in regulating age-related myocardial fibrosis[12]. This is based largely on work demonstrating that TGFβ is chemotactic for fibroblasts, stimulates fibroblast proliferation, and increases the synthesis of a number of ECM proteins[19, 43, 46]. Animals that have diminished levels of TGFβ (TGFβ+/-), show decreased age-related fibrosis and preserved diastolic function[133]. However, given the complexity in TGFβ regulation, many investigators have advocated looking at downstream mediators of TGFβ, especially when identifying and developing anti-fibrotic therapies. CTGF is one of the proteins downstream of TGFβ that has been shown to be involved in ECM deposition, wound repair, angiogenesis, migration, differentiation, and cell survival/proliferation in animal models of hypertension-related myocardial fibrosis or myocardial infarction[114, 130, 134]. A similar link between CTGF expression and age-related fibrosis in the myocardium has not been addressed. Likewise, the relationship between expression of other highly active pro-fibrotic factors, such as FGF and PDGF, and myocardial fibrosis in the aging heart has not been investigated.

In this study, we have characterized the expression of several pro-fibrotic factors early in the trajectory of aging and examined how they relate to collagen homeostasis. Furthermore, we have demonstrated that disruption of collagen crosslinking with LOX inhibition can have profound effects on overall collagen homeostasis beyond its structural

effects on collagen, which might offer novel insights into the development of age-related myocardial fibrosis.

4.2 Results

4.2.1 Physiological Measurements

A minimum of 6 mice were evaluated per group. Mice were grouped based on age (± 1wk): 8wk, 12wk, 40wk. Body weight and heart weight were collected and only body weight increased significantly by 40wk (Table 4.1). Hypertrophy was defined as HW/BW ratio and did not differ significantly between groups.

4.2.2 Significant Myocardial Fibrosis Develops With Age

Myocardial fibrosis was assessed using Sirius red for collagen visualization. Representative images illustrated an increase in interstitial and perivascular collagen in older animals, with darker red indicating the presence of denser collagen fibers in the myocardium of 40wk compared to 8wk or 12wk animals (Figure 4.1A, B, C). The amount of collagen was semi-quantified and reported as a percentage of total cross-section area affected. The myocardium of mice at 40wk had significantly more collagen deposition (10.2±1.3%) compared to mice at either 8wk (5.7±1.8%) or 12wk (5.5±1.2%) (Figure 4.1D; $p<0.05$).

4.2.3 Mechanisms Involved In The Observed Collagen Increase

Collagen type I is the most abundant ECM protein within the myocardium[135]. It is actively and continually synthesized, processed (including crosslinking) and degraded. We therefore assessed collagen homeostasis within the myocardium and its relationship to aging.

Collagen synthesis: The relative expression of collagen type I α I (COL1A1) mRNA was assessed by qPCR in myocardium and did not change significantly between 8wk to 12wk, but was significantly elevated by 40wk (15.2±4.9fold) (Figure 4.1E; $p<0.05$). This suggests that the increase in collagen deposition observed during aging is in part due to an increase in new collagen mRNA production. Having shown that collagen increased both in mRNA and protein as early as 40wk of age, we stained sections of myocardium for SMA in order to assess the presence of myofibroblasts (activated fibroblasts), which are responsible for ECM production. We were able to identify myofibroblasts in the interstitium of 40wk old mice but not in the myocardium of younger animals (Figure 4.1F).

Collagen crosslinking: Hydroxyproline content within the myocardium was quantified and represents a measure of the total collagen content per microgram of tissue. The proportion of crosslinked collagen was assessed by comparing the amount of hydroxyproline in non-solubilized (crosslinked) to that in solubilized (non-crosslinked) fractions of homogenized myocardium. There was a significant increase in total collagen in myocardium of 40wk animals compared to 8wk, supporting the Sirius red semi-quantification. Furthermore, at 40wk the increase in collagen appeared to be mainly comprised of non-soluble or crosslinked collagen (Figure 4.2A).

LOX is the primary enzyme responsible for the crosslinking of collagen. LOX mRNA expression did not change significantly by 40wk compared to 8wk (Figure 4.2B). The amount of the active isotype of LOX protein did not change significantly either by 40wk, as assessed by western blot (2.48±0.68fold; $p>0.05$) (Figure 4.2C, D).

ECM degradation/MMP activity: A major pathway of ECM degradation involves the matrix metalloproteinases, notably MMP2 and MMP9[136]. The MMPs are themselves regulated by the tissue inhibitors of MMPs, such as TIMP1 which is known to degrade MMP2[137]. We therefore assessed the expression and activity of these molecules in the setting of age-related fibrosis. MMP2 mRNA expression did not change significantly with age (Figure 4.3A). However, the regulator of MMP2, TIMP1 did increase significantly by 40wk (10.95±4.49 vs 1.08±0.22fold; $p<0.05$) (Figure 4.3B). The ratio of MMP2:TIMP1 was significantly reduced at 40wk compared to 8wk (0.28±0.08 vs 1.01±0.06fold; $p<0.05$), suggesting a decrease in overall MMP2 activity and reduced collagen degradation (Figure 4.3C). To confirm age-related changes on the activities of MMP2 and MMP9 within the myocardium, their activities were directly assessed using gelatin zymography. MMP2 activity did not change significantly with aging. In contrast MMP9 activity decreased significantly by 40wk relative to 8wk (-3.95±1.07; $p<0.05$) (Figure 4.3D, E, F), suggesting that MMP activity was reduced in aging animals, resulting in less degradation and favoring collagen accumulation.

4.2.4 Age-Related Fibrosis Is Associated With A Significant Up-Regulation Of Pro-Fibrotic Pathways Including TGFβ

Pro-fibrotic factors are small molecules secreted within the extracellular milieu that are known to promote the expression and deposition of ECM proteins and increase proliferation and motility of fibroblasts[130]. One such growth factor, TGFβ, is recognized as a key fibrotic signaling molecule in many fibrotic disorders[2]. As such, we investigated the involvement of the TGFβ signaling pathway in age-related myocardial fibrosis. The relative mRNA expression of TGFβ was assessed by qPCR. By

40wk of age TGFβ mRNA expression was significantly elevated (2.9±1.0fold) compared to 8wk or 12wk, within the myocardial tissue (Figure 4.4A; $p<0.05$). The SMAD2/3 protein expression and SMAD3 phosphorylation were determined by immunoblotting and was used to assess TFGβ receptor activation, as this is a key step in the pro-fibrotic pathway of TGFβ. Total SMAD2/3 protein expression increased significantly with aging. In conjunction, the relative amount of phosphorylated SMAD2 also significantly increased at 40wk compared to 8wk, further supporting that TGFβ signaling increased with age (Figure 4.4B, C; $p<0.01$).

We also assessed production of a downstream fibrotic mediator of TGFβ, CTGF. CTGF mRNA expression was significantly increased at 40wk (7.0±2.8fold) compared to 8wk or 12wk (Figure 4.4D; $p<0.05$). The amount of CTGF in the serum, which has previously been suggested as a biomarker for heart failure[138], was also significantly increased by 40wk (5.52±0.45ng/mL) compared to 8wk (0.46±0.40ng/mL), with no significant change at 12wk (Figure 4.4E; $p<0.01$). Taken together, these data strongly support that TGFβ signaling is significantly up-regulated in aging myocardium.

The expression of two other pro-fibrotic factors known to increase fibroblast proliferation and collagen deposition, namely PDGF and FGF were also assessed within the myocardium[139, 140]. PDGF and FGF mRNA levels were significantly up-regulated at 40wk (7.0±2.0fold and 2.5±0.5fold) compared to younger animals (Figure 4.4F, G; $p<0.05$).

4.2.5 Age-Related Fibrosis Is Reversible By Disrupting Collagen Homeostasis

Taken together, we have shown that as early as 40wks, significant changes can be identified within the myocardium that are consistent with the development of age-related

fibrosis. Our findings suggest that an imbalance between ECM deposition and degradation favoring increased accumulation of collagen is already established and responsible for age-related fibrosis. Furthermore, these changes in the ECM are associated with significant increases in pro-fibrotic signaling such as TGFβ, CTGF, PDGF and FGF, suggesting that these molecules are likely key regulators of the process through a mechanism that is yet to be defined.

In order to better understand the links between collagen homeostasis and pro-fibrotic signaling, we sought to disrupt one of the final stages of the post-transcriptional regulation of collagen synthesis: crosslinking of lysine groups initiated by LOX[141]. The LOX inhibitor BAPN was administered to 38wk mice for 2wk and these animals were compared to untreated 40wk mice. Using analysis of Sirius red stained cross-sections we were able to show that collagen deposition was significantly ($p<0.05$) reduced in BAPN exposed 40wk animals (5.84±0.30% vs 10.17±1.34%; Figure 4.5A, B). In fact, collagen deposition in BAPN treated mice at 40wk did not significantly differ from that observed in young myocardium at 8wk (5.74±1.70%) (Figure 4.5B; $p<0.05$). In support of the effects of BAPN on crosslinking, there were significant reductions in the amount of crosslinked collagen (40wk+BAPN 1.33±0.09; 40wk 1.69±0.10; $p<0.05$) and total collagen (40wk+BAPN 2.41±0.21; 40wk 1.69±0.09; $p<0.05$) within the myocardium after exposure to BAPN compared to at 40wk (Figure 4.5C).

4.2.6 LOX Inhibition Also Affects Collagen Homeostasis Beyond Collagen Crosslinking

BAPN exposure resulted in a significant reduction in collagen mRNA expression compared to age-matched animals at 40wk (3.50±0.29 vs 15.22±4.90fold; $p<0.05$). Expression in BAPN treated myocardium was not significantly elevated compared to

8wk (Figure 4.5D). Similarly, following BAPN exposure the mRNA expression of TGFβ, CTGF, PDGF and FGF were significantly reduced from 40wk controls (TGFβ 1.37±0.19 vs 2.79±1.06fold; CTGF 0.83±0.22 vs 7.63±2.47fold; PDGF 1.40±0.21 vs 8.56±1.72fold; FGF 1.19±0.12 vs 2.25±0.53fold; $p<0.05$) and did not differ significantly from the levels observed in 8wk myocardium (Figure 4.5E). Supporting these findings, serum CTGF levels were also significantly reduced after BAPN exposure (2.65±0.08 vs 5.52±0.45ng/mL) (Figure 4.5F; $p<0.01$). These findings suggest that LOX inhibition with BAPN affects crosslinking of collagen but also affects collagen production and pro-fibrotic signaling. BAPN treatment also decreased LOX mRNA expression within the myocardium compared to 40wk mice and returned mRNA expression to that observed at 8wk (Figure 4.5G). BAPN exposure was associated with a significant ($p<0.05$) reduction in the active isoform of LOX protein within the myocardium, although this remained elevated relative to 8wk (40wk; 2.48±0.38fold, 40wk + BAPN; 1.67±0.11fold) (Figure 4.5H, I). In summary, LOX inhibition with BAPN was able to reverse age-related fibrosis. However, the mechanism for this effect appears to be beyond the structural effects of reducing collagen crosslinking and suggests a complex relationship between ECM proteins and the molecular signals involved in ECM regulation.

4.2.7 Functional Effects Of BAPN Exposure

Echocardiography was used to assess cardiac function at 8wk and at 40wk, both before and after 2wk BAPN exposure (Table 4.1). Comparing the early (E) to late mitral inflow velocities (A) or E/A ratio measured using tissue Doppler is a common method for assessing diastolic function[142]. E/A was significantly ($p<0.05$) reduced at 40wk compared to 8wk. However, this decrease was ameliorated after BAPN exposure, with no

significant difference in animals treated with BAPN compared to 8wk (Figure 4.6A, B, C, G). This suggests that BAPN treatment for 2wk was sufficient for recovery of diastolic function. There were no significant changes in the m-mode measurements of cardiac structure (Table 4.1) except for an increase in LVPWd with exposure to BAPN, compared to at 8wk (Figure 4.6D, E, F, H). The maintenance of EF and FS suggests that systolic function was maintained at 40wk and was not affected by BAPN exposure.4.2.8 Cellular Response To LOX Inhibition

We used an *in vitro* system to investigate in more depth the mechanism behind the inhibition of collagen synthesis by LOX in the myocardium. Primary cardiac fibroblasts were used, as these are the cell type primarily responsible for ECM production[2]. Cells were isolated from animals at 40wk of age and exposed to media (negative control), BAPN and/or TGFβ. There was no difference ($p<0.05$) between any of the groups in the percentage of SMA^+ cells, a marker of myofibroblast activation or in the total number of cells after 24hr of BAPN (Figure 4.7A). There was also no significant difference ($p<0.05$) in viability between groups after 48hr (Figure 4.7A). This suggests that the increase in collagen synthesis observed *in vivo* was not due to an increase in fibroblast differentiation, proliferation or cell viability. The mRNA expression of TGFβ was also assessed to determine if BAPN directly regulated its expression by fibroblasts. BAPN significantly increased TGFβ expression compared to media control (Figure 4.7B; $p<0.05$).

	8wk			40wk			BAPN		
	Mean	SEM	n	Mean	SEM	n	Mean	SEM	n
LVIDd (cm)	0.39	0.02	5	0.38	0.02	5	0.35	0.03	4
LVIDs (cm)	0.28	0.01	5	0.27	0.02	5	0.24	0.03	4
EF	58.76	2.32	5	59.33	1.17	5	65.44	4.51	4
FS (%)	27.48	1.50	5	27.65	0.97	5	32.85	2.99	4
IVSd (cm)	0.10	0.01	5	0.11	0.01	5	0.09	0.01	4
IVSs (cm)	0.12	0.01	5	0.14	0.01	5	0.14	0.01	4
LVPWd (cm)	0.11	0.01	5	0.11	0.01	5	0.13^{+}	0.01	4
LVPWs (cm)	0.13	0.01	5	0.13	0.01	5	0.16	0.02	4
E (cm/s)	59.56	3.67	4	53.27	3.89	5	50.36	6.31	4
A (cm/s)	27.25	2.85	4	30.55	1.44	5	23.34^{++}	1.96	4
E/A	2.25	0.24	4	1.76	0.16	5	2.14	0.14	4
HW (mg)	138.5	7.6	10	162.9	8.6	6	154.7	6.3	8
BW (g)	27.2	1.0	10	33.8*	0.7	6	32.6*	1.0	8
HW/BW (mg/g)	5.1	0.2	10	4.8	0.2	6	4.8	0.2	8

Table 4.1 Echocardiography Data

2-dimensional m-mode and tissue Doppler echocardiography were carried out on 8wk, 40wk and 40wk+BAPN groups. M-mode measurements included the interior diameter in diastole (LVIDd) and systole (LVIDs), ejection fraction (EF), fractional shortening (FS), septal wall thickness in diastole (IVSd), systole (IVSs) and left ventricular posterior wall thickness in diastole (LVPWd) and systole (LVPWs). Doppler measurements included the early and late mitral inflow velocities (E and A) and the E/A ratio was calculated. Heart weight, body weight and hypertrophic index (HW/BW) were also measured. *$p < 0.05$ compared to 8wk; $^{+}p < 0.05$, $^{++}p < 0.01$ compared to 40wk group.

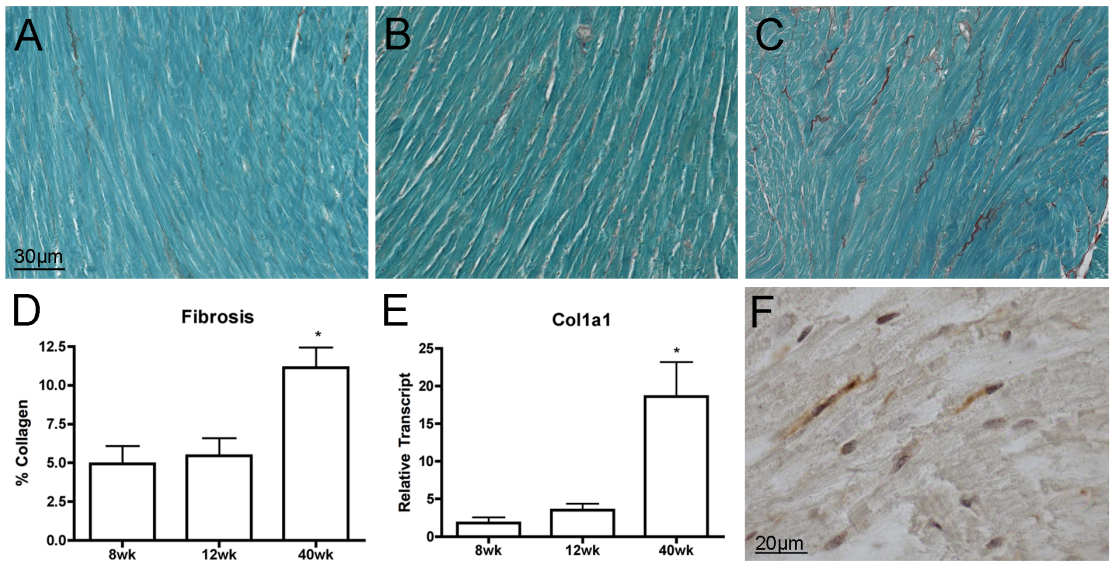

Figure 4.1 Age-Related Fibrosis Development

Fibrosis was assessed using Sirius red staining. Representative images from 8, 12 and 40wk myocardium are shown at 25x (A, B, C). The percentage of whole cross-section of myocardium stained with Sirius red was semi-quantified using image analysis software (D). Expression of COL1A1 mRNA in whole myocardium was assessed using qPCR and compared to the housekeeping gene 18S and relative to the 8wk group (E). Immunohistochemistry was done on paraffin fixed myocardial sections for SMA, with a representative image from 40wk shown at 63X (F). n=6; *$p<0.05$.

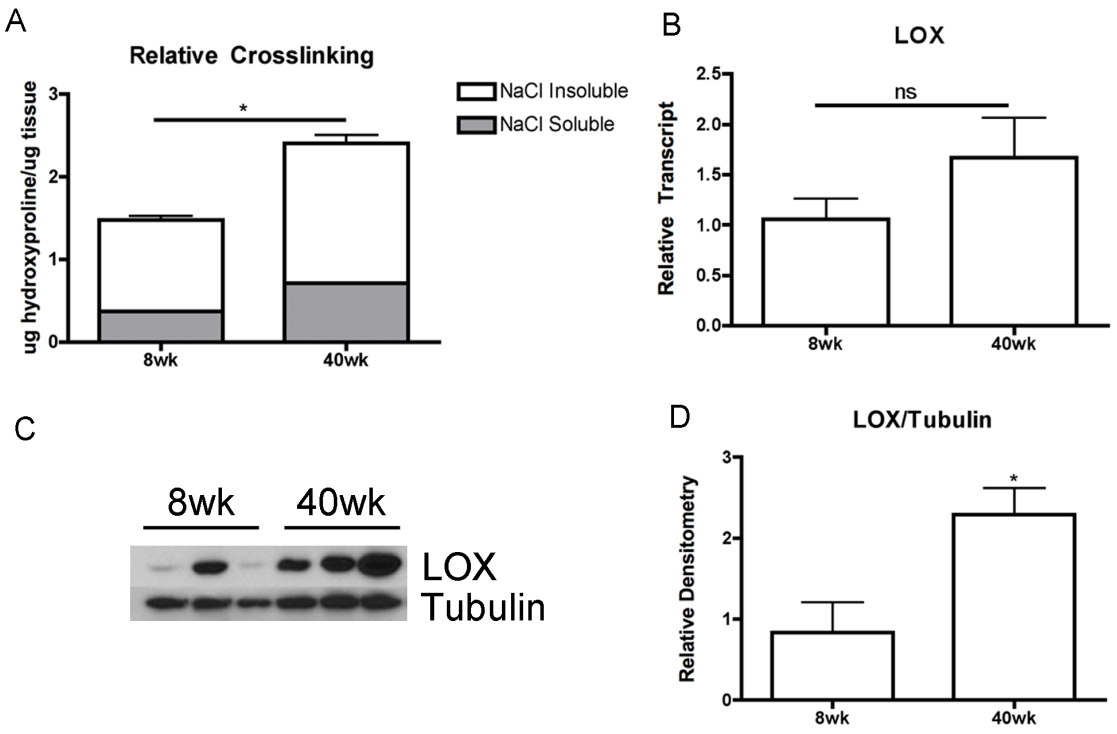

Figure 4.2 Collagen Crosslinking

The amount of collagen cross-linking was determined by assessing hydroxyproline levels in NaCl soluble (non-crosslinked) and insoluble (crosslinked) fractions of whole myocardium (A). Expression of LOX (B) mRNA in whole myocardium was assessed using qPCR and compared to the housekeeping gene 18S, relative to the 8wk group. LOX protein levels were assessed by immunoblotting (C) and semi-quantified using densitometry (D). n=3; *$p<0.05$.

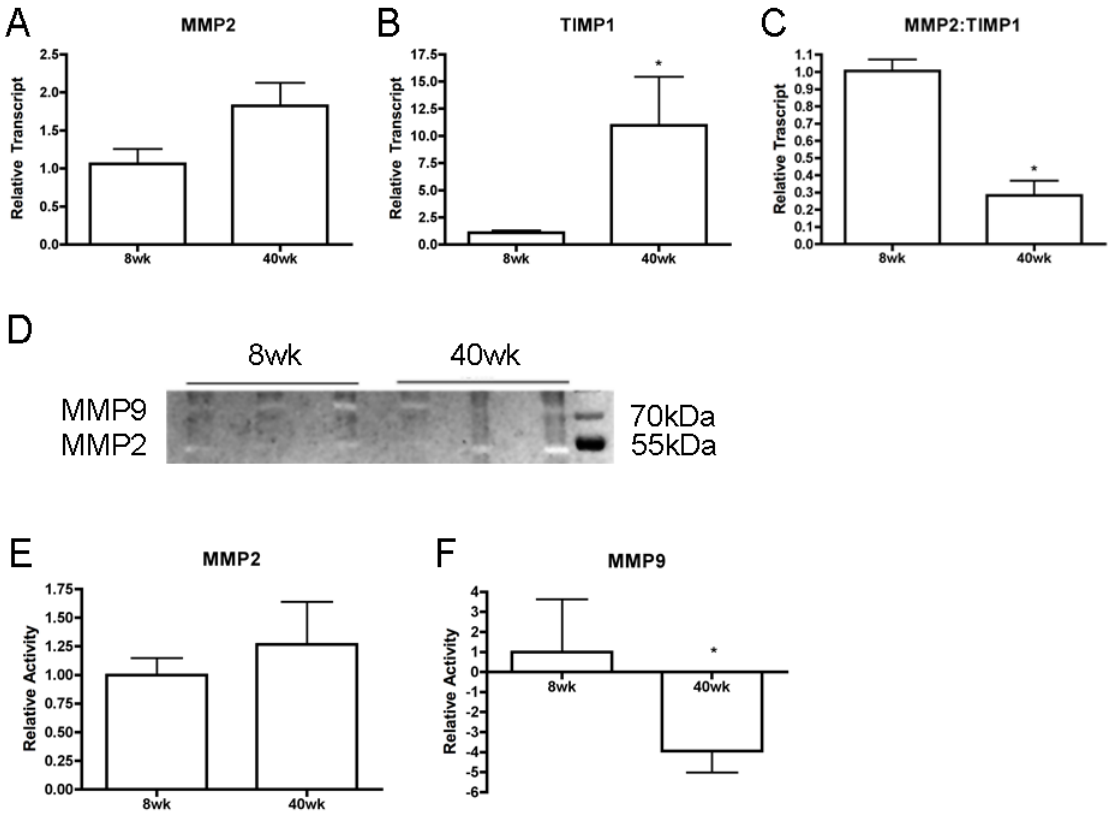

Figure 4.3 MMP Activity

The mRNA expression of MMP2 (A) and TIMP1 (B) were assessed by qPCR and the ratio of MMP2:TIMP1 expression is reported (C). Enzymatic activity of MMP2 and MMP9 was assessed using gelatin zymography. A representative gel is shown (D) and MMP2 (E) and MMP9 (F) activity were semi-quantified using densitometry. n=6; *$p<0.05$.

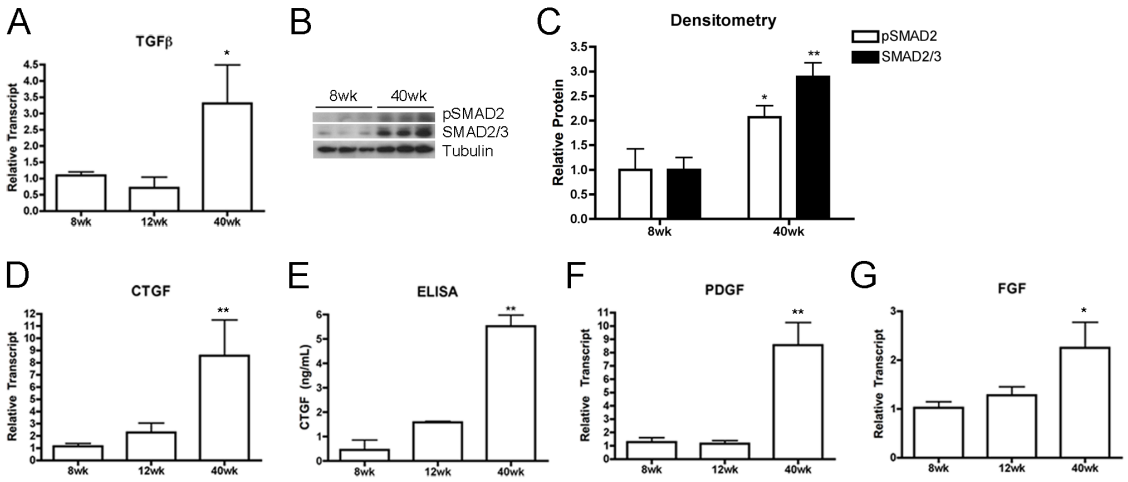

Figure 4.4 Fibrotic Growth Factors And Aging

TGFβ mRNA expression was assessed using qPCR and compared to 18S housekeeping gene, relative to the 8wk group (A). Downstream signaling of TGFβ was determined by assessing SMAD2 phosphorylation with immunoblotting. A representative blot with tubulin as a loading control showing SMAD2/3 and phosphoSMAD2 levels is shown (B), which were semi-quantified using densitometry (C). CTGF mRNA expression was assessed using qPCR (D). CTGF protein levels were assessed in the serum using ELISA (E) (n=3). PDGF (F) and FGF (G) mRNA expression were determined using qPCR. n=6 unless otherwise noted; *p<0.05, **p<0.01.

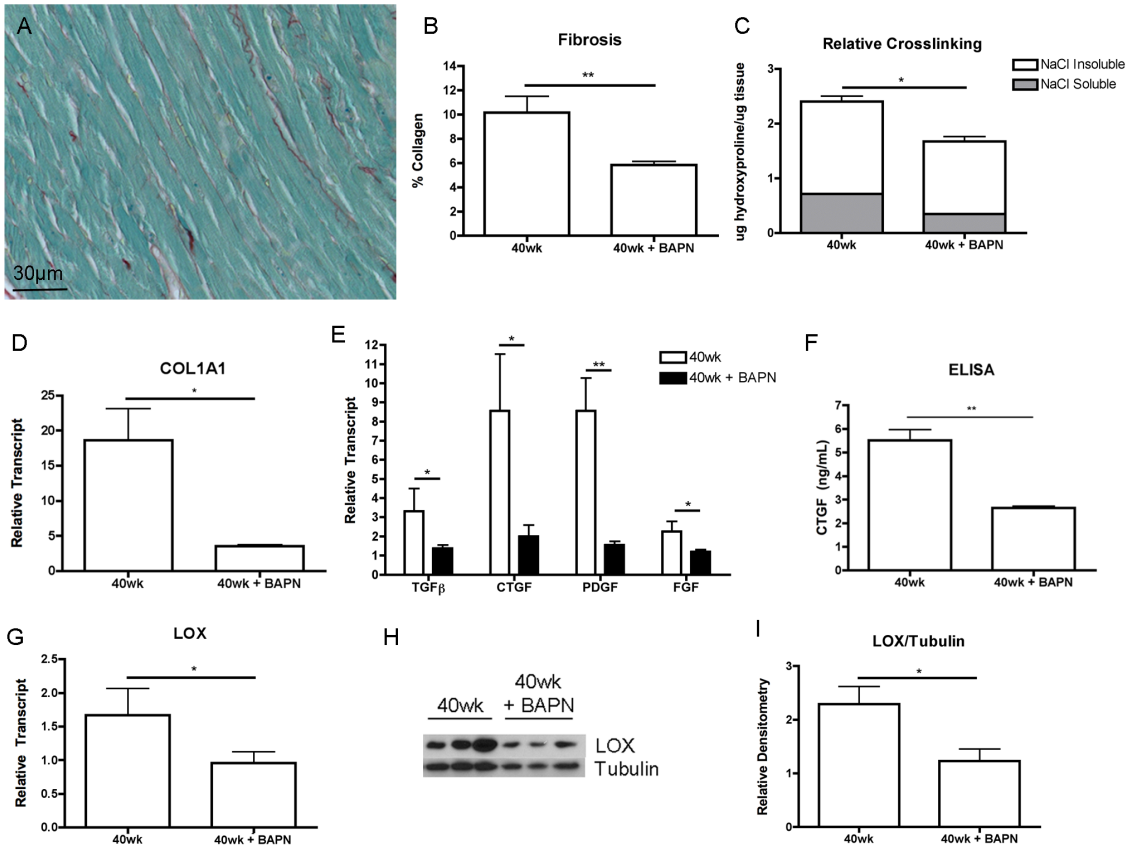

Figure 4.5 LOX Inhibition And Collagen Processing

LOX inhibitor BAPN was administered by micro-osmotic mini-pump for 2wk prior to sacrificing animals at 40wk. Fibrosis was assessed in the myocardium using Sirius red staining of formalin fixed, paraffin embedded cross-sections. A representative image of 40wk myocardium after BAPN exposure is shown at 25x (A). The percentage of whole cross-section of myocardium stained with Sirius red was semi-quantified using image analysis software (B). The amount of collagen cross-linking was determined by assessing hydroxyproline levels in NaCl soluble and insoluble fractions of whole myocardium sections (C). The mRNA expression COL1A1 (D), TGFβ, CTGF, PDGF and FGF (E) were assessed by qPCR and compared to housekeeping gene 18S and are reported relative to the 8wk group. CTGF protein concentration in serum was quantified using

ELISA (F). LOX mRNA expression was assessed using qPCR and compared to 18S and is reported relative to the 8wk group (G). LOX protein levels were assessed by immunoblotting (H) and semi-quantified using densitometry (I). n=6; *$p<0.05$, **$p<0.01$.

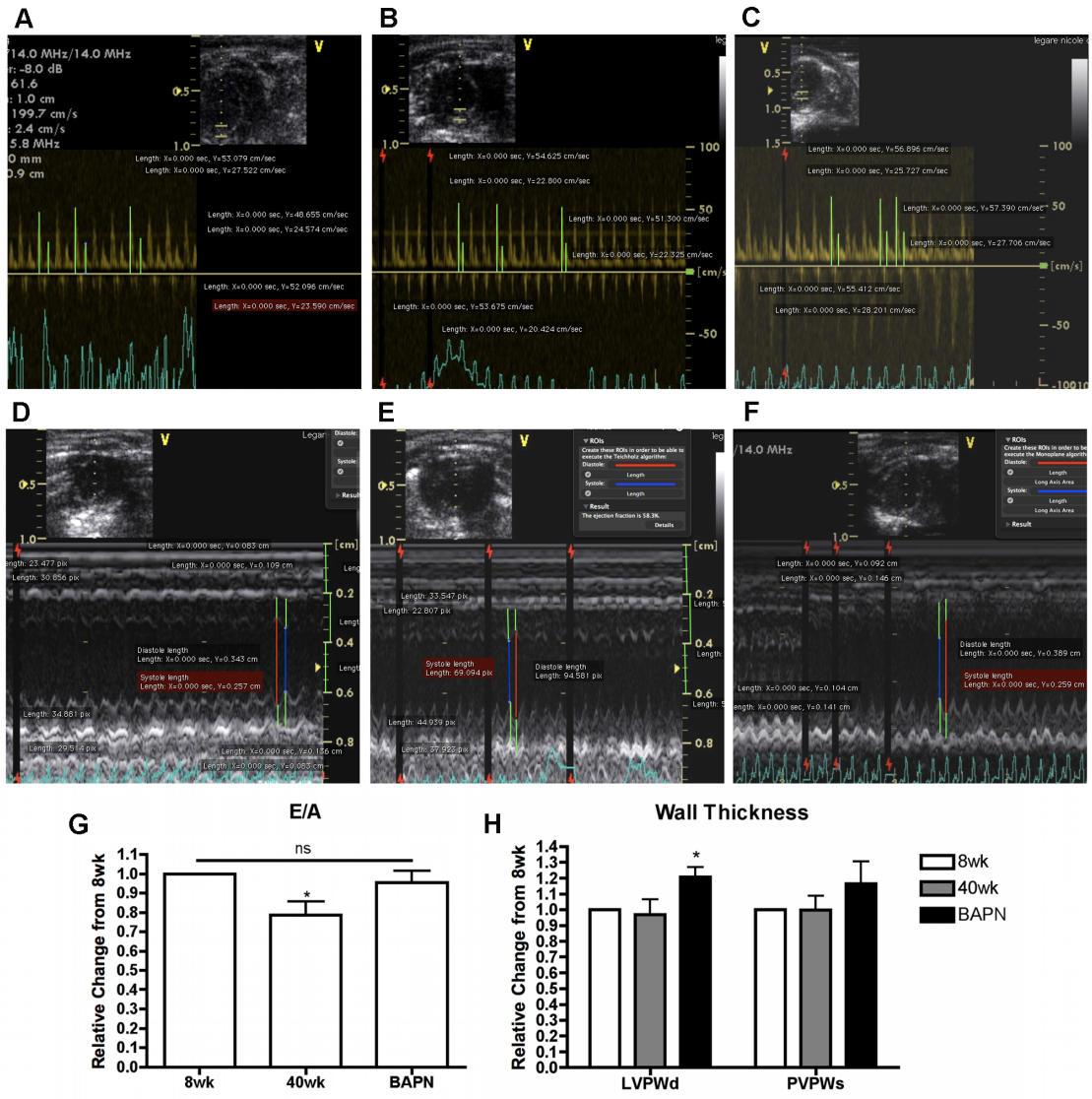

Figure 4.6 Functional Effects Of LOX Inhibition

Representative images are shown for tissue Doppler (A, B, C) and 2-dimensional m-mode (D, E, F) echocardiography that were used to assess cardiac function in 8wk (A, D), 40wk(B, E) and 40wk+BAPN (C, F) animals. Doppler measurements included the early and late mitral inflow velocities (E and A) and the relative change in E/A ratio from 8wk was calculated (G). Relative change in wall thickness from 8wk was calculated (H). n=5; *p<0.05.

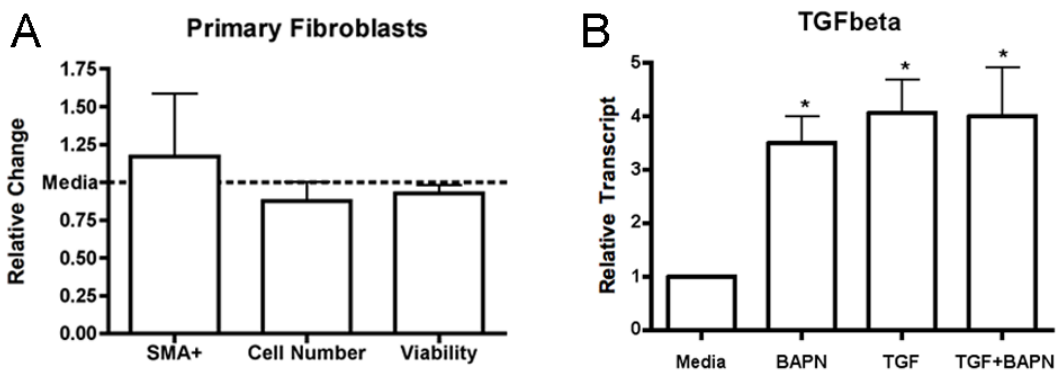

Figure 4.7 *In Vitro* Effects Of LOX Inhibition

Cardiac fibroblasts were isolated from 40wk mice and treated with either: 1 – media, 2 – BAPN (200μM), 3 - TGFβ (10ng/mL) or 4 - TGFβ+BAPN. Immunofluoresence was used to stain for SMA with the nuclear dye Hoescht used to indicate the nuclei after 24hr. The relative percentage of SMA+ cells was calculated and the average from 5 fields of view taken (A). The total number of cells was determined at 24hr by counting nuclei and is reported as an average of 5 fields of view for each replicate (A). Following 48hr treatments the cell-titer blue assay was used to assess the viability of cells relative to the media only control (2% BSA in DMEM) (A). The mRNA expression of TGFβ (B) was assessed by qPCR with 18S used as the housekeeping gene and expression reported relative to the media only control group (2% BSA in DMEM). n=3; *$p<0.05$.

4.3 Discussion

Normal aging has been associated with important changes in the myocardium, most notably the development of age-related myocardial fibrosis. The majority of previous studies of age-related myocardial fibrosis have described changes between 8-12wk and 56-64wk[91, 143]. In the present study we have demonstrated a significant increase in interstitial and perivascular collagen as early as 40wk of age in mice. The age of our mice is equivalent to an age of about 40yr in humans, suggesting that age-related changes seen in the myocardium begin early in the development of age-related myocardial fibrosis[144]. In addition, very few studies have thus far focused on changes that occur solely as a result of aging, but attempt to compare differences between fibrosis models (transgenic expression of AngII in cardiomyocytes[145], senescence accelerated mice[4], ischemia reperfusion[39]) or comparing anti-hypertensive regimes in the setting of advanced age[146]. While important information about responsiveness at different ages is learned from these studies, key gaps remain in our knowledge of baseline alterations in fibrotic signaling within the myocardium during aging; specifically how this contributes to the development of myocardial fibrosis.

The progressive nature of the reduction in diastolic functional during aging is well established, as both tissue Doppler and transmitral flow measurements indicate[142, 147]. The functional effects of increased collagen were evident within the early time frame used in the present manuscript, in accordance with a known correlation between increasing collagen content in the myocardium and decreased function at advanced ages[8, 9]. The present study is therefore intended to focus on the underlying mechanisms

of collagen homeostasis and their contribution to the increase in myocardial fibrosis seen in aging.

The growth factor TGFβ is a well-described pleiotropic protein with one of its roles promoting fibrosis, through increasing fibroblast proliferation and production of ECM proteins, including collagen[12]. TGFβ has previously been reported to increase in the myocardium during aging, however why this occurs remains poorly understood[40, 148]. We confirmed that there was an increase in TGFβ signaling in the myocardium as early as 40wk. In addition to TGFβ we also report for the first time that there is age-related increase in the production of its downstream mediator CTGF. This increased TGFβ signaling occurred concurrently with a significant increase in myocardial collagen accumulation, suggesting that the increase in TGFβ is contributing to the increased deposition of ECM proteins during aging. This is further supported by the observed increase in the number of myofibroblasts, which are believed to be the major effector cell type responsible for ECM production and an important source of pro-fibrotic cytokines. However, despite providing further evidence that increased TGFβ signaling is likely involved in age-related fibrosis we have not elucidated the exact mechanism behind why this occurs.

Our findings also suggest that the increase in collagen was partially due to an increase in crosslinked collagen. This increase in crosslinking did not appear to be due to an increase in mRNA for LOX, the primary enzyme responsible for crosslinking. However, others have reported increases in active LOX protein during aging[56], although this was not observed in our model. Collagen crosslinking in turn is understood to have a significant impact on turnover by inhibiting collagen breakdown[149]. Our

findings suggest that aging was not associated with more LOX but instead significant changes in key MMPs (MMP 2 and 9) and TIMPs (TIMP 1) that favor less degradation and an increase in ECM accumulation, the hallmark of fibrosis.

Given the apparent importance in collagen crosslinking in age-related fibrosis we sought to alter this process by inhibiting LOX. BAPN functions by covalently and irreversibly binding to LOX, thereby inhibiting its function[150]. The result of this inhibition is a reduction in collagen crosslinking, reducing the stability of newly deposited collagen, which ultimately results in more collagen breakdown and the release of breakdown products into the extracellular environment. Administering BAPN at a constant rate using an osmotic pump significantly decreased the amount of collagen within the myocardium after only 2wk.

Previous studies have used the administration of BAPN in combination with either aortic banding or AngII exposure as a model of aortic aneurism; increased pressure in combination with reduced structural integrity of the elastic lamina result in failure of the vessel wall[120, 151]. Similarly, due to the copper dependency of LOX its activity can be inhibited with copper chelation or a copper-deficient diet. Either of these methods when used chronically result in severe adverse effects, including vessel and ventricle rupture due to lack of structural collagen and elastin[152]. However, in the present study there were no adverse effects observed, as the ventricular diameter did not increase and wall thicknesses did not decrease during BAPN exposure, possibly due to the short duration of BAPN administration in our model.

The in-vitro experiment yielded surprising results, with LOX inhibition resulting in increased TGFβ expression. This is counter to the *in vivo* observations, suggesting a

more complex mechanism, or the involvement of a different cell type *in vivo*. Our *in vitro* data did support that LOX directly inhibits TGFβ activity, as previously reported[153]. At the same time, TGFβ can increase LOX expression and activity[154] acting as a feedback mechanism to regulate TGFβ expression and crosslinking of TGFβ-induced, newly synthesized collagen. Furthermore, LOX has been reported to regulate the activity of other fibrotic factors, such as through oxidizing the PDGF receptor (PDGFR-B), resulting in increased PDGFR-B activity[141]. These mechanisms were beyond the scope of the current study, but remain an area of interest.

We provide novel evidence that modulating collagen homeostasis could hold potential as a future therapeutic route to reducing the burden of myocardial fibrosis in heart failure by demonstrating that the process can be reversed. This is the first time to our knowledge that LOX inhibition has been reported to also result in the significant down-regulation of pro-fibrotic factors. This would suggest that LOX inhibition and therefore LOX have systemic effects on the regulation of collagen, beyond direct involvement in collagen crosslinking. This regulation of fibrotic factors occurred both in whole myocardium (decreased fibrotic factor expression) and in isolated fibroblasts (increased fibrotic factor expression). The mechanism explaining our observation remains unclear, but suggests that collagen or the products of its breakdown could be key in regulating collagen homeostasis through unidentified signaling or feedback mechanisms.

CHAPTER 5: BLOOD PRESSURE DEPENDANCE OF ANGIOTENSINII INDUCED MYOCARDIAL FIBROSIS

This work appears in part in the publication:

Rosin N.L., Sopel M, Falkenham A., Myers T.L., Légaré J.F. Myocardial migration by fibroblast progenitor cells is blood pressure dependent in a model of AngII myocardial fibrosis. *Hypertension Research*. 2012 Apr;35(4):449-56. Doi:10.1038/hr.2011.217. Epub 2012 Jan 19.

Contribution:

NR – contributed to study design, carried out experimentation, collected and analyzed data, and prepared the manuscript

MS, AF – contributed to study design and carried out experimentation

TM – collected data and assisted with analysis

JFL – assisted in manuscript preparation

5.1 Introduction

There is growing evidence that the RAAS, specifically AngII, is implicated in the development of myocardial fibrosis, a common pathological feature of many cardiovascular conditions [20, 33, 155, 156]. RAAS activation and increased levels of AngII can be seen in patients with cardiovascular diseases, including atherosclerosis, hypertension, cardiac hypertrophy and heart failure [20, 157, 158]. Conversely, inhibition of RAAS activation by ARBs has been shown to significantly improve patient survival and limit the progression of cardiac remodeling and heart failure [159].

Investigations in small animals have confirmed that AngII exposure can result in myocardial fibrosis [29-32, 160-163]. Such experiments have supported a direct relationship between RAAS activation via AngII and fibrosis. Animal models of fibrosis using AngII have proven very helpful in understanding some of the molecular events leading to the development of fibrosis. However, AngII is also a potent vasoconstrictor capable of causing significant hypertension, making it difficult to dissociate the effects of hypertension versus AngII on the myocardium. In fact, whether hypertension or RAAS activation is the mechanism responsible for remodeling has been a longstanding debate [72, 161].

Using a mouse model of AngII infusion, our laboratory has been able to characterize the early molecular and cellular events occurring in the myocardium within 1 week of exposure to AngII. We have shown that animals exposed to AngII develop hypertension and early infiltration (1d) by fibroblast progenitor cells called fibrocytes [37]. We and others have also provided evidence that strategies to limit the migration of fibrocytes inhibit the development of fibrosis, supporting an effector role for these cells.

In this manuscript, we have utilized our experience with the AngII infusion model to better characterize early events in the development of fibrosis. Specifically, we evaluated the effects of RAAS activation in the absence of hypertension using the antihypertensive drug hydralazine, which acts on smooth muscle cells as a vasodilator independent of the RAAS system.

5.2 Results

5.2.1 Model Establishment

At 8wk of age animals were randomly assigned to one of three experimental groups and infused with one of the following: a) AngII (2.0 µg/kg/min, n=10); b) AngII with hydralazine (6.9 mg/kg/min; n=4); or c) saline (control, n=10). Infusion of AngII, a known vasoconstrictor, resulted in a significant increase in mean arterial blood pressure compared to the saline control (Figure 4.1). Coadministration of AngII with hydralazine allowed normalization of the blood pressure to levels similar to those of the saline control animals (Figure 4.1A). Furthermore, hydralazine also inhibited the myocardial hypertrophic effects of AngII, as the AngII+hydralazine animals had a significantly lower heart weight/body weight ratio (Figure 4.1B), which was comparable to that of the saline controls (AngII, 6.7±0.3mg/g; AngII+hydralazine, 5.7±0.2mg/g; saline, 5.2±0.2mg/g). Serum levels of aldosterone were evaluated using a standard ELISA and showed that AngII and AngII+hydralazine animals had elevated serum aldosterone levels compared to the saline controls, although significance was not reached (Figure 4.1C). Taken together, our findings suggest that the hypertensive effects of AngII can be controlled with the antihypertensive agent hydralazine while maintaining RAAS activation, thus creating a

model with which to examine the early cellular and molecular events occurring in these animals.

5.2.2 Myocardial Fibrosis

The degree of myocardial fibrosis in experimental animals was determined by quantifying the collagen depositions within the myocardium using heart sections stained with Sirius red, as previously described [37]. AngII infusion resulted in multifocal areas of extensive collagen deposition compared to saline-infused control animals ($p<0.01$; Figure 4.2A, B). When hydralazine was also infused, there was a significant reduction in collagen deposition evident within the myocardium, which approached levels seen in the saline controls, expressed as the percentage surface of an area of myocardium affected ($p<0.01$; Figure 4.2C, D). These findings were confirmed by evidence of significant collagen-1 transcript up-regulation in AngII animals (103.0 ± 36.2fold), with levels returning to baseline when hydralazine was co-administered ($p<0.01$; Figure 4.2E).

5.2.3 Cellular Infiltration

Previous work from our laboratory has shown that myocardial fibrosis is temporally preceded by the infiltration of fibroblast progenitor cells into the myocardium [37]. In the present experiment, AngII exposure resulted in multi-focal areas of cellular infiltration and myocyte loss compared to saline controls (Figure 4.3A, B). When the animals were given AngII in combination with hydralazine, minimal cellular infiltration was identified after 7d of exposure (Figure 4.3C). We have adapted a grid-scoring method to quantify the degree of cellular infiltration between groups, confirming that significant myocardial cellular infiltration was evident in AngII-exposed animals and was inhibited by hydralazine ($p<0.01$; Figure 4.3D). The cells that were observed to infiltrate

the myocardium were mononuclear in appearance, with no evident polymorphonuclear cells. Immunohistochemistry was used to confirm that a significant proportion of the cells observed in AngII-exposed animals were $SMA^+/CD133^+$ fibrocytes, as previously reported (Figure 4.4) [37]. In contrast, animals that received both AngII and hydralazine had minimal infiltration by $SMA^+/CD133^+$ cells. Taken together, our findings confirm that myocardial fibrosis is dependent upon the accumulation of $SMA^+/CD133^+$ fibrocytes prior to ECM deposition and that this process is blood pressure dependent, given that hydralazine can inhibit this response.

5.2.4 Myocardial Pro-Fibrotic Cytokine Environment

Transcript levels of a well-known profibrotic factor, CTGF, were significantly increased in the myocardium at 7d (7.8±0.8fold) after AngII exposure ($p=0.008$; Figure 4.5). The co-administration of AngII with hydralazine resulted in a significant reduction in CTGF back to baseline levels seen in the saline control animals (Figure 4.5). Similar findings were observed for the proinflammatory cytokines TNFa (4.6±0.8fold) and IL1b (6.4±2.6fold) in animals receiving AngII, with a return to baseline in the animals co-administered AngII+hydralazine ($p<0.05$; Figure 4.5).

5.2.5 Myocardial Chemokine Expression Associated With Fibrocyte Migration

To investigate which factors in the myocardial microenvironment may be recruiting the infiltrating cells, we used relative qRT-PCR to assess the transcript levels of the cytokines that are chemotactic for fibroblast progenitor cells, CXCL12 and CCL2 [95, 164]. There was a significant increase in CXCL12 mRNA (3.2±0.4fold; $p=0.008$) expression in the myocardium of animals exposed to AngII at 7 d compared to the baseline expression of the normalized housekeeping gene (Figure 4.6). Similarly, there

was a significant increase in CCL2 mRNA expression in the myocardium of AngII-exposed animals (3.8±1.0fold; p=0.015). The addition of hydralazine resulted in complete inhibition of the upregulation of CXCL12 and CCL2 in the myocardium, resulting in levels similar to those seen in the control animals (Figure 4.6).

5.2.6 Effects Of Hydralazine At The Cellular Level

The effects of hydralazine, other than those resulting from vasodilation and blood pressure reduction, were also investigated. We first looked at the induction of the transcription factor hypoxia-inducible factor 1 (Hif1α), which has been suggested as a downstream effector of hydralazine. The transcript levels, measured by qPCR, were significantly increased after 7d of AngII exposure (5.0±0.8fold; p=0.016); however, when hydralazine was administered in combination with AngII, the levels of Hif1α were not elevated but were similar to baseline levels seen in the control animals (Figure 4.7).

Our previous work has shown that in areas of myocardial infiltration by fibrocytes, a significant number of these cells are proliferating [37]. We therefore investigated the effects of hydralazine on proliferation both *in vivo* and *in vitro*. As previously described, the infiltrating $SMA^{+}/CD133^{+}$ cells were shown to have a high proliferative index, as demonstrated by strong positivity for Ki67 after AngII exposure. In contrast, animals that received both AngII and hydralazine had a significant reduction in the positivity for Ki67, suggesting that hydralazine may affect the proliferation of fibrocytes (Figure 4.8). To confirm these findings we used an *in vitro* assay with primary fibroblasts, assessing the relative proliferation of primary fibroblast cultures as determined by BrdU incorporation. Our *in vitro* findings suggested that the proliferation of fibroblasts after hydralazine exposure, in the presence or absence of AngII, was

significantly reduced by 30.6% from the level of the saline controls (Figure 4.8). Similar findings were obtained with an MTT assay (results not shown). Taken together, these results indicate that hydralazine may have some effect at the cellular level that could modulate the development of fibrosis, independently of blood pressure reduction.

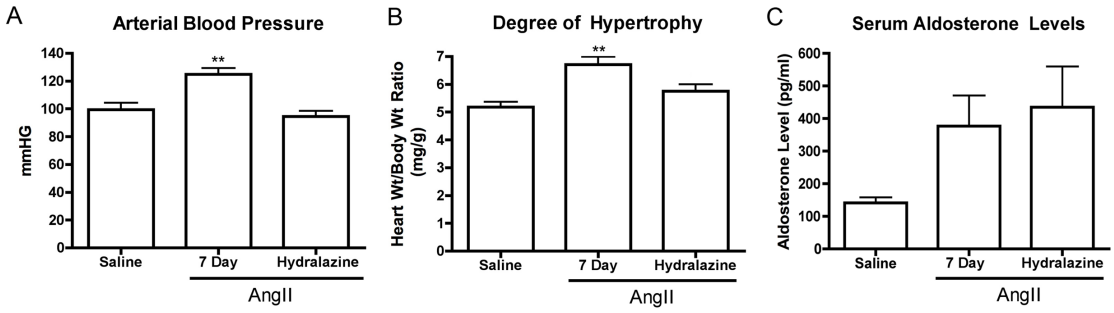

Figure 5.1 Establishing The Model

Hemodynamic measurements were taken via a tail cuff blood pressure system (at 7d) and compared between groups (AngII 2.0µg/kg/min; hydralazine 6.9µg/kg/min) Systolic blood pressure measurements are shown as mean±SEM (A). The cardiac mass index was expressed as heart weight/body weight ratio at 7d (B). Serum levels of aldosterone at 7d were measured by ELISA and expressed as pg/ml (C). **$p<0.01$.

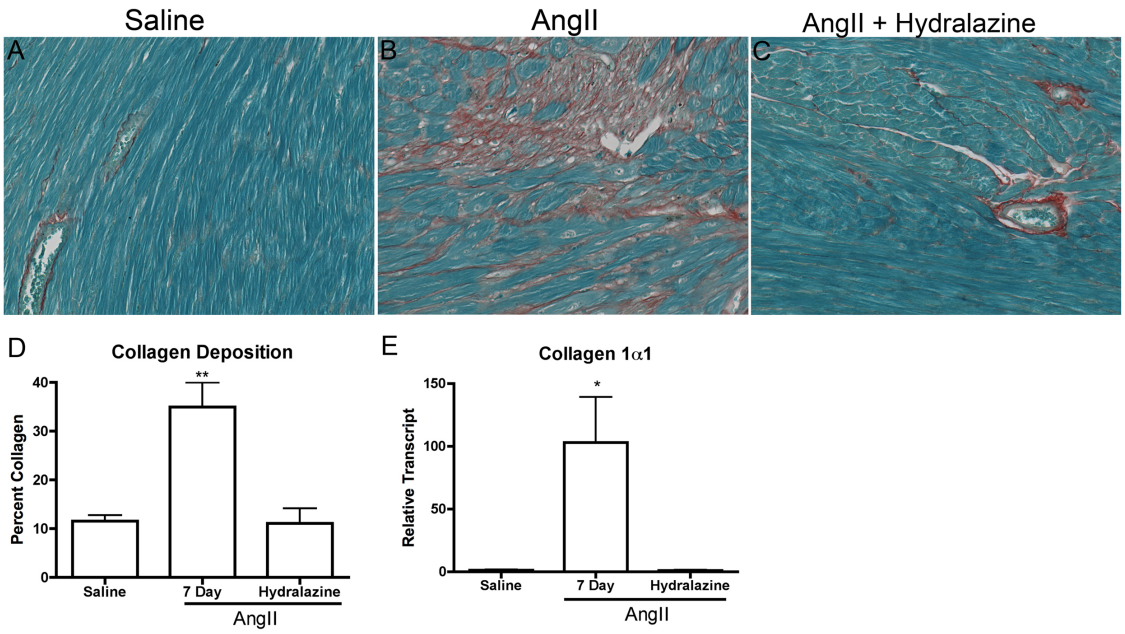

Figure 5.2 Myocardial Fibrosis

The collagen deposition in heart sections from the experimental groups was assessed using a standardized Sirius red and fast green stain. Representative sections are shown from control animals (A), 7d AngII-exposed animals (B) and 7d AngII+hydralazine exposed animals (C). Collagen in the heart sections was quantified using image analysis software and expressed as the percentage area affected (D). Collagen deposition was also quantified using whole heart extracts and processed for qPCR for pro-Collagen-1 (E). Images were captured at 25X. **$p<0.01$, *$p<0.05$.

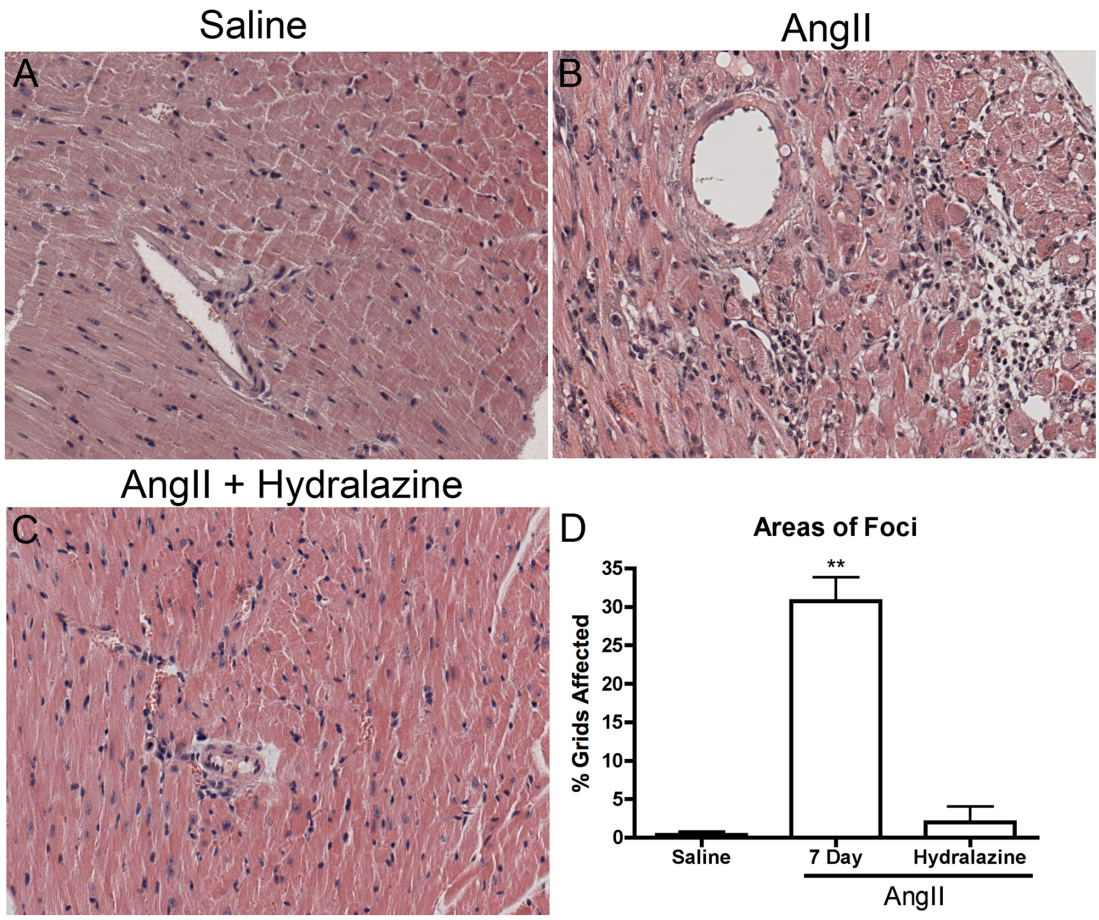

Figure 5.3 Cellular Infiltration

The hearts from animals receiving the saline control (A), AngII for 7d (B) or AngII+hydralazine for 7d (C) were stained with H&E. The quantification of infiltrating cells was performed using a modified grid-analysis technique, comparing the number of grids affected from a representative cross section of the myocardium (heart) taken at low power (5x magnification) from each group (D). Images were captured at 25X. **$p<0.01$.

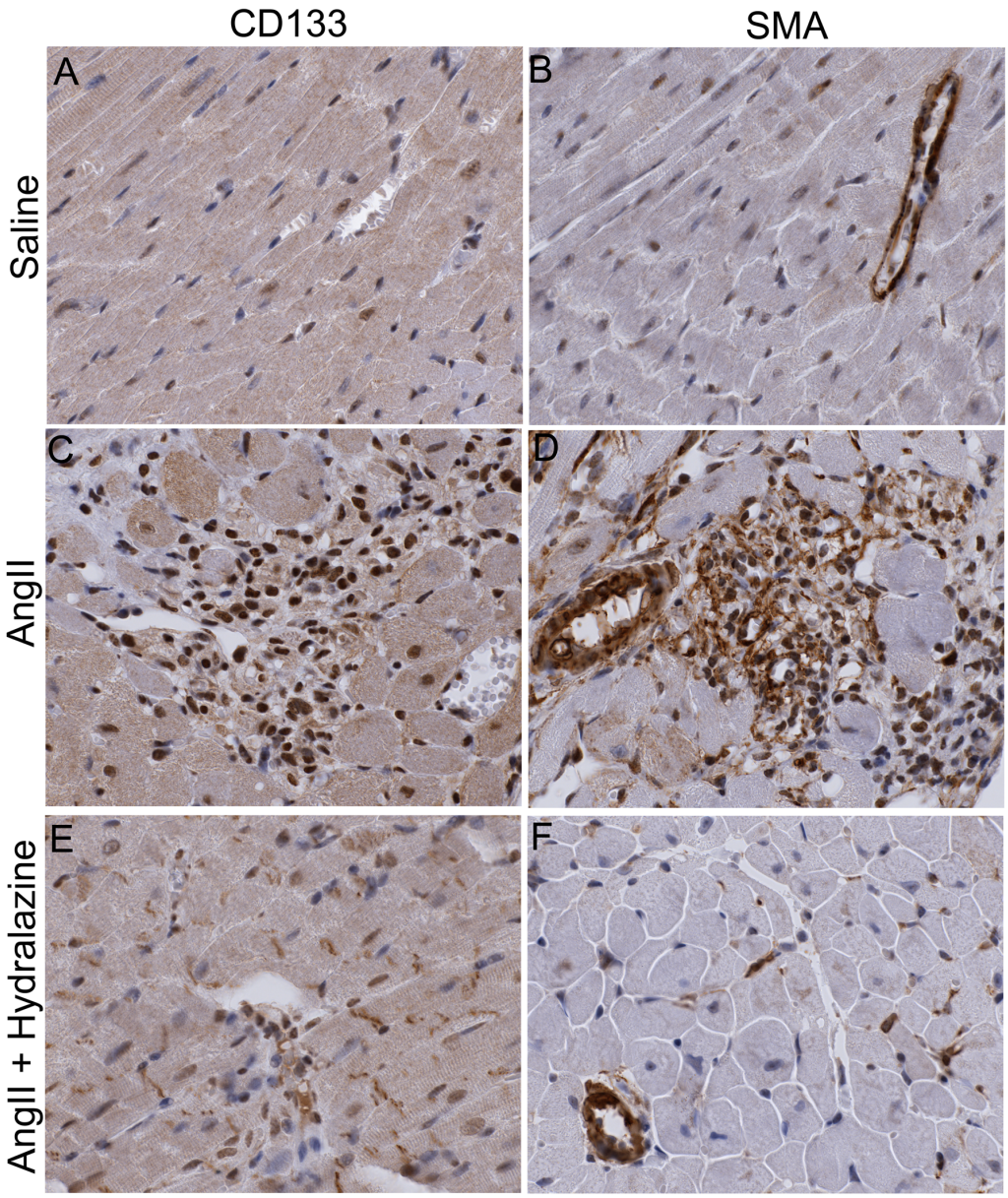

Figure 5.4 Immunohistochemical Staining

Immunohistochemistry for CD133 (A, C, E) and SMA (B, D, F) was used to identify positive cellular infiltrate in heart sections. Representative sections from animals receiving the saline control (A, B), AngII for 7d (C, D) or AngII+hydralazine for 7d (E, F) are shown. Images were captured at 63X.

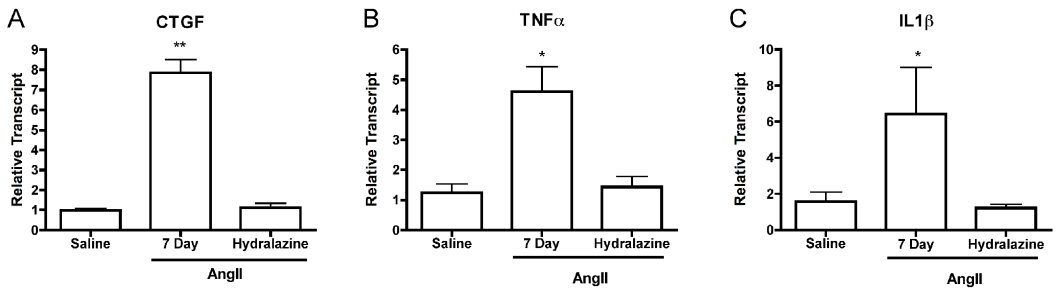

Figure 5.5 Pro-Fibrotic Microenvironment

qPCR was used to assess the myocardial expression of CTGF (A), TNFα (B) and IL-1β (C) transcripts relative to the housekeeping gene. **$p<0.01$, *$p<0.05$.

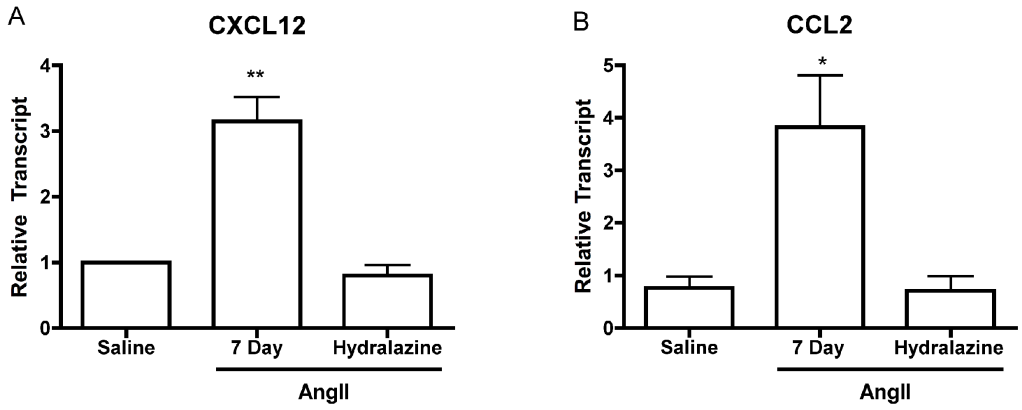

Figure 5.6 Chemokine Expression

qPCR was used to assess myocardial expression of CXCL12 (A) and CCL2 (B) transcript levels relative to the housekeeping gene (E). **p<0.01, *p<0.05.

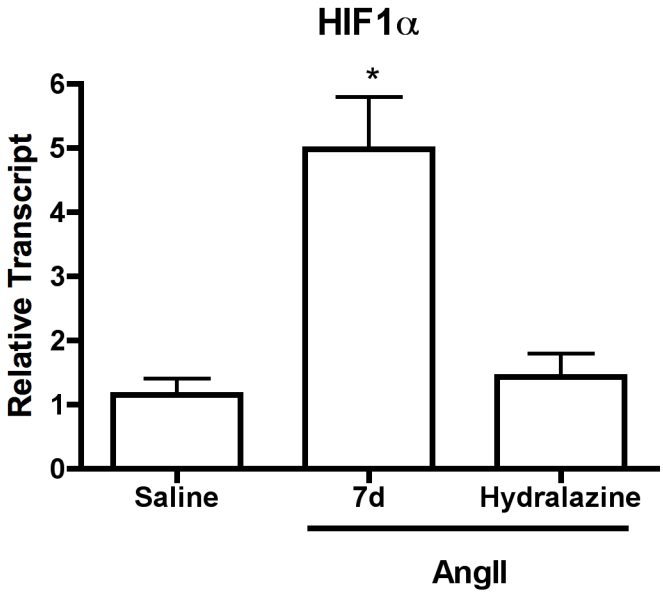

Figure 5.7 Transcription Factor Expression

qPCR was used to assess the myocardial Hif1α transcript expression relative to the housekeeping gene. *p<0.05.

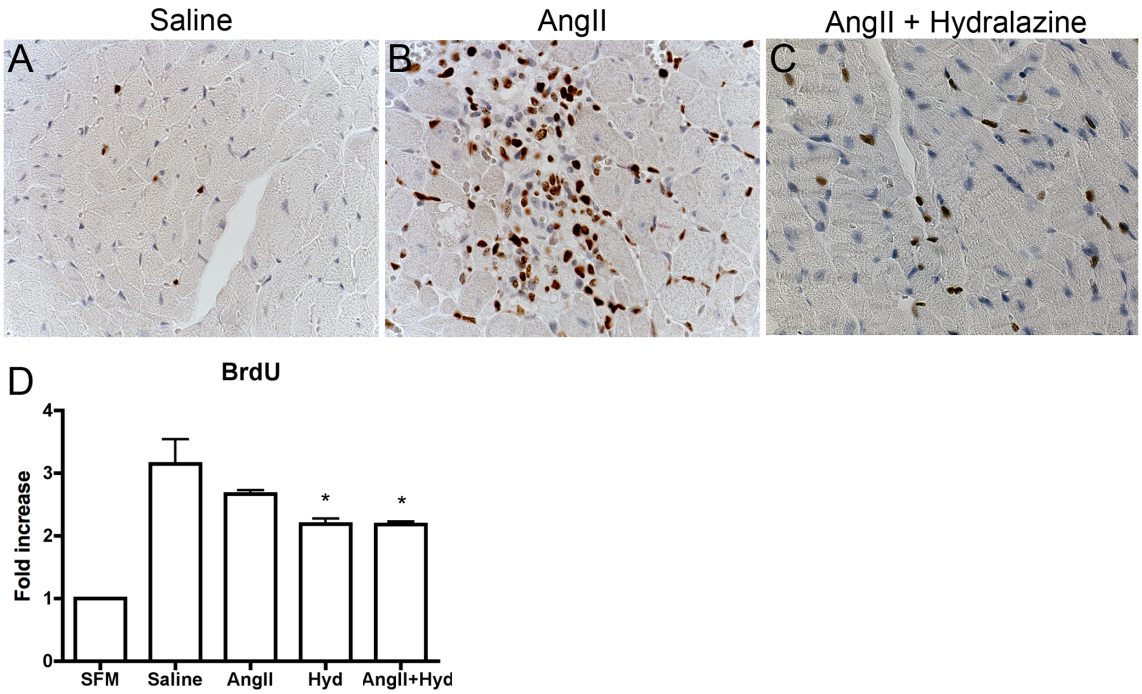

Figure 5.8 Cellular Effects Of Hydralazine

Immunohistochemistry for Ki67 was used to illustrate the proliferative index of infiltrating fibrocytes. Representative sections from animals receiving saline (A), AngII (B) or AngII+Hydralazine (C) are shown. Images were captured at 63x. The BrdU assay for proliferation was used on primarily isolated fibroblasts after exposure to saline, AngII (100nM), hydralazine (40nM) or AngII+Hydyralazine (D). Relative proliferation was expressed as the fold increase compared to serum-free media (SFM). *$p<0.05$.

5.3 Discussion

AngII infusion models have been well described and are known to result in increased blood pressure, myocardial hypertrophy and a characteristic ECM deposition within the myocardium that is typical of myocardial fibrosis [164-166]. In the mouse model used here, the physiological response to AngII resulted in blood pressure elevation and the early development of myocardial hypertrophy within 7d of exposure. Using this model, we attempted to create a situation in which RAAS up-regulation via AngII infusion was maintained without the resultant hypertensive response. We achieved this by co-administration of hydralazine.

Hydralazine was chosen based on its antihypertensive properties of lowering blood pressure in a dose-dependent manner without acting on AngII receptors [167, 168]. RAAS up-regulation was demonstrated in the animals that received AngII+hydralazine, as evidenced by an elevation in serum aldosterone, which is a downstream mediator and marker of RAAS activation. Our primary observation using this model was that the addition of hydralazine to AngII resulted in normalization of the blood pressure and inhibition of the fibrosis that is normally seen in animals receiving AngII. Taken together, these results indicate that AngII and its effects on promoting myocardial fibrosis appear, at least in part, to be blood pressure dependent.

Studies from our laboratory and other research groups have recently identified bone-marrow-derived fibroblast progenitor cells as the primary cells recruited to the myocardium prior to the development of fibrosis [37, 169]. We were able to show minimal infiltration by $SMA^{+}/CD133^{+}$ fibrocytes in animals receiving AngII+hydralazine

compared to animals receiving AngII. These findings support a direct relationship between cell migration and the development of fibrosis.

Fully characterizing the mechanism by which AngII results in myocardial fibrosis is beyond the scope of this manuscript. However, using our model, in which RAAS up-regulation was maintained without hypertension, we explored key pathways previously described as potentially being involved in promoting fibrogenesis. We chose to assess CTGF as a profibrotic cytokine based on evidence that it is produced by cardiomyocytes, providing a mechanism by which AngII acts directly on the myocardium and promotes a profibrotic environment. AngII has been shown to increase CTGF expression within the myocardium and specifically in cardiomyocytes *in vitro* [170, 171]. CTGF also appears to be capable of inducing both profibrotic and proinflammatory gene expression in cultured cardiomyocytes [115]. In fact, CTGF has been suggested to be the primary mediator of AngII-induced myocardial fibrosis [114]. Our findings suggest that CTGF, which was significantly up-regulated in AngII-exposed animals, was completely inhibited by the administration of hydralazine. Similar findings were observed with the classic proinflammatory cytokines TNFa and IL1b. Although we provide no direct evidence that hydralazine inhibits the production of these cytokines, we provide strong evidence of an association between early fibrocyte migration and profibrotic cytokine production in the myocardium.

Interactions between chemokines and their respective receptors have emerged as key mechanisms in the directed migration of leukocytes and fibrocytes [172-176]. Fibrocytes have previously been shown to express the chemokine receptors CCR7 and CXCR4 [103, 177, 178]. Recently, Haudek et al. was able to show that CCR2 plays a

critical role in regulating fibrocyte migration in a model of myocardial fibrosis [169]. Using $CCR2^{-/-}$ animals, they were able to show a significant reduction in AngII-dependent fibroblast progenitor cell migration (fibrocytes) and a reduction in fibrosis. In the present manuscript, we did not attempt to modulate fibrocyte migration by blocking specific chemokines. However, our findings support previous studies by others that have suggested a key role for CXCL12 and CCL2 in regulating fibrocyte migration and accumulation.

It is generally assumed that fibroblasts and myofibroblasts are the cells responsible for ECM deposition. As such, there is a large body of literature that supports the direct effects of AngII, via the AT_1R, in promoting fibroblast proliferation, myofibroblast differentiation and fibrosis [29-32]. We provide evidence that the interaction of AngII with its receptor may be sufficient, but not necessary, for fibrosis. Our findings are in keeping with other studies that have suggested that the effects of AngII on fibrosis are blood pressure dependent [167, 168, 179]. Some reports have even suggested that blood pressure can affect the migration of fibrocytes ($CD45^+/SMA^+$) into the myocardium, but these reports did not elucidate a definitive mechanism [168]. In contrast, transgenic mice that overexpress AT_1R and develop hypertrophy and fibrosis do so without developing hypertension, emphasizing the multifactorial pathways capable of promoting ECM deposition and fibrosis [180]**.** However, these findings were based on transgenic mice that had abnormal RAAS regulation based on overexpression of only the AT_1R. Data from spontaneously hypertensive models suggest that hydralazine was unable to fully inhibit the development of fibrosis, but these findings can be explained by mechanisms independent of RAAS activation [181].

In contrast to our findings in the present manuscript, there are examples in the literature of cases in which a reduction in blood pressure to normotensive levels did not abrogate organ damage, suggesting that fibrosis may be blood pressure independent under certain circumstances [181, 182]. However, some of these studies had other important differences that should be taken into consideration, such as the presence of metabolic syndrome using genetically mutated mice, in which obesity, dietary supplementation, glucose intolerance and hyperinsulinemia likely contributed to end organ damage [181]. The same can be said for a model combining aldosterone administration, uninephrectomy and a high salt diet, in which increased load on the remaining kidney likely contributed to organ damage [182]. Furthermore, hydralazine has traditionally been administered in the drinking water, whereas in the current study, we used a more direct administration of hydralazine through an osmotic mini-pump, providing a constant dosage over time [182, 183]. Our approach may have resulted in a higher effective dose, as the drug was delivered more directly to the circulation.

Some experimental studies have shown a beneficial effect of mineralocorticoid antagonists in reducing myocardial fibrosis that was suggested to be independent of blood pressure effects. These results have been explained by reductions in myocardial oxidative stress, suggesting that oxidative stress may be the common pathway by which AngII activation and hypertension can lead to myocardial fibrosis [184, 185]. Although we did not specifically examine oxidative stress, our findings suggest that aldosterone up-regulation may not be sufficient for fibrosis, given the absence of fibrosis in AngII+hydralazine animals that had increased levels of aldosterone in their serum. Finally, the mechanisms should be considered by which hydralazine might reduce

fibrosis, other than its antihypertensive effect. One mechanism that was recently suggested is that hydralazine may induce Hif1α, which can in turn affect multiple genes as a transcription factor that mediates adaptive responses to injury, such as ischemia [186, 187]. Our findings support a significant up-regulation of Hif1α with AngII exposure but, when coadministered with hydralazine, Hif1α levels returned to baseline. From our data, it is not possible to conclude that hydralazine has any direct effect on Hif1α. We can conclude only that in animals without hypertension or myocardial histologic changes that are receiving AngII+hydralazine, there appears to be no significant upregulation in mRNA encoding Hif1α.

In the present manuscript, we attempted to separate RAAS activation from hypertension and thereby identify potential mechanisms for the development of myocardial fibrosis. This separation was necessary because the downstream effects of RAAS activation that lead to myocardial fibrosis are not fully characterized. Clinical trials published to date using RAAS blocking agents, such as ARBs and ACEi, have established a clear benefit for patients, with a significant reduction in the number of adverse cardiac events [159, 161]. This is in contrast to clinical studies that have used hydralazine and achieved similar reductions in blood pressure but failed to offer the same clinical benefit as RAAS inhibition [188-190]. In the present manuscript, we provide no explanation for this discrepancy. Taken together, these results suggest that blood pressure reduction may not be the sole factor influencing myocardial events such as fibrosis. The data obtained in the present study support the notion that although fibrosis appears to be partly dependent on blood pressure elevation, the anti-fibrotic properties of hydralazine may extend beyond its antihypertensive effects. We observed a reduction in fibrocyte and

fibroblast proliferation in response to hydralazine both *in vivo* and *in vitro*. Although discerning the cellular mechanism responsible for this anti-proliferative response is beyond the scope of this manuscript, our findings suggest that regulation of the anti-fibrotic properties of hydralazine, by mechanisms other than the vasodilator effects, should be considered.

In summary, we provide evidence that the effects of AngII on the development of myocardial fibrosis appear to be at least partly blood pressure dependent. We also provide evidence that blood pressure elevation seems necessary for early fibrocyte migration and for the development of a pro-fibrotic environment, although the mechanisms for this are unclear at present.

CHAPTER 6: THE ROLE AND REGULATION OF CTGF IN ANGII-INDUCED MYOCARDIAL FIBROSIS

This work appears in part in the publication:

Rosin N.L., Sopel M., Falkenham A., Lee T.D., Légaré J.F. The regulation and role of connective tissue growth factor in angII induced myocardial fibrosis. *American Journal of Pathology*. 2013 Mar; 183(3):714-26. Doi: 10.1016/j.ajpath.2012.11.014. Epub 2012 Dec 31.

Contribution:

NR – designed the study, carried out experimentation, collected and analyzed data, and prepared the manuscript

MS, AF – assisted with experimentation and data collection

TL, JFL – assisted with study design and critical review of the manuscript

6.1 Introduction

Myocardial fibrosis is a common pathological feature of many cardiovascular disorders characterized by an over-abundant deposition of ECM molecules in combination with a deficit in ECM degradation[2, 3]. The excess ECM protein results in loss of contractility and increased stiffness, ultimately leading to organ dysfunction and end-stage heart failure[2, 5]. Current understanding of the molecular mechanisms culminating in increased matrix deposition is incomplete, warranting further investigation into the pathways involved.

One molecule, AngII has been implicated in the development of fibrosis in the myocardium as well as in other fibrotic disorders[19, 71]. This hormone is a member of the RAAS and as such is involved in blood pressure regulation, however it has also been correlated with conditions that lead to organ fibrosis[74, 75]. The exogenous administration of AngII to rodents through a subcutaneous osmotic pump has become a well-established model resulting in myocardial fibrosis and functional deterioration[37, 86].

Recent evidence published by us, and others has demonstrated that AngII exposure leads to an influx in hematopoetic progenitor cells, termed fibrocytes, into the myocardium. This occurs before ECM deposition[37, 95, 96]. Fibrocytes possess both hematopoietic markers (CD34, CD45 and CD133) and mesenchymal markers (Collagen type I, fibronectin and vimentin)[97, 98]. Supporting evidence for the involvement of fibrocytes has been described in fibrotic disorders of the lung, kidney, liver and skin[99-102]. While there is increasing evidence confirming the importance of fibrocytes in fibrotic conditions, there remains a significant paucity of mechanistic information, such

as the tissue microenvironment with which these cells interact and the cytokine signaling that elicit their contribution to ECM production.

The current paradigm concerning pro-fibrotic signaling suggests that one of the first molecules involved in fibrosis development after AngII exposure is TGFβ[45, 107]. TGFβ has been suggested to interact directly with cardiomyocytes, which then produce other growth factors, such as CTGF[171]. In fact, recent studies have suggested that both the well-described TGFβ downstream regulation through the SMAD signaling pathway and a SMAD-independent TGFβ signaling pathway mediate the up-regulation of CTGF[191, 192]. Transgenic rodent models selectively overexpressing CTGF in fibroblasts result in increased systemic tissue fibrosis[193]. In addition, increased levels of CTGF have been correlated with the development of fibrotic pathologies, including dermal, renal, liver, pulmonary, and cardiac fibrosis[37, 194, 195]. Due to its strong link to fibrotic diseases, CTGF has also been suggested as a biomarker for fibrosis[94, 194]. Notwithstanding this evidence, a direct causal link between CTGF and fibrosis development after AngII exposure has yet to be established.

In the current study we have characterized the effects of AngII exposure *in vivo* on CTGF levels in the myocardium and its effects in relation to infiltrating fibrocytes. We have shown for the first time that CTGF is the first pro-fibrotic cytokine to be upregulated by resident cells in response to AngII exposure, through TGFβ dependent signaling. We also provide evidence that in response to CTGF, infiltrating fibrocytes are capable of contributing to the process of ECM deposition and thereby fibrosis development. We also show that this up-regulation is dependent on TGFβ signaling in the form of early SMAD2 phosphorylation.

6.2 Results

6.2.1 Bone-Marrow Derived Progenitors Are Mobilized From The Bone Marrow And Infiltrate Into The Myocardium After AngII Exposure

Previous work from our laboratory has demonstrated that AngII exposure results in significant multi-focal areas of cellular infiltration within the myocardium by 1d[37]. This cellular infiltration is then followed by significant collagen deposition in areas of infiltration over 3-7d of AngII exposure. GFP chimeric mice that constitutively express eGFP under control of the actin promoter in bone marrow derived cells were used initially to compare animals exposed to AngII or saline control. Chimeric mice exposed to AngII for 3d were found to have a significant proportion of infiltrating cells in the myocardium, identified in H&E stained sections, which were positive for GFP when compared to saline control (Figure 5.1A, B, E, F). Thus suggesting that bone marrow derived cells were the predominant cell type.

Immunofluorescence was used to show that infiltrating cells also expressed SMA that colocalized with GFP in AngII exposed animals, but co-labeled cells were absent from saline treated animals (Figure 5.1C, D, G, H). CD133 a marker of progenitor cells was observed to co-localize with GFP^+ cells using confocal microscopy (Figure 5.1I-K). Similarly, collagen type I expressed by mesenchymal cells such as myofibroblasts co-localized with GFP^+ cells as well as resident fibroblasts and ECM seen throughout the myocardium (Figure 5.1L-N). Taken together, these findings confirm our previous work suggesting that a significant proportion of myocardial infiltrating cells are fibrocytes known to express bone marrow (hematopoetic-GFP, CD133) and mesenchymal markers (SMA, Coll-1) [37, 196]. Flow cytometry was used to identify double positive fibrocytes

in the circulation. The percentage of CD45+/vimentin+ double positive cells, indicative of fibrocytes in PBMCs, was significantly higher in animals exposed to AngII when compared to saline control (Figure 5.2A, B). Taken together, AngII infusion resulted in early mobilization of fibrocytes from the bone marrow into the circulation and significant migration to the myocardium within 3d of exposure.

6.2.2 CTGF Is The First Pro-Fibrotic Cytokine Seen In The Myocardium After AngII Exposure

Previous work by us, and others suggested that TGFβ and CTGF may be the predominant pro-fibrotic cytokines associated with AngII dependent myocardial fibrosis[37, 170]. Increased numbers and additional time-points were added to historical data[37]. The expression of CTGF within the myocardium relative to both housekeeping gene and saline control was significantly increased (23-fold) as early as 6hr after AngII exposure ($p < 0.01$), preceding myocardial cellular infiltration or ECM deposition shown to be significant by 1d and 3d respectively[37, 196]. CTGF mRNA levels were then seen to drop off at 12hr before increasing again at 24hr by 19fold ($p<0.01$) (Figure 5.3A). As the second wave of CTGF expression occurs there is a concurrent increase in TGFβ mRNA levels that reached significance at 24hr of AngII exposure (4fold) and peaked at 3d compared to saline control ($p<0.01$) (Figure 5.3B). The increase in CTGF expression when compared to TGFβ was earlier and several fold higher, suggesting a role for CTGF in the subsequent fibrosis development (Figure 5.3C).

Although there was no change in TGFβ mRNA expression in the first 12hrs of AngII exposure, early downstream activation of the TGFβ pathway was observed, as SMAD2 phosphorylation in relation to total SMAD2/3 protein levels increased

significantly by 6hr (Figure 5.3D, E). SMAD2 phosphorylation concomitant with CTGF mRNA expression suggests that the early peak in CTGF is at least in part TGFβ dependent. Up-regulation of CTGF expression was confirmed by showing a significant increase in the presence CTGF protein relative to saline controls at 3d of AngII exposure by western blotting of cardiac extracts (Figure 5.3F, G). The majority of CTGF appeared to be localized to the cardiomyocytes and not the infiltrating cells suggesting that resident cells may be a source of early CTGF production (Figure 5.3H, I).

6.2.3 Myocardial Resident Cells Produce CTGF In Response To AngII

In addition to cardiomyocytes, myocardial tissue contains large numbers of endothelial cells due to its rich capillary blood supply. Given our evidence that CTGF production was up-regulated in the myocardium prior to fibrocyte migration and appeared to be localized to resident cells, we sought to confirm that cardiomyocytes or endothelial cells produce CTGF after AngII exposure. To achieve this we conducted *in vitro* stimulation assays using isolated neonatal cardiac myocytes and microvascular endothelial cells. The majority of isolated cardiomyocytes stained positive for CTnI, both by flow cytometry (97%) and immunofluorescence (94%) suggesting high purity (Figure 5.4A, B). Stimulation of isolated cardiomyocytes for 6hr with AngII significantly increased the CTGF mRNA expression 2.1fold compared to vehicle only control ($p < 0.05$). The addition of neutralizing anti-TGFβ antibody in combination with AngII exposure abrogated the increase in CTGF expression *in vitro*, suggesting that the change in expression was TGFβ dependent (Figure 5.4C). This finding confirms that cardiomyocytes are capable of producing significant amounts of CTGF in response to AngII.

Similarly, endothelial cells significantly increased CTGF mRNA expression following 6hr of AngII exposure *in vitro* (2.8-fold) when compared to saline control. Once again the increase in CTGF mRNA seen after AngII exposure was was abrogated by the addition of neutralizing anti-TGFβ antibody ($p<0.05$) (Figure 5.5). Taken together, these data provide supporting evidence that resident cells are responsible for the observed early peak in CTGF expression in response to AngII. Furthermore, this up-regulation in CTGF remains dependent on TGFβ signaling as demonstrated by the inhibitory effects of TGFβ neutralizing antibody.

6.2.4 Fibrocytes Isolated And Cultured In Vitro From AngII Exposed Myocardium Also Contribute To CTGF Expression

While our findings suggest that CTGF is produced initially by resident cells, they may not explain our observation *in vivo* of a second peak in CTGF mRNA expression that appears to coincide with the increase in fibrocyte accumulation in the myocardium at 24hr of AngII exposure. Therefore, we examined the possibility that infiltrating cells could also contribute to the high level of CTGF found in whole tissue after AngII exposure. Infiltrating fibrocytes (after AngII exposure) were isolated as previously described[37]. Fibrocyte purity was assessed by confirming co-expression of a mesenchymal marker collagen type I and the hematopoetic marker CD45 (Figure 5.6A). Using this approach, the mean purity of fibrocyte cultures was 50%. Control animals yielded less than 1% fibrocytes (Figure 5.6B). Direct exposure of the isolated fibrocyte population to AngII resulted in a significant 2.6-fold increase in CTGF mRNA expression compared to saline control, which was reduced to saline control levels by the addition of neutralizing anti-TGFβ antibody ($p < 0.05$) (Figure 5.6C). This suggests that a

fibrocyte rich population in which no cardiomyocytes are present is also capable of CTGF up-regulation and expression. These findings may explain the observed second peak in CTGF mRNA we observed in the myocardium of AngII exposed animals after 12hr of AngII exposure.

6.2.5 Fibrocytes Proliferate In Response To CTGF

We next focused on a potential role for CTGF in fibrocyte accumulation and ECM deposition. On examination of histological sections from animals exposed to AngII for 3d we observed significant positive staining of Ki67, a proliferation marker, in areas of fibrocyte infiltration when compared to saline control (Figure 5.7A, B). This would suggest that fibrocyte accumulation is dependent on both influx from the circulation and from proliferation. Fibrocyte proliferation in the myocardium occurred concurrently with the elevation of CTGF. As such, we investigated the effect of CTGF exposure on the proliferation of fibrocytes in an *in vitro* setting. Isolated fibrocytes exposed to CTGF resulted in significant proliferation as assessed by Ki67 positivity when compared to media control ($p < 0.05$) (Figure 5.7C). This was confirmed using a second proliferation assay, the MTT assay ($p < 0.05$) (Figure 5.7D). These data suggest that increased fibrocyte proliferation within the myocardium after AngII exposure (3d) is in part due to the increase in CTGF observed at this time.

6.2.6 Fibrocytes Differentiate To ECM Producing Cells Under The Influence Of CTGF

To investigate the effect of CTGF on fibrocyte differentiation, fibrocytes were isolated as above and exposed to CTGF. There was a significant increase in the mRNA expression of collagen type 1, α1 subunit (COL1A1), with a 2.3-fold increase compared to saline control (Figure 5.8A). This suggests that fibrocytes can, under appropriate

conditions, become a source of ECM in the myocardium particularly after AngII exposure and in the presence of CTGF. Given that we have demonstrated that AngII up-regulates the expression of CTGF (Figure 5.6), this would create a positive feedback loop promoting a profibrotic environment.

Fibrocytes isolated from peripheral blood were enriched over 14d with or without CTGF. Cells that were not exposed to CTGF over the duration had a significantly lower SMA to CD133 ratio, compared to early isolates (1d). On the other hand, fibrocytes exposed to CTGF during the 14d enrichment did not show a significant reduction in SMA:CD133 (Figure 5.8B). Taken together, this suggests that CTGF exposure may allow fibrocytes to maintain a higher mesenchymal protein expression and therefore favor differentiation of fibrocytes into ECM producing myofibroblast-like cells.

CTGF has been shown to increase the motility and migration of several types of cancer cells and vascular endothelial cells but this effect has yet to be evaluated with fibrocytes [197-199]. Using a well-described scratch assay, CTGF resulted in a non-significant 1.02-fold change in recovered distance compared to media control (Figure 5.9), suggesting that CTGF failed to affect the motility of isolated fibrocytes.

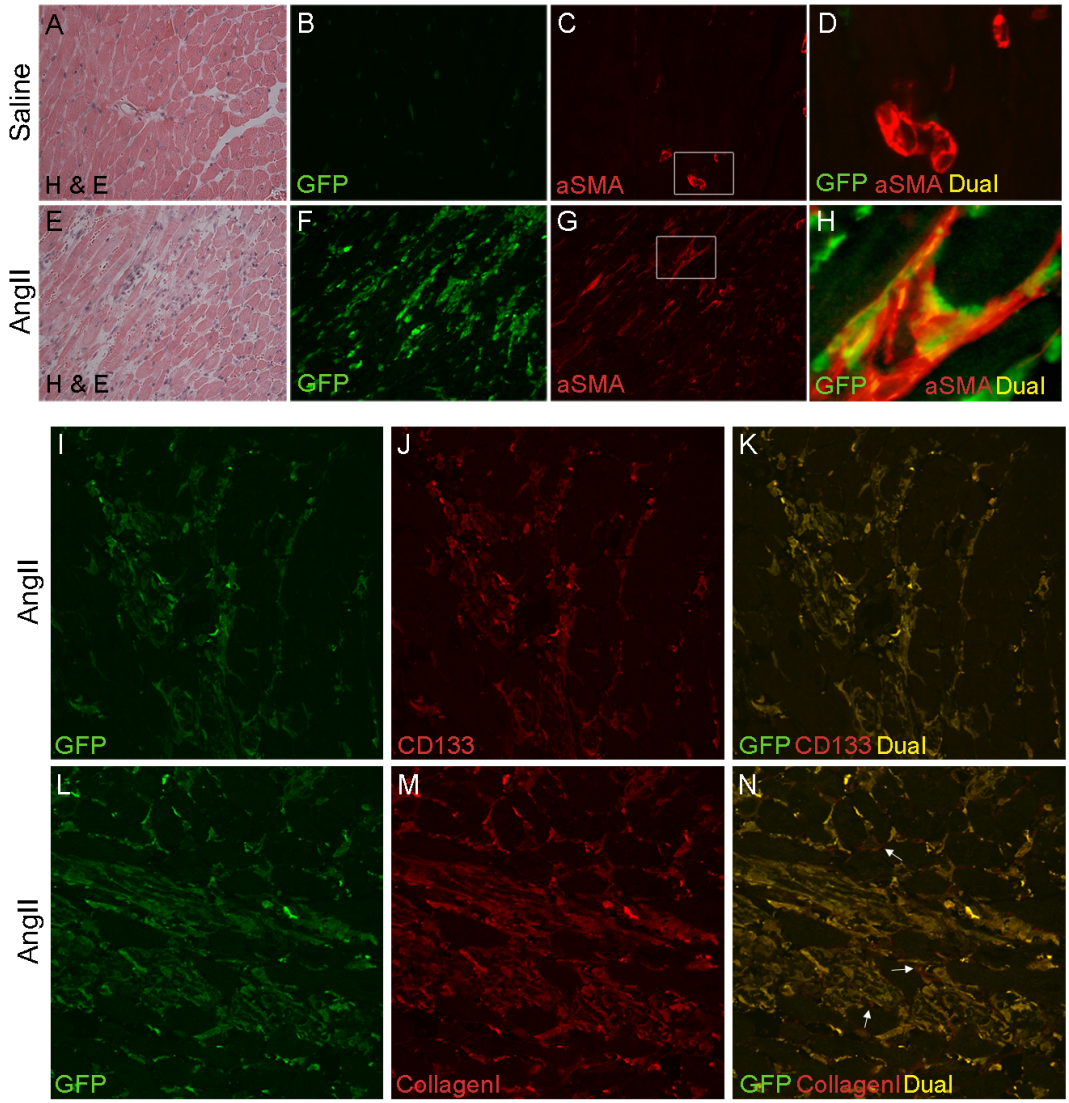

Figure 6.1 Fibrocyte Infiltration

Chimeric animals with transplanted GFP+ bone marrow cells received saline (A, B, C, D) or AngII (2.0μg/kg/min) for 3d (E, F, G, H, I-N). Areas containing infiltrating cells were identified by H&E stain (A, E) and characterized by immunofluorescent staining for GFP (B, F, I, L) and SMA (C, G), CD133 (J), Col1 (M). Merged images of green and red channels show dual staining indicating GFP+/SMA+ (D, H), GFP+/CD133+ (K), GFP+/Col1+ (N) cells in the area of infiltration. White arrows indicate areas of uniquely

Col1+ staining (N). Images were captured at 25X and 100X (A-H) and 63X confocal (I-N), with representative images shown. n=3.

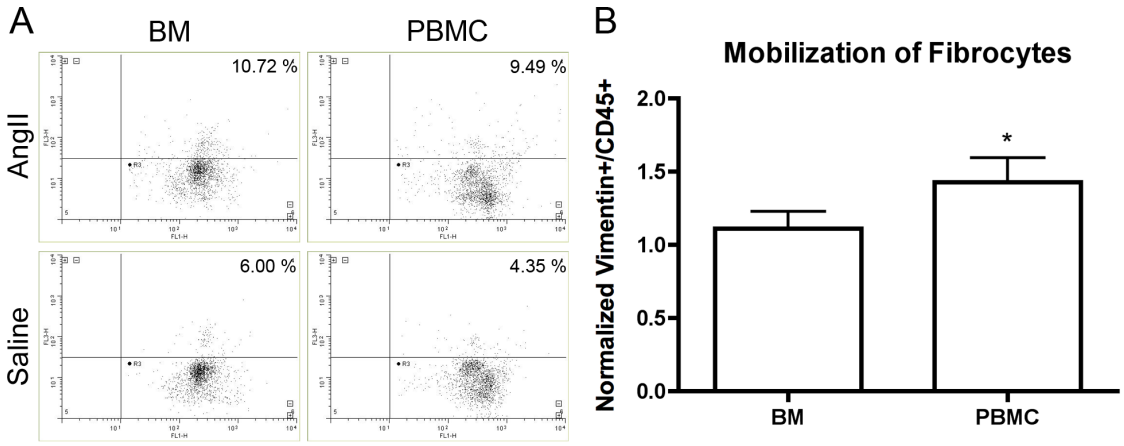

Figure 6.2 Fibrocyte Mobilization

Animals received saline as a control or AngII for 3d and bone marrow (BM) and peripheral blood mononuclear cells (PBMCs) were isolated for assessment of CD45 and vimentin presence by flow cytometry (A). Quantification of relative levels of vimentin+ cells within the CD45+ population in bone marrow and peripheral blood is shown (B). n=5; *p<0.05.

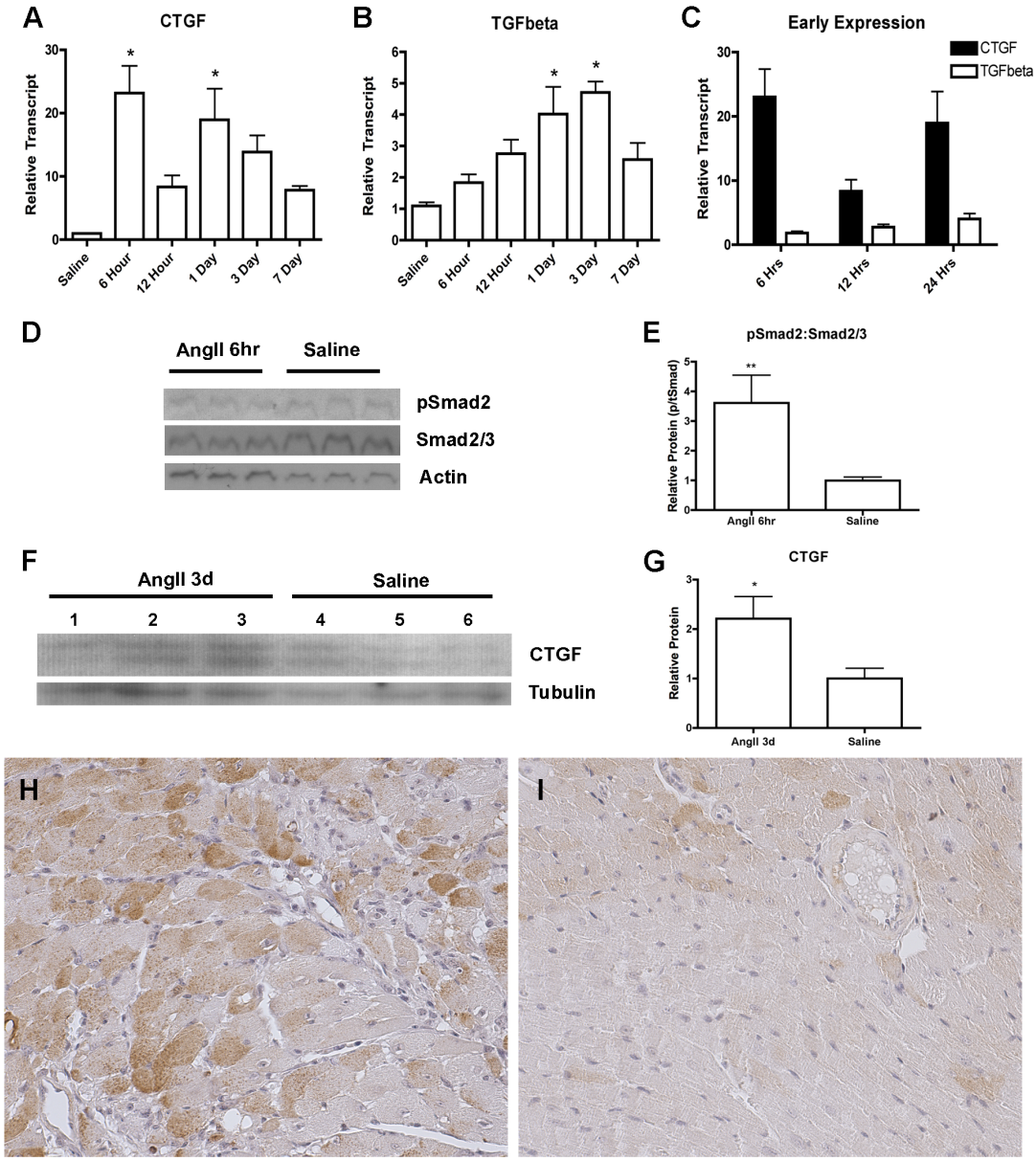

Figure 6.3 CTGF And TGFβ Production

qPCR was used to assess myocardial expression for CTGF (A), TGFβ (B) and the early expression compared (C). Transcript levels are reported relative to housekeeping gene ribosomal 18S (n=8). Immunoblotting was used to determine SMAD2 phosphorylation and total SMAD2/3 protein levels (D), with densitometry used for semi-quantification of

pSMAD2:SMAD2/3 ratio (E) (n=6). Immunoblotting was used to determine CTGF and βtubulin protein production in whole myocardium (D). CTGF protein was semi-quantified relative to the housekeeping protein β-tubulin (E) (n=6). Representative blots with 3 samples in each experimental group (AngII; lanes 1-3 and saline; lanes 4-6) are shown (D, F). Immunohistochemistry was used to localize CTGF within the myocardium. Representative sections from animals treated with AngII (2.0μg/kg/min) for 3d (F) or saline as a control (G) are shown. Images were captured at 40x. *$p<0.05$.

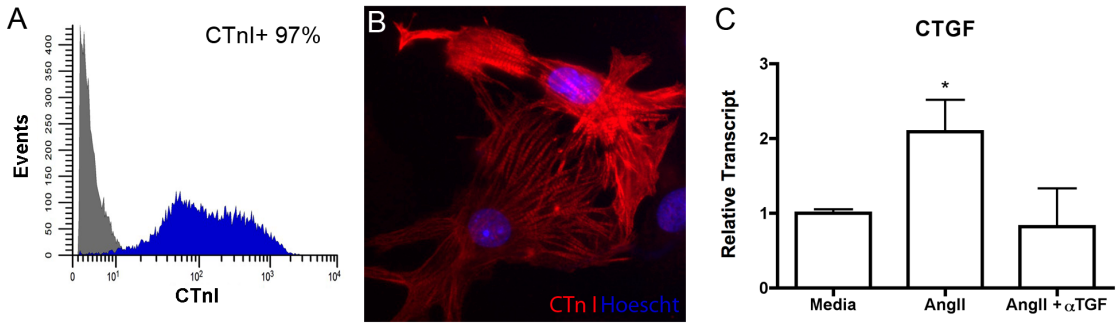

Figure 6.4 Cardiomyocytes Produce CTGF

Cardiomyocytes were isolated from neonatal mice. Purity was assessed using CTnI staining by flow cytometry (A) and immunofluoresence with nuclei counterstained with Hoescht (B). Cultured cardiomyoctes were stimulated with AngII (100nM), AngII + neutralizing anti-TGFβ antibody (αTGF; 15μg/mL) or saline control for 6hr. CTGF mRNA expression was assessed by qPCR and compared to the housekeeping gene 18S (C). Images were captured at 63x. n=8; *p<0.05.

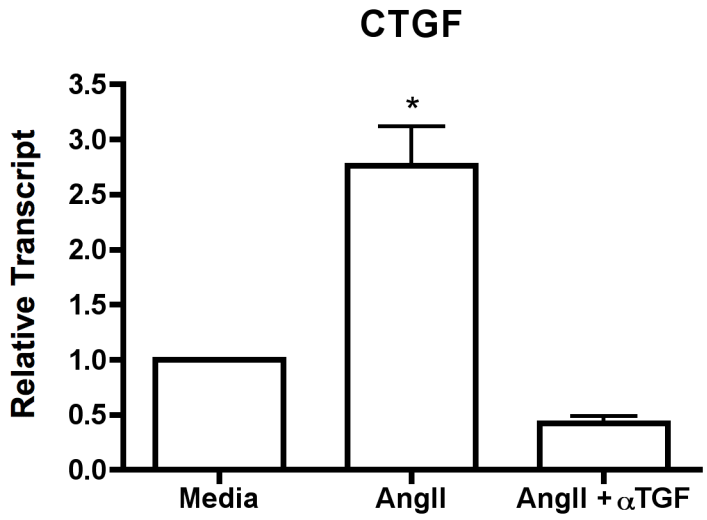

Figure 6.5 Microvascular Endothelial Cells Produce CTGF

B.End3 endothelial cells were stimulated with AngII (100nM), AngII + neutralizing anti-TGFβ antibody (αTGF; 15μg/mL) or saline control for 6hr. CTGF mRNA expression was assessed by qPCR and compared to the housekeeping gene 18S (C). n=3; *$p<0.05$.

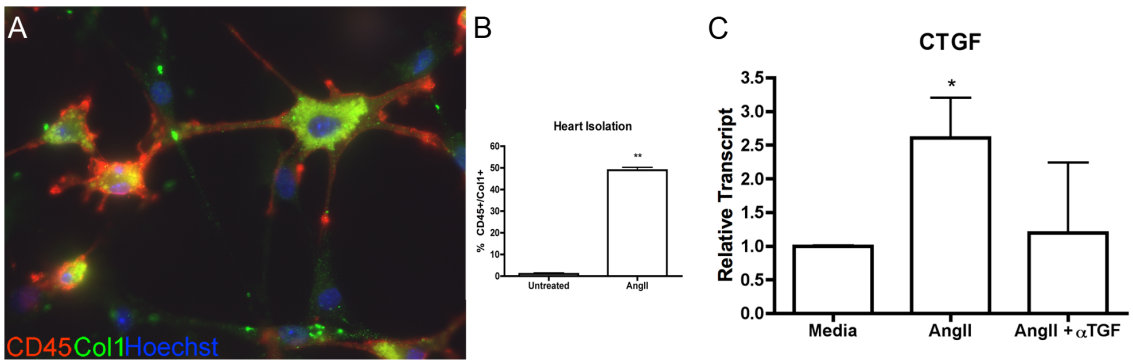

Figure 6.6 Isolated Fibrocytes Produce CTGF

Fibrocytes were isolated from the myocardium of mice exposed to AngII (2.0μg/kg/min) for 3d. Purity was assessed by immunofluoresent staining for $CD45^{+}/ColI^{+}$ with nuclei counterstained with Hoescht (A). Purity was quantified by calculating the percentage of $CD45^{+}/ColI^{+}$ cells relative to the total number of nuclei (B). Isolated fibrocytes were stimulated with AngII (100nM), AngII + anti-TGFβ neutralizing antibody (αTGF; 15μg/mL) or saline control for 6hr. CTGF mRNA expression was assessed by qPCR and compared to the housekeeping gene 18S (C). Images were captured at 63x. n=5; *p<0.05, **p<0.01.

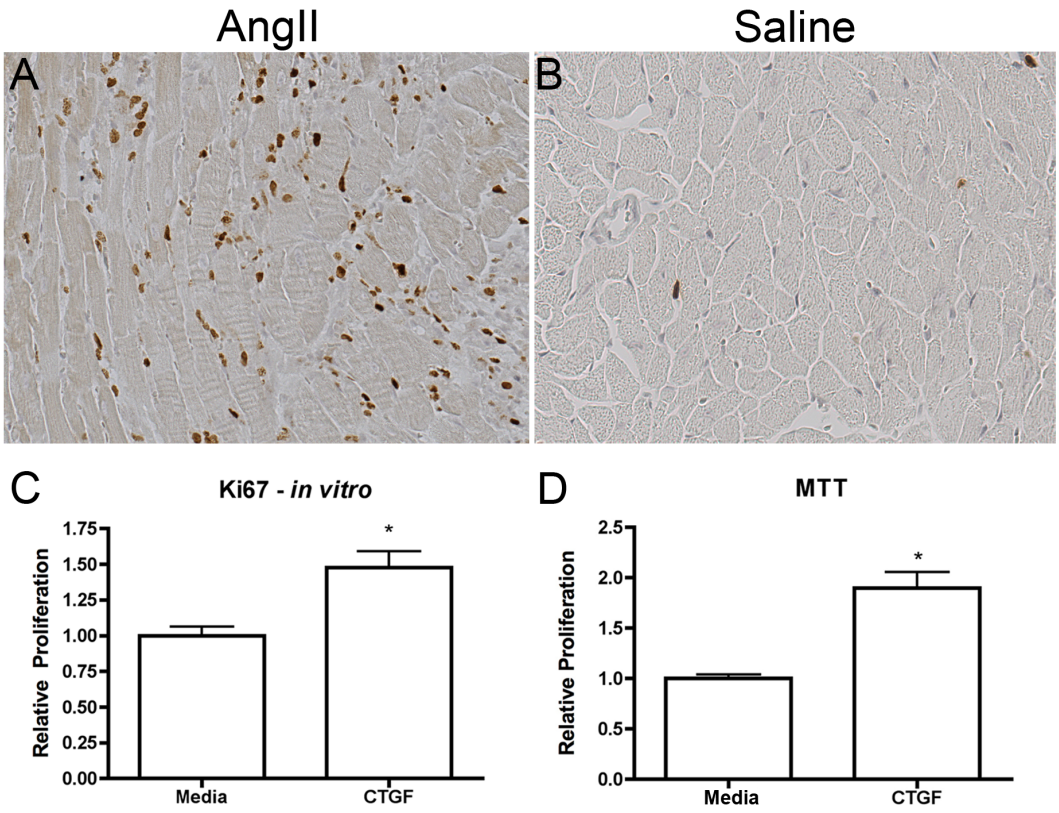

Figure 6.7 Fibrocytes Proliferate In Response To CTGF

Immunohistochemistry was used to identify Ki67 positive cells within the myocardium of animals exposed to AngII (A) or saline control (B) for 3d. Isolated fibrocytes were exposed to CTGF (125ng/mL) or vehicle control for 24hr. Proliferation was assessed by counting cells positive for immunofluorescent staining of Ki67 relative to the number of nuclei in 5 fields of view per sample captured at 25x (C) and MTT assay (D). Representative images were captured at 40x. n=6; *$p<0.05$.

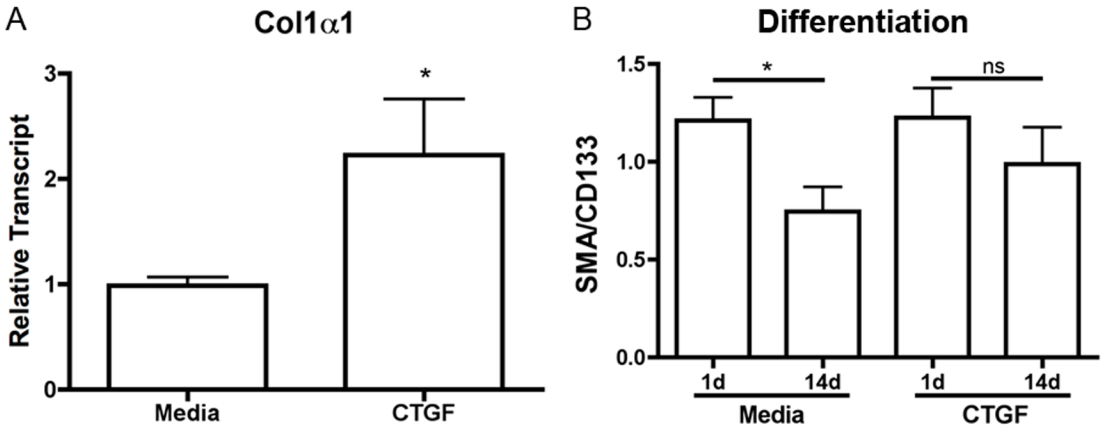

Figure 6.8 Fibrocytes Differentiate And Produce ECM In Response To CTGF

Isolated fibrocytes were exposed to AngII, CTGF or vehicle control for 6hr. The COL1A1 transcript expression was assessed by qPCR relative to housekeeping gene 18S (A) (n=6). PBMCs were enriched for fibrocytes in media containing CTGF (125ng/mL) or vehicle control and maintained in culture for 1 or 14d. Immunofluorescent staining for SMA and CD133 was done and the area of positive staining was normalized to the total number of nuclei positive and reported as a ratio of SMA/CD133 staining from 5 fields of view per sample captured at 25x. n=4; *$p<0.05$.

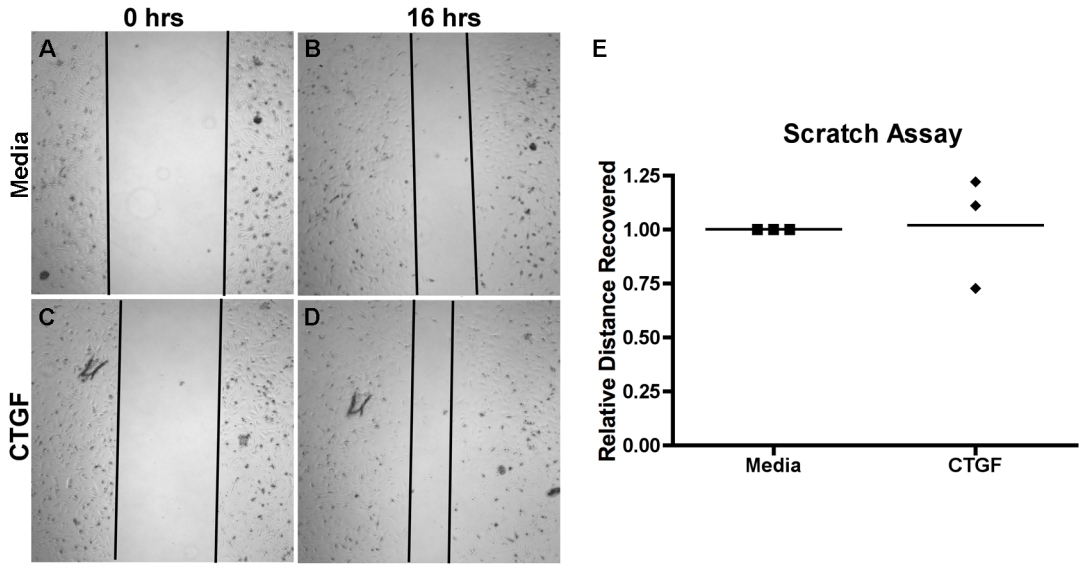

Figure 6.9 CTGF Does Not Affect The Mobility Of Isolated Fibrocytes

Isolated fibrocytes were cultured and scraped from a section of the plate. Images captured immediately (0hr; A, C) or after 16hr (B, D) of culture in media containing either PBS (A, B) as control or CTGF (125ng/mL) (C, D). Representative images were captured at 10x (A-D). Pixel counts were used to semi-quantify the relative distance recovered compared to initial scratch size (E). n=3.

6.3 Discussion

6.3.1 Bone Marrow-Derived Progenitor Cells Mobilize And Migrate To The Myocardium

We have previously reported that fibrocytes, a bone marrow-derived fibroblast progenitor population, represent the majority of infiltrating cells seen to accumulate in the myocardium after AngII exposure[37, 196]. The effector role of fibrocytes has been suggested in many fibrotic pathologies including models focusing on cardiomyopathy[95, 164], cardiac hypertrophy[119], pulmonary fibrosis[100] and renal fibrosis[74]. Strategies aimed at eliminating fibrocytes have resulted in the inhibition in the development of myocardial fibrosis supporting the causal relationship between fibrocytes and myocardial fibrosis [95, 169, 200]. In the present study we demonstrate that following 3d of AngII exposure, cells that have migrated to the myocardium are bone marrow-derived (GFP^+) and stain positive for the progenitor marker CD133, mesenchymal markers SMA or ColI confirming that the infiltrating cells are fibrocytes. We have also provided evidence that fibrocyte numbers increase in peripheral blood after AngII exposure supporting a hypothesis of mobilization of these progenitor cells from the bone marrow in response to AngII. Given these findings, we investigated the parameters that induce fibrocyte accumulation in the myocardium and the propagation of the fibrotic response.

6.3.2 Fibrotic Mediators: Interaction Between CTGF And TGFβ

We observed significant increases in CTGF mRNA and protein in the myocardium well before the accumulation of fibrocytes, suggesting a link between CTGF production by resident cells and fibrocyte accumulation. Immunocytochemistry labeling

for CTGF suggested that cardiomyocytes were a significant cellular source of CTGF. Further support for this hypothesis came from experiments using cultured cardiomyocytes, which demonstrated that AngII exposure results in significant increase in CTGF mRNA expression. Microvascular endothelial cells were also able to produce CTGF mRNA in response to AngII, suggesting that other resident myocardial cells contribute to the early increase in CTGF mRNA *in vivo*. The importance of CTGF in fibrosis development has been suggested by others, and a link between AngII and CTGF has been implicated by data showing that CTGF expression could be abrogated in animal models by ARB treatment[114]. These data suggest that the initial increase in CTGF expression seen in our model after AngII exposure was a direct result of signaling by resident cardiomyocytes and endothelial cells which represent a large proportion of all myocardial cells [201].

Traditionally, CTGF is believed to be regulated via TGFβ signaling. CTGF was first described as a TGFβ response factor in human endothelial cells (HUVECs) and was found to be expressed by cultured skin fibroblasts in response to TGFβ as early as 30 min after exposure[202, 203]. The role of TGFβ as a key regulator of fibrosis development has previously been described and explains why in the AngII infusion model, there was an increase in TGFβ mRNA in the myocardium after 1d of exposure[45, 107]. We provide evidence for the first time that in a mouse model of AngII exposure, CTGF is expressed first (6hr) within the myocardium by resident cells including cardiomyocytes and endothelial cells, well before the observed increase in TGFβ expression (1d).

While TGFβ mRNA was not up-regulated until 1d of AngII exposure, earlier TGFβ signaling was likely the result of activation of latent TGFβ protein, with

dissociation of the latency associated polypeptide resulting in the early increase in CTGF mRNA expression detected (6hr) [204]. Once TGFβ is activated, it binds the TGFβ receptors leading to a conformational change that results in kinase activity of the receptor[205]. Ultimately, this results in the phosphorylation of SMAD2, which when complexed with SMAD3 and co-SMAD4, translocate to the nucleus and regulate the expression of CTGF mRNA[191]. We have provided novel supporting evidence that SMAD2 phosphorylation increases early, by 6hr of AngII infusion *in vivo*. This was concurrent with the increase in early CTGF mRNA seen at 6hr. Taken together with our in-vitro observation that CTGF expression after AngII exposure appears to be TGFβ dependent, this suggests that AngII exposure resulted in early TGFβ activation with downstream phosphorylation of SMAD2, which was responsible for the observed increase in CTGF mRNA expression. This is supported by evidence that AngII induced ECM synthesis can be limited by TGFβ neutralizing antibody or truncated TGFβ type II receptors[206].

During the course of AngII exposure, the initial increase in CTGF expression was followed by a reduction in CTGF mRNA at 12hr. At 24hr, CTGF expression in the myocardium rebounded, coinciding with increased infiltration of fibrocytes.
In fact, we demonstrated that fibrocytes enriched in culture up-regulate CTGF expression in response to AngII exposure, providing convincing evidence that fibrocytes could be contributing to the increased expression of CTGF in the myocardium observed at 24hr of AngII exposure. However, this second wave of CTGF expression also coincided with increased TGFβ expression, which is known to contribute to CTGF expression. Thus

making it difficult to determine the relative contribution from newly infiltrating fibrocytes or due to TGFβ signaling in resident cells [202, 203].

A third mechanism, perhaps equally important, by which CTGF expression is modulated is through an autoregulatory feedback pathway in which CTGF can up-regulate its own expression[193]. Furthermore, CTGF can up-regulate TGFβ expression, which is consistent with our observations that increased TGFβ expression occurred concurrently with increased CTGF expression[207].

Cumulatively, our results suggest that multiple cell types and feedback mechanisms likely contribute to the increased CTGF expression in the myocardium after AngII exposure. The early response to AngII is mediated by CTGF produced by resident cells in a TGFβ dependent manner. The secondary increase in CTGF expression, while likely TGFβ-dependent, is likely dependent on both resident cells (cardiomyocytes and endothelial cells) and infiltrating fibrocytes.

6.3.3 CTGF Regulation Of Fibrocyte Proliferation And ECM Production

The timing of CTGF expression in the myocardium suggested that CTGF plays an important role in the early environment that leads to myocardial fibrosis following AngII exposure. As fibrocytes are the predominant infiltrating cell type in the myocardium after AngII exposure[37] and many fibrotic conditions feature CTGF up-regulation, it followed that CTGF may promote fibrosis by acting on fibrocytes. In our AngII model, we demonstrated that fibrocytes in the myocardium were highly proliferative. Thus, we believed CTGF might promote fibrosis through fibrocyte proliferation, as CTGF had minimal effect on the motility of cultured fibrocytes. Several studies provide evidence supporting this theory by demonstrating that CTGF increases proliferation in cultured

fibroblasts[112, 208]. We therefore investigated the effects of CTGF on isolated fibrocytes in culture. Consistent with our *in vivo* findings, CTGF exposure led to increased fibrocyte proliferation *in vitro*. This suggests that the increase in CTGF production in the myocardium after AngII exposure contributed to the observed increase in fibrocyte accumulation within the myocardium through increasing fibrocyte proliferation.

Fibrocytes are progenitor cells that under certain conditions are capable of differentiation into collagen producing myofibroblasts. We sought to investigate the effect of CTGF on the maturation and differentiation of fibrocytes. We have provided evidence for the first time that fibrocyte enriched cell culture exposed to CTGF resulted in a significant increase in COL1A1 mRNA supporting the differentiation of fibrocytes toward an ECM producing phenotype. In support of our observation, some investigators have shown increased expression of ECM proteins by fibroblasts after exposure to CTGF[97, 128]. Furthermore, there is also evidence suggesting that inhibiting CTGF *in vitro* is sufficient to reduce collagen type 1 and SMA protein production by stimulated fibroblast cell lines and primary isolated fibroblasts, thus supporting a role for CTGF in promoting and maintaining fibroblast differentiation and phenotype[127, 128, 208].

Taken together, our results suggest that CTGF is involved in the regulation of myocardial fibrosis after AngII exposure. We have provided two mechanisms by which CTGF contributes to the pro-fibrotic microenvironment: (1) increased fibrocyte proliferation contributing to fibrocyte accumulation and (2) promoting fibrocyte differentiation into ECM producing cells.

6.3.4 Mechanism Of Action Of CTGF

There has not yet been a CTGF receptor identified and, as such, the molecular mechanisms of action continue to be investigated. Although the exact molecular mechanisms of CTGF signaling is beyond the scope of the current manuscript, there are a number of possible pathways that may be involved in regulation of ECM production and cellular proliferation in response to CTGF. Separate domains of CTGF have been suggested to be responsible for regulating proliferation or differentiation, supporting this hypothesis[208]. One possible pathway that is likely involved is the mitogen-activated protein (MAP) kinase cascades, specifically p38, which is involved in regulating proliferation and collagen type 1 expression[209]. In fact, p38 positively regulates COL1A1 expression by primary fibroblasts and is significantly phosphorylated after cells are exposed to CTGF[210]. Moreover, exposure to CTGF results in reduced phosphorylation of MAP kinases, ERK1/2 and JNK, which have been suggested to repress COL1A1 expression, resulting in increased COL1A1 expression when CTGF is present[210, 211]. Taken together, these studies suggest that activation of the p38 MAP kinase pathway in combination with repression of the ERK1/2 and JNK pathways could control COL1A1 expression and proliferation of fibrocytes in response to CTGF.

Although mice constitutively lacking CTGF die shortly after birth[212] anti-fibrotic intervention through blockade of CTGF has shown some positive results in animal models of skin, kidney and lung fibrosis[213-215]. Potential strategies for interrupting the effects of CTGF were thoroughly reviewed by Brigstock and have included monoclonal antibody, antisense oligonucleotide and siRNA interventions. Preliminary results published from recent stage 1 clinical trials suggested that a

humanized anti-CTGF antibody decreased kidney failure in a cohort of patients with diabetic nephropathy[216]. These potential therapeutic strategies, however, have not yet been successfully deployed for the treatment of myocardial fibrosis[217]. With this in mind, we provide evidence that CTGF contributes to the proliferation of fibrocytes and may have autocrine effects, which could be necessary to promote the pro-fibrotic environment required for the development of myocardial fibrosis as opposed to myocardial healing. We have provided support for a pro-fibrotic role for CTGF in the development of myocardial fibrosis after AngII exposure downstream of TGFβ, conceivably allowing for opportunity to interrupt the fibrotic role of TGFβ without affecting its immunomodulatory properties. As such, CTGF may still present a therapeutic target for reducing fibrosis in cardiac diseases, although this requires further evaluation.

CHAPTER 7: INTERRUPTION OF COLLAGEN HOMEOSTASIS ALTERS THE FIBROTIC RESPONSE TO ANGII EXPOSURE

Rosin N.L., Légaré J.F.

NR – designed the study, carried out experimentation, collected and analyzed data, and prepared the manuscript

JFL – assisted with study design and critical review of the manuscript

7.1 Introduction

AngII is a vasoregulatory hormone that is introduced in animals as a model of hypertrophy and myocardial fibrosis induced by an increase in blood pressure [37, 130]. In addition to inducing hypertension, AngII also signals locally within the myocardium through recognition by AT_1R and AT_2R. AT_2R is highly expressed in the embryo stage, with lower expression in adult myocardium[218]. AT_2R acts in a cell specific manner as a compensatory signal to regulate AT_1R activity[218]. All cell types express AT_1R and its downstream signaling is partially dependent on the cell type where it is located. When AngII binds to AT_1R located on cardiomyocytes there is resultant cellular hypertrophy[219], whereas when bound to AT_1R located on fibroblasts there is increased fibroblast proliferation and ECM production[220].

Aged mice have increased fibrosis by 40wk, as assessed by increased Col1A1 mRNA expression, Sirius red staining and hydroxyproline content in the myocardial tissue (Rosin *et al.* submitted; Chapter 4). This is accompanied by an increase in profibrotic factors including TGFβ, CTGF, PDGF and FGF that regulate the production of ECM proteins including collagen. However, unlike the AngII-induced model of myocardial fibrosis in 8wk old mice, which has a significant amount of mononuclear cell infiltration into the myocardium[37], there were no infiltrating cells detected in the myocardium of aged animals. Therefore, it follows that fibrotic signaling during age-related myocardial fibrosis influences the reactive potential of mainly resident cell populations including cardiomyocytes, fibroblasts, endothelial cells or macrophages, without inducing an inflammatory reaction. This suggests that extracellular profibrotic

signaling in AngII-induced fibrosis may be different than that resulting in age-related myocardial fibrosis.

When aged spontaneously hypertensive rats were treated for an extended period with ARB or ACE inhibitor the majority of hypertrophy and fibrosis were ameliorated, however this was not the case with hydralazine treatment [79]. This suggests that reducing blood pressure without inhibiting AngII signaling in aged animals was not sufficient to inhibit fibrosis development and therefore that AngII signaling contributes to age-related fibrosis development beyond inducing hypertension [26]. This is in contrast to the AngII-induced fibrosis model, in which hydralazine ameliorated myocardial fibrosis (Chapter 5).

Although old mice had higher collagen content in the heart, they developed more hypertrophy and a much 'looser' scar after ischemia reperfusion injury[39]. These mice also had increased expression of chemokines (CCL2, MIP1α, MIP2), pro-inflammatory cytokines (TNFα, IL1β, IL6, MCSF), and mesenchymal proteins (SMA, collagen, osteopontin) as well as decreased myofibroblast accumulation when compared to young mice. This suggests that fibroblast proliferation, accumulation or differentiation to the myofibroblast phenotype in aged mice was impaired compared to the response in young mice.

The objective of the present study was to determine if age alone, or the associated accumulation of myocardial fibrosis and fibrotic signaling contribute to the fibrotic response to AngII exposure. We used BAPN to inhibit LOX, thereby inhibiting collagen crosslinking and altering collagen homeostasis prior to AngII exposure [10]. Treatment with BAPN reduces the amount of established myocardial fibrosis and fibrotic signaling

in 40wk animals to that observed in 8wk animals (Rosin in press; Chapter 3). BAPN treated animals were then exposed to AngII to evaluate the fibrotic response and determine if this was dependent on age alone or on the underlying presence of collagen and pro-fibrotic factors.

7.2 Results

7.2.1 Cellular Infiltration After AngII Exposure

We have previously reported that at 8wk, within 1d of AngII exposure there is a significant amount of mononuclear cell infiltration within the myocardium. This effect was maintained after 3d of AngII exposure in the 8wk group (22.0±2.8 %). There was a similar area affected by cellular infiltration after AngII exposure in animals at 40wk (21.1±3.6 %), but infiltration was nearly double in 40wk + BAPN animals (45.1±2.2%) (Figure 6.1 A). This suggests that the processes and/or mediators involved in cellular infiltration did not change with age, but did change due to LOX inhibition and the reduction in collagen crosslinking.

7.2.2 AngII Exposure Results In Increased Myocardial Fibrosis

The relative increase in the percentage of the myocardial cross-section area that was fibrotic after AngII exposure was assessed by % Sirius red staining and was significant in the 8wk, 40wk and 40wk + BAPN groups compared to saline (2.1±0.3 fold, 1.6±0.2 fold and 1.9±0.1 fold) (Figure 6.1 B). However, there was no significant difference between the three groups exposed to AngII.

7.2.3 Regulation Of Collagen Homeostasis

Collagen homeostasis is maintained through the regulation of 1- new collagen synthesis, 2- stabilization of collagen by crosslinking and 3- collagen degradation.

Collagen Synthesis

In order to assess if the increase in fibrosis was due to an increase in new collagen synthesis we measured the amount of collagen type I subunit, (Col1A1) mRNA transcript within the myocardium. After AngII Col1A1 mRNA was elevated significantly in all groups compared to the 8wk saline control (8wk 60.8±24.05 fold; 40wk 42.9±13.9 fold; 40wk + BAPN 33.6±6.1 fold). The 8wk and 40wk + BAPN group increased, but the 40wk group did not change significantly after AngII exposure compared to their respective saline controls (8wk 60.8±24.5 fold, $p<0.05$; 40wk 3.8±1.2 fold, $p>0.05$; 40wk + BAPN 11.2±2.4 fold, $p<0.05$). This dampened response to AngII exposure in the 40wk group may be due to the significantly higher baseline expression of Col1A1 transcript at 40wk (18.6±4.6 fold, $p<0.05$) compared to the 8wk group (Figure 6.2 A). This suggests that the absolute amount of new collagen synthesized in each group is similar and possibly limited by an unknown feedback mechanism after AngII exposure.

Therefore, we assessed if new collagen synthesis and the aforementioned feedback mechanism were regulated at the level of known fibrotic signaling. The primary fibrotic signaling pathway involved in the development of myocardial fibrosis after AngII exposure is the TGFβ pathway. This includes TGFβ and downstream mediator CTGF, which increase the activation of fibroblasts and their production of collagen[107]. We have previously reported significant early increases after 3d of AngII exposure in the TGFβ pathway at 8wk including increased TGFβ and CTGF mRNA production,

SMAD2/3 phosphorylation and CTGF serum protein concentration (Chapter 5). We have also observed increases in the TGFβ pathway signaling by 40wk in age-related myocardial fibrosis development (Chapter 3).

After AngII exposure in the 40wk group there was no significant increase in either TGFβ or CTGF mRNA expression compared to the 40wk saline control group (TGFβ 0.9±0.1 fold; CTGF 3.5±1.8 fold). However, both TGFβ and CTGF mRNA expression increased significantly in the 40wk + BAPN group after AngII exposure (TGFβ 2.3±0.4fold; CTGF 11.2±2.4 fold $p<0.05$) (Figure 6.2 B, C). Taken together, this suggests that either the ability to respond to AngII is reduced during aging or that there is regulatory feedback that is maintaining a maximum threshold of expression of these factors.

MMP Activity

MMP2 and 9 are enzymes that actively degrade ECM proteins and these MMPs are in turn regulated by TIMPs (TIMP1 regulates MMP2). The expression of MMP2, 9 and TIMP1 are regulated by TGFβ, potentially as part of a feedback mechanism to maintain collagen homeostasis. The MMP2:TIMP1 mRNA ratio gives an estimation of the amount of MMP2 protein that is active. We have previously reported that in the myocardium of animals at 8wk exposed to AngII there is a significant decrease in MMP2:TIMP1, due to TIMP1 expression increasing substantially in combination with no change in the MMP2 mRNA expression. Similarly, in the 40wk and 40wk + BAPN groups there was a significant decrease in the ratio of MMP2:TIMP1 after AngII exposure (40wk, 0.12±0.05fold; 40wk + BAPN, 0.01±0.003fold; $p<0.05$) (Figure 6.3C). There was also a decrease in the MMP2:TIMP1 ratio in both the baseline 40wk and 40wk

+ BAPN groups compared to the 8wk group, however the ratio in the 40wk + BAPN group did not significantly change compared to the 40wk group. This suggests that the overall amount of MMP2 protein that is active in the ECM decreased in response to AngII exposure in each group. However, the the MMP2:TIMP1 ratio changed in response to AngII exposure significantly in the 40wk + BAPN group compared to the 40wk group. This suggests that inhibition of collagen crosslinking had more effect on TIMP1 expression and the MMP2:TIMP1 ratio than age alone, possibly as a feedback pathway to regulate the amount of collagen being degraded. This also suggests that in the 40wk + BAPN group with, in which collagen crosslinking was inhibited, there was a compensatory decrease in the amount of active MMP2 available to degrade the newly deposited, but not yet crosslinked collagen.

7.2.4 Cellular Response To Signaling

Primary fibroblasts were isolated from mice at 40wk and stimulated with AngII (100nM) in order to determine whether these cells were able to respond to direct AngII signaling. Previously reported data suggest that AngII signaling in fibroblasts isolated from young mice increases fibrotic signaling and collagen production. Similarly, there were increases in the mRNA expression of COL1A1 (2.2±0.4fold; $p<0.05$), TGFβ (2.6±02fold; $p<0.05$), CTGF (3.6±0.7fold; $p<0.05$) and LOX (3.5±0.2fold; $p<0.05$) by fibroblasts from 40wk mice *in vitro* (Figure 6.5). This suggests that alterations in the response to AngII at 40wk in the myocardium were not due to inhibited fibroblast recognition of or direct response to AngII.

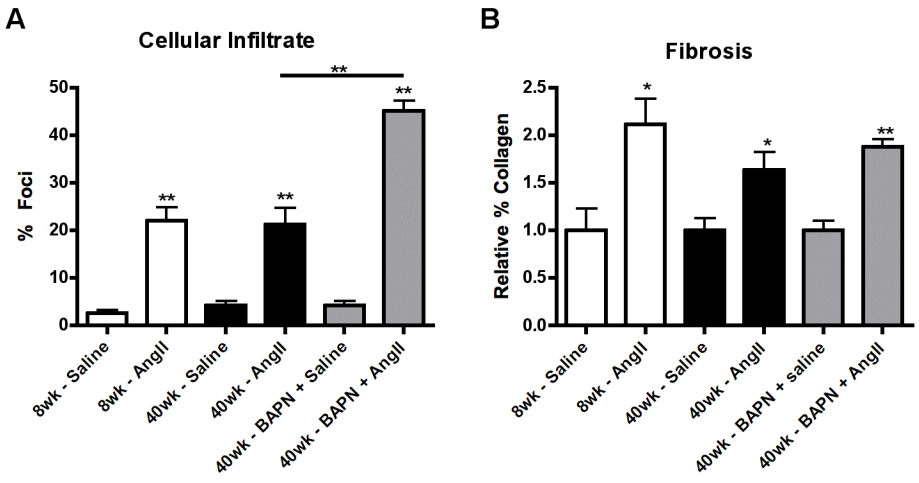

Figure 7.1 Fibrosis And Cellular Infiltration

Animals were treated with BAPN for 2wk (104.2µg/kg/min), AngII for 3d (2.0µg/kg/min) or BAPN followed by AngII. Fibrosis was assessed using Sirius red staining. The percentage of whole cross-section of myocardium stained with Sirius red was semi-quantified using image analysis software (A). The quantification of infiltrating cells was performed using a modified grid-analysis technique, comparing the number of grids affected from a representative cross section of the whole myocardium stained with H&E (B). n=6 (except for BAPN treated groups; n=3); *$p<0.05$, **$p<0.01$ compared to age-matched saline control.

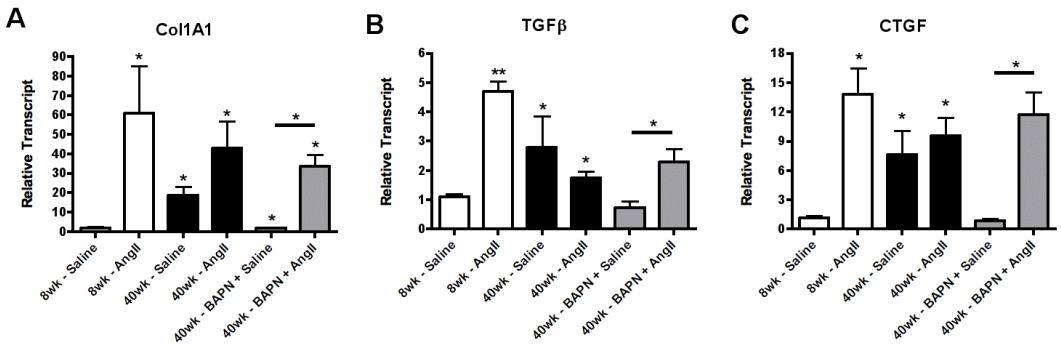

Figure 7.2 Collagen And Fibrotic Factor Expression

Expression of COL1A1 (A), TGFβ (B) and CTGF (C) mRNA in whole myocardium was assessed using qPCR and compared to the housekeeping gene 18S and is reported relative to the 8wk saline group. n=6 (except for BAPN treated groups; n=3); *$p<0.05$, **$p<0.01$ compared to 8wk saline control.

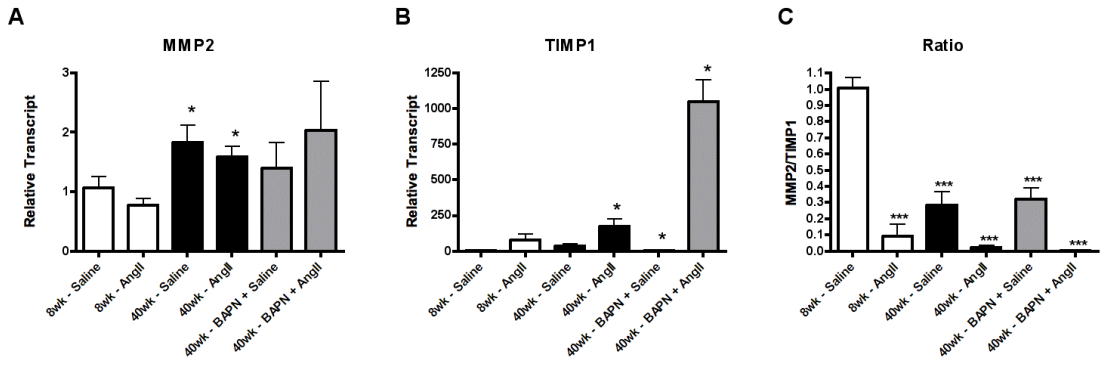

Figure 7.3 Collagen Degradation

Expression of MMP2 (A), TIMP1 (B) mRNA in whole myocardium was assessed using qPCR and compared to the housekeeping gene 18S and is reported relative to the 8wk saline group. The MMP2:TIMP1 ratio was calculate (C). n=6 (except for BAPN treated groups; n=3); *$p<0.05$, **$p<0.01$ compared to 8wk saline control.

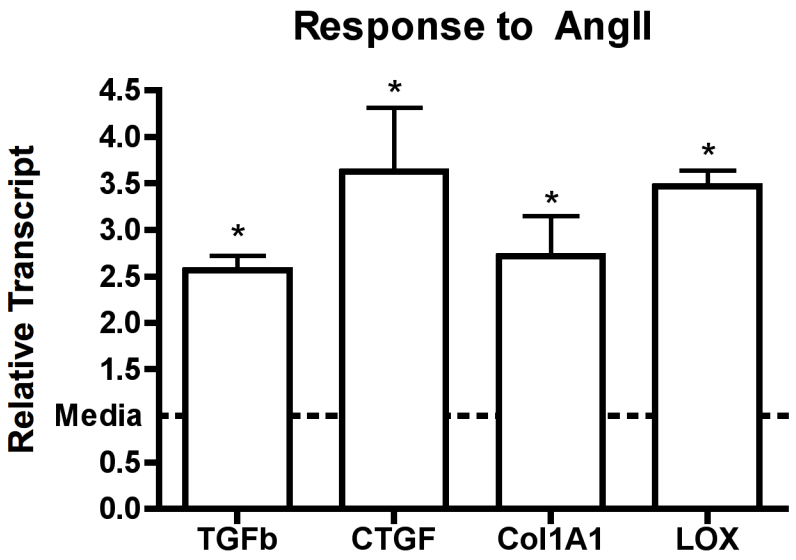

Figure 7.4 Cellular Response To AngII Exposure

Primary fibroblasts were isolated from the myocardium of animals at 40wk and treated with AngII (100nM) for 6hr. Expression of TGFβ, CTGF, Col1A1 and LOX mRNA was assessed using qPCR and compared to the housekeeping gene 18S and is reported relative to the media control. n=3; *$p<0.05$.

7.3 Discussion

Overall, this evidence suggests that the fibrotic signaling response by older animals to AngII exposure is dampened compared to at 8wk. Treatment with BAPN prior to AngII exposure ameliorated the reduction in the response to AngII, suggesting that the reduced fibrotic response was a due to established fibrosis and elevated fibrotic signaling and not due to age alone. There was an elevated baseline expression of all of the growth factors assessed and in collagen synthesis at 40wk compared to 8wk. This suggests two potential mechanisms: that the ability to respond to AngII is diminished during aging; or that there is regulatory feedback mechanism initiated that results in a threshold of fibrotic factors and collagen that is reached, regardless of the baseline expression.

After AngII exposure there was no difference in the amount of infiltration between the 8wk and 40wk groups, suggesting that AngII-initiated chemotactic signals and the migration of mononuclear cells to the myocardium were not affected by aging at 40wk. However, there was significantly more infiltration in the 40wk + BAPN group after AngII exposure, suggesting that the amount of established fibrosis can also have an effect on the ability of the infiltrating cells to migrate into the tissue. Surprisingly, the increased amount of cellular infiltration in the 40wk + BAPN group after AngII exposure did not result in an greater increase in fibrosis after 3d compared to either 8wk or 40wk after AngII, measured either with quantification of Sirius red staining or new collagen mRNA synthesis. This suggests that effector cells that infiltrated may have had a reduced ability to respond to local AngII and/or pro-fibrotic mediators or that an unknown regulatory mechanism may be involved in maintaining collagen homeostasis.

There was a compensatory increase in TIMP1 expression after AngII exposure, which was exacerbated by pretreatment with BAPN. This may be due to the reduction in crosslinked collagen observed after 40wk animals were treated with BAPN (Chapter 3). The inhibition of crosslinking results in collagen being more exposed to degradation by MMP2, which resulted in a compensatory increase in TIMP1 after AngII exposure to disrupt further degradation from occurring.

Ultimately, we did not observe differences in deposited collagen protein after AngII exposure at 40wk compared to 8wk. However, there was a reduced increase (a less robust response) in Col1A1 expression after AngII and the fibrotic growth factors did not change significantly. Interestingly, there were increases in cellular infiltration, fibrotic factor expression and MMP2:TIMP1 due to AngII exposure when comparing between animals with and without prior treatment with BAPN, suggesting that established fibrosis contributes to AngII-induced myocardial fibrosis development more than age alone (at least at 40wk).

CHAPTER 8: DISCUSSION

8.1 Summary Of Findings And Comparison To Literature

There are many similarities between the signaling pathways observed in age-related and AngII-induced myocardial fibrosis development. In particular, the involvement of TGFβ and consequent downstream signaling underscores the complex signaling mechanisms in AngII and/or hypertension to age-related myocardial fibrosis. Moreover, the complex interplay between collagen synthesis, crosslinking and degradation and the role of each of these parameters in fibrosis development are incompletely understood. The data shown in this thesis provide novel insights into these interactions, their regulation and contribution to the development of myocardial fibrosis.

The TGFβ pathway has been reported to be more active during aging, with a potential outcome of increased fibroblast proliferation, activation/differentiation to myofibroblasts and the expression of ECM proteins within the myocardium[221]. We have shown for the first time that the pro-fibrotic downstream regulators of TGFβ, including SMAD phosphorylation and CTGF expression, were increased within the myocardium as early as 40wk in our mouse model. Alterations in these downstream effectors are more specific for the fibrotic effects of the TGFβ pathway than solely assessing changes in TGFβ mRNA expression or protein concentrations. This is because TGFβ is secreted from the cell in association with an inhibitory latancy-associated peptide that must be removed before TGFβ is biologically active and able to initiate downstream signaling[45].

This is also the first time, to our knowledge that increases in collagen deposition within the myocardium were observed as early as 40wk of age, which is considered middle-aged in mice. Previous studies have generally focused on age-related changes in much older mice, at 56-64wk. It is at this older age, and in very old mice (approximately 72wk and later), when changes have been reported in aging biomarkers[144]. The early initiation of the age-related pro-fibrotic changes in the myocardium could support the potential targeting of these in the development of preventative treatments in the development of myocardial fibrosis.

Limitations of many aging studies, including our own, include such possible confounding age-associated effects of diabetes, excessive weight or alterations in calcium handling in older mice[222], which are generally not adjusted for when comparing to younger mice. In this study, we did not measure the serum glucose levels in any group, however this would be one method of assessing if there were changes during aging that could contribute to the alterations in fibrotic factors and collagen deposition that were observed. The strain of inbred mice used, C57Bl/6, have extensive records available through the breeding facility (Jackson Labs) that have reported that this strain is susceptible to high-fat diet induced type 2 diabetes and atherosclerosis. However, mice used in the current studies were fed a standard diet that should not induce diabetes.

A causative role for TGFβ in the development of age-related myocardial fibrosis has been reported in studies using a strain of mice heterozygous for a loss-of-function mutation in TGFβ (TGFβ+/-)[133]. Aged TGFβ+/- mice have less fibrosis than their age-matched wild type counterparts but still showed more fibrosis compared to younger mice. This suggests that increased activity in the TGFβ pathway contributes to the

development of age-related fibrosis in some manner but that this link is more complex. The reasons for increased TGFβ pathway signaling in aging have not yet been determined. Possible causative mechanisms for increases in TGFβ signaling include increased upstream activators, including AngII and endothelin-1 (ET1), hormonal regulators of blood pressure and cardiotrophin-1 (CT1) that increase the production of fibrotic factors in other animal models of myocardial fibrosis, and by fibroblasts *in vitro* [76, 223]. Of interest in this context is the fact that AngII has been reported to increase in the serum in aging models and both of its receptors have been reported to increase in the myocardium during aging [40, 41].

ET1 is a potent vasoconstrictor that is up-regulated in hypertensive and hypertrophic pathologies[224]. It is produced by endothelial cells and fibroblasts and acts locally through both autocrine and paracrine signaling through two g-protein receptors, ETA and ETB, that are expressed on most cell types including fibroblasts, endothelial cells and cardiomyocytes[223]. Both ETA and ETB are up-regulated during aging and in response to hypertension[76]. In addition to having hypertensive properties ET1 is hypertrophic, pro-fibrotic (increasing expression of CTGF, TGFβ), pro-inflammatory and contributes to oxidative stress, while it also has pro-survival properties[77, 224]. When AngII is infused into mice that have had ET1 selectively knocked out of vascular endothelial cells, there is a significant decrease in interstitial and perivascular fibrosis, partially due to decreases in expression of TGFβ and CTGF[223]. Due to the up-regulation of ET1 receptors with age, it is likely that ET1 signaling is involved in age-related fibrosis development as well, although a causative link in this setting has not yet been established.

CT1 is another molecule that is up-regulated after AngII exposure, in spontaneously hypertensive rats, in the presence of heart failure and that increases with aging[225]. It is produced by both cardiomyocytes and fibroblasts directly after AngII exposure as well as in response to mechanical stress, such as in during hypertrophy. CT1 is a member of the IL6 family of cytokines and signals through a heterodimeric receptor composed of gp130 and leukemia inducible factor. This receptor complex is expressed on cardiomyocytes and signaling results in cardiomyocyte growth and interruption of calcium handling by decreasing production of calsequestrin[94].

In the AngII model of hypertension-induced myocardial fibrosis, CTGF is up-regulated in the myocardium and systemically very early after AngII exposure. We focused on the role of CTGF for two reasons; (i) existing literature has established that CTGF is a potential target as a regulator of fibrosis development in many organ systems; and (ii) that it acts in a TGFβ-dependent manner (as opposed to the inflammatory signaling properties of TGFβ). We have shown for the first time that within 6hr there was a 20-fold increase in mRNA expression of CTGF. There was also an increase in CTGF mRNA *in vitro* by fibrocytes, fibroblasts, endothelial cells and cardiomyocytes after AngII exposure. This suggests that any or all of these cell types can contribute to the increase in CTGF that was observed in the animal model. CTGF is known to have many pro-fibrotic roles; increasing fibroblast proliferation, differentiation to myofibroblast phenotype and increasing the production of ECM proteins such as collagen[195]. We were able to confirm that CTGF increases proliferation, metabolic activity and the production of collagen mRNA by fibrocytes *in vitro*. This expands on previously

published studies, in which CTGF elicited similar effects by fibroblasts, supporting an effector function of both CTGF and fibrocytes in AngII-induced myocardial fibrosis.

The increase in CTGF after AngII *in vitro* was ameliorated with the anti-TGFβ blocking antibody in each of these cell types. In addition, there were increases in CTGF expression by fibroblasts after exposure to TGFβ (unpublished data 198±69fold; $p<0.01$) [109]. Taken together, these data suggest that the increase in new CTGF expression observed after AngII exposure was dependent on the presence of functional TGFβ and not a result of direct AngII signaling either through AT_1R or AT_2R, further supporting the specificity of CTGF as a downstream mediator of fibrotic-specific functions of TGFβ.

In our AngII model we found that hydralazine treatment administered through a mini-pump resulted in reduction of blood pressure, decreased cellular infiltration and decreased fibrotic factor expression. This ultimately reduced the amount of fibrosis that developed as a response to AngII exposure. Hydralazine is a vasodilator that lowers blood pressure through an AngII independent mechanism, by opening calcium dependent potassium channels in vascular smooth muscle cells[226]. This suggests that while direct AngII signaling through the local AT_1R/AT_2R contributes to fibrosis (by enhancing fibroblast differentiation, proliferation and ECM production) it is not sufficient in the absence of increased blood pressure to result in AngII induced myocardial fibrosis. However, other effects of hydralazine have been reported that do not affect vasodilation, such as increases in HIF1α expression and reduction in reactive oxygen and nitrogen species[187, 227]. In addition, isolated fibroblasts exposed to hydralazine had reduced proliferation, suggesting a secondary mechanism of action of hydralazine that is not blood pressure-mediated.

When aged spontaneously hypertensive rats are treated with hydralazine at an equal pressor dose to ARB or ACEi, most of the hypertrophy and fibrosis were ameliorated [26]. Clinically, hydralazine is only used for short durations due to the vasorelaxation not being maintained over time, an effect that may have been countered in our model by constant infusion of hydralazine from an osmotic pump. Alternately, clinical studies comparing non-RAAS hypertensive drugs such as hydralazine, calcium channel blockers or diuretics with either ARB or ACEi report that there is improvement in hypertrophy and moderate reductions in fibrosis only after treatment that interrupted RAAS signaling [183, 189, 228-230]. Unfortunately, studies using anti-hypertensive agents (ARB or ACEi) in clinical trials for elderly patients with HFpEF (heart failure with EF>40) have thus far demonstrated either no change or only moderate reduction of myocardial fibrosis and only moderate improvement in diastolic function[23-25]. This suggests that neither reducing blood pressure alone, or blocking the effects of AngII are sufficient to ameliorate fibrosis and resulting diastolic dysfunction.

As such, the involvement of direct AngII signaling through local or resident cells expressing AngII receptors should be considered when investigating myocardial fibrosis development. We addressed the involvement of direct AngII signaling using an *in vitro* model. However, this does not take into account other physical effects of hypertension, such as cellular hypertrophy and stretching of the cells that likely also contribute to age-related fibrotic signaling and collagen production.

We have reported that significant improvement to cardiac function is possible after a short exposure to BAPN, which reduced established age-related fibrosis. This appears to be due to a reduction in the amount of collagen in the myocardium after

crosslinking is inhibited. Both crosslinking and new collagen synthesis were reduced after exposure to BAPN, and it remains unclear what contribution the reduction in crosslinking compared to reduction in new collagen synthesis had on the overall reduction in deposited collagen that was observed.

We did not observe a significant increase in LOX mRNA expression or protein in the myocardium by 40wk, which may be due to high variability in the limited number of samples assessed. Nonetheless, we observed an increase in crosslinked collagen within the myocardium by 40wk. This suggests that there is an ongoing crosslinking of collagen that occurred over time that may not be reliant on an elevated amount of active crosslinking occurring at any one point in time. This also suggests that reduced degradation may contribute to the accumulation of collagen.

Reducing collagen cross-linking with a LOX inhibitor such as BAPN has previously been shown to decrease diastolic stiffness and hypertrophy[10, 231]. However, this is the first time to our knowledge that LOX inhibition resulted in changes in fibrotic factor expression. This suggests that LOX inhibition and therefore LOX have systemic effects on the regulation of collagen, beyond the direct involvement on collagen crosslinking. Altered expression of fibrotic factors after LOX inhibition occurred both in whole myocardium (after 3d) and in isolated fibroblasts (after 6hr). This suggests that the alteration of expression was due to a signaling or feedback between LOX and TGFβ and was not a secondary response to the associated interruption of collagen cross-linking.

The mechanisms of the LOX and TGFβ interaction are potentially more complicated than solely through the previously reported direct inhibition of TGFβ activity by LOX[153]. Previous literature suggests that LOX regulates protein synthesis

of HIF1α enzymatically through the mitogen activated kinase pathway (PI3K) and through reactive oxygen species production (H_2O_2)[232]. Elevation of HIF1α in turn increases the expression of TGFβ, thereby increasing fibroblast proliferation and collagen expression[233]. TGFβ also increases LOX expression and activity[154] acting as a feedback mechanism, regulating TGFβ expression and crosslinking of newly TGFβ-induced collagen production.

LOX inhibition reduces the crosslinking of ECM proteins other than collagen, including elastin[120, 151]. As discussed previously, increasing pressure through induction of hypertension in combination with LOX inhibition leads to lathyrism, a side-effect of reducing the structural support of the aorta and resulting in aneurisms[152]. In mice that were treated with BAPN alone we did not observe any signs of this side effect, heart function improved and the ventricular wall thickness increased. The short exposure period of our model to BAPN and the discontinuation of BAPN prior to the initiation of AngII exposure were used to counter the potential for aneurism development.

The intention of pre-treating 40wk animals with BAPN prior to AngII exposure was to evaluate the role of the pre-existing collagen within the myocardium on AngII-dependent myocardial fibrosis development. However, the intention of this design was confounded by the significant reduction in all pro-fibrotic signaling after exposure to BAPN alone. With BAPN exposure, changes in fibrosis development after AngII would likely be influenced by the altered fibrotic factor profile compared to age-matched controls. There was an increase in cellular infiltrate after AngII, however the fibrotic response was not as robust as in the age-matched controls animals. This suggests that signaling differences, including fibrotic factor expression that decreased significantly

after BAPN exposure may also influence the response to AngII. Alternately, either fewer of the cells responded or they were not able to respond with the same magnitude to AngII signaling compared to young animals.

Possible alterations in other signaling pathways due to aging could contribute to alterations in the fibrotic response, such as inflammatory signals that influence cellular migration. These were not investigated in the present study, but remain an area of interest. There are also age-related alterations in myocardial and cellular responses that are not yet fully understood. The ages of both myocardial/resident cells and bone-marrow derived infiltrating cells in a model of pressure overload contribute to age-related increases in fibrosis development[38]. However, isolated cardiac fibroblasts from old mice stimulated with TGFβ have less downstream phosphorylation of SMAD2 compared to cell isolated from young mice[39]. This may explain in part the increase in pro-fibrotic signaling observed in myocardium of 40wk mice; a compensatory increase in signaling could be used to counter the reduced ability of cells to respond to necessary reparative signals.

In this thesis we utilized both *in vivo* and *in vitro* experimentation. The *in vivo* experimentation is limited by our ability to understand complex *in vivo* interactions that we cannot control. *In vitro* studies allow for this control but have their own limitations. In this thesis, for example, the primary cardiac fibroblast and fibrocyte isolation was dependent on selective adherence and may have contained contaminating cells, specifically fibroblasts of other origins in the case of the fibrocytes. The isolation protocol selects for cells that adhere early, which severely limits the other cell types that may be contaminants. In addition, all observed cells expressed established mesenchymal

markers (collagen and SMA) [36], suggesting that cultured cells used for further experimentation were either fibroblasts or fibrocytes. These cell types represent a spectrum of differentiation towards myofibroblasts, the activated phenotype [234], suggesting that similar results for collagen and pro-fibrotic factor production are expected. Therefore, it is very difficult if not impossible to separate these populations completely. The origin of myofibroblasts was not the primary focus of the studies reported here, but there is evidence that they arise from many sources; resident fibroblasts, fibrocytes (hematopoetic progenitor cells), endothelial or epithelial mesenchymal transition and pericytes all differentiate into myofibroblasts [36, 235].

The primary cardiomyocytes were isolated from n1 neonatal mice and have different expression profiles of some receptors and proteins compared to adult cardiomyocytes[236]. Therefore, neonatal cardiomyocytes may respond differently to AngII than adult cardiomyocytes. Adult isolated cardiomyocytes have a finite duration of culture *in vitro* and do not proliferate well, which neonatal cardiomyocytes are capable of doing. Because we compared treatments with time-points longer than one-day we used neonatal cardiomyocytes in the current study. The primary neonatal cardiomyocytes maintained contractile ability and signal conduction for two weeks in culture. They also maintained cardiomyocyte morphology and the expression of cardiac troponin. In addition, experiments with both primary cultured cell types were used to confirm observations made in the animal models.

8.2 Future Directions

The aging studies were designed to look at how fibrosis and its development changed between groups. This did not address whether changes in fibrotic factor expression were causative or even maintained over time, which would be of key importance to understanding fibrosis development. A longitudinal study including repeated testing of fibrosis and/or fibrotic factors within the myocardium would be one method of addressing the snap shot approach of the current studies. Recent publications using MRI with, or without, the use of contrast agents have quantified collagen accumulation after MI in mice (without contrast agent using T2 mapping [237]) or in an aged patient population (with contrast agent using T1 mapping [238]); a related technique could be applied to imaging the development of myocardial fibrosis in aging mice over time. This would allow for assessment of changes that occur over time in the same individual. Correlating heart function and LOX function/amount of collagen crosslinking in a patient population would also be interesting to investigate. Specifically adjusting for cofounders such as diabetes, hypertension and treatment regimens would further our understanding of the effect of these on crosslinking, and hence on heart function.

Further investigation into the causative role of LOX and/or the interaction with TGFβ would be necessary to assess the therapeutic potential of interrupting this interaction. Animals that have reduced TGF-β (TGF-β1+/-) show decreased age-related fibrosis and preserved diastolic function, but the effects of reducing TGFβ production and activity on LOX regulation have not been assessed to our knowledge[133]. Additionally, there are newly synthesized compounds that reversibly inhibit LOX[239] that may reduce the deleterious side-effects that have been reported with BAPN

exposure. These compounds, inducible genetic knockouts of LOX or removal of LOX activity *in vitro* (siRNA or antibody based inhibition) could be used to further understand the signaling mechanisms behind the reduction in TGFβ and downstream fibrotic factor expression.

In regards to the pretreatment of BAPN followed by AngII exposure, investigating the mechanism responsible for the increased cellular infiltration would be necessary in considering the use of LOX inhibition clinically. One method for determining the cause of increased migration would be to assess the protein expression profiles of chemokines in this group using a high-throughput array. Recent studies using the AngII model have brought attention to certain chemokines, including CX3CL1, CCL2 and CXCL12[106]. However, interruption of these signaling axis individually have not had the expected anti-inflammatory effects hypothesized. This suggests that there are other chemokines involved or that there is a more complex array of chemokines responsible for migration/infiltration into the myocardium after AngII exposure.

REFERENCES

1. Creemers, E.E. and Y.M. Pinto, *Molecular mechanisms that control interstitial fibrosis in the pressure-overloaded heart.* Cardiovasc Res, 2011. **89**(2): p. 265-72.
2. Berk, B.C., K. Fujiwara, and S. Lehoux, *ECM remodeling in hypertensive heart disease.* J Clin Invest, 2007. **117**(3): p. 568-75.
3. Gurtner, G.C., et al., *Wound repair and regeneration.* Nature, 2008. **453**(7193): p. 314-21.
4. Reed, A.L., et al., *Diastolic dysfunction is associated with cardiac fibrosis in the senescence-accelerated mouse.* Am J Physiol Heart Circ Physiol, 2011. **301**(3): p. H824-31.
5. Sun, Y., *Intracardiac renin-angiotensin system and myocardial repair/remodeling following infarction.* J Mol Cell Cardiol, 2009.
6. Brilla, C.G., B. Maisch, and K.T. Weber, *Myocardial collagen matrix remodelling in arterial hypertension.* Eur Heart J, 1992. **13 Suppl D**: p. 24-32.
7. Weber, K.T., et al., *Patterns of myocardial fibrosis.* J Mol Cell Cardiol, 1989. **21 Suppl 5**: p. 121-31.
8. Weis, S.M., et al., *Myocardial mechanics and collagen structure in the osteogenesis imperfecta murine (oim).* Circ Res, 2000. **87**(8): p. 663-9.
9. Asif, M., et al., *An advanced glycation endproduct cross-link breaker can reverse age-related increases in myocardial stiffness.* Proc Natl Acad Sci U S A, 2000. **97**(6): p. 2809-13.
10. Kato, S., et al., *Inhibition of collagen cross-linking: effects on fibrillar collagen and ventricular diastolic function.* Am J Physiol, 1995. **269**(3 Pt 2): p. H863-8.
11. MacKenna, D.A., et al., *Contribution of collagen matrix to passive left ventricular mechanics in isolated rat hearts.* Am J Physiol, 1994. **266**(3 Pt 2): p. H1007-18.
12. Biernacka, A. and N.G. Frangogiannis, *Aging and Cardiac Fibrosis.* Aging Dis, 2011. **2**(2): p. 158-173.
13. Besse, S., et al., *Is the senescent heart overloaded and already failing?* Cardiovasc Drugs Ther, 1994. **8**(4): p. 581-7.
14. Bradshaw, A.D., et al., *Age-dependent alterations in fibrillar collagen content and myocardial diastolic function: role of SPARC in post-synthetic procollagen processing.* Am J Physiol Heart Circ Physiol, 2009. **298**(2): p. H614-22.
15. Barasch, E., et al., *Association between elevated fibrosis markers and heart failure in the elderly: the cardiovascular health study.* Circ Heart Fail, 2009. **2**(4): p. 303-10.
16. Yancy, C.W., et al., *2013 ACCF/AHA Guideline for the Management of Heart Failure: Executive Summary: A Report of the American College of Cardiology Foundation/American Heart Association Task Force on Practice Guidelines.* Circulation, 2013. **128**(16): p. 1810-52.
17. Zile, M.R., et al., *Prevalence and significance of alterations in cardiac structure and function in patients with heart failure and a preserved ejection fraction.* Circulation, 2011. **124**(23): p. 2491-501.
18. Chen, W. and N.G. Frangogiannis, *The role of inflammatory and fibrogenic pathways in heart failure associated with aging.* Heart Fail Rev. **15**(5): p. 415-22.

19. Wynn, T.A., *Cellular and molecular mechanisms of fibrosis.* J Pathol, 2008. **214**(2): p. 199-210.
20. Kim, S. and H. Iwao, *Molecular and cellular mechanisms of angiotensin II-mediated cardiovascular and renal diseases.* Pharmacol Rev, 2000. **52**(1): p. 11-34.
21. Ganau, A., et al., *Ageing induces left ventricular concentric remodelling in normotensive subjects.* J Hypertens, 1995. **13**(12 Pt 2): p. 1818-22.
22. Lakatta, E.G. and D. Levy, *Arterial and cardiac aging: major shareholders in cardiovascular disease enterprises: Part II: the aging heart in health: links to heart disease.* Circulation, 2003. **107**(2): p. 346-54.
23. Cleland, J.G., et al., *The perindopril in elderly people with chronic heart failure (PEP-CHF) study.* Eur Heart J, 2006. **27**(19): p. 2338-45.
24. Massie, B.M., et al., *Irbesartan in patients with heart failure and preserved ejection fraction.* N Engl J Med, 2008. **359**(23): p. 2456-67.
25. Yusuf, S., et al., *Effects of candesartan in patients with chronic heart failure and preserved left-ventricular ejection fraction: the CHARM-Preserved Trial.* Lancet, 2003. **362**(9386): p. 777-81.
26. Ito, N., et al., *Renin-angiotensin inhibition reverses advanced cardiac remodeling in aging spontaneously hypertensive rats.* Am J Hypertens, 2007. **20**(7): p. 792-9.
27. Jones, E.S., M.J. Black, and R.E. Widdop, *Angiotensin AT2 receptor contributes to cardiovascular remodelling of aged rats during chronic AT1 receptor blockade.* J Mol Cell Cardiol, 2004. **37**(5): p. 1023-30.
28. Saupe, K.W., et al., *Effects of AT1 receptor block begun late in life on normal cardiac aging in rats.* J Cardiovasc Pharmacol, 2003. **42**(4): p. 573-80.
29. Dostal, D.E., G.W. Booz, and K.M. Baker, *Angiotensin II signalling pathways in cardiac fibroblasts: conventional versus novel mechanisms in mediating cardiac growth and function.* Mol Cell Biochem, 1996. **157**(1-2): p. 15-21.
30. Sadoshima, J. and S. Izumo, *Molecular characterization of angiotensin II--induced hypertrophy of cardiac myocytes and hyperplasia of cardiac fibroblasts. Critical role of the AT1 receptor subtype.* Circ Res, 1993. **73**(3): p. 413-23.
31. Crabos, M., et al., *Characterization of angiotensin II receptors in cultured adult rat cardiac fibroblasts. Coupling to signaling systems and gene expression.* J Clin Invest, 1994. **93**(6): p. 2372-8.
32. Zhou, G., et al., *Effects of angiotensin II and aldosterone on collagen gene expression and protein turnover in cardiac fibroblasts.* Mol Cell Biochem, 1996. **154**(2): p. 171-8.
33. Towbin, J.A., *Scarring in the heart--a reversible phenomenon?* N Engl J Med, 2007. **357**(17): p. 1767-8.
34. Fan, D., et al., *Cardiac fibroblasts, fibrosis and extracellular matrix remodeling in heart disease.* Fibrogenesis Tissue Repair, 2012. **5**(1): p. 15.
35. Baum, J. and H.S. Duffy, *Fibroblasts and myofibroblasts: what are we talking about?* J Cardiovasc Pharmacol, 2011. **57**(4): p. 376-9.
36. Krenning, G., E.M. Zeisberg, and R. Kalluri, *The origin of fibroblasts and mechanism of cardiac fibrosis.* J Cell Physiol, 2010. **225**(3): p. 631-7.

37. Sopel, M.J., et al., *Myocardial fibrosis in response to Angiotensin II is preceded by the recruitment of mesenchymal progenitor cells.* Lab Invest, 2010. **91**(4): p. 565-78.
38. Sopko, N.A., et al., *Bone marrow support of the heart in pressure overload is lost with aging.* PLoS One, 2011. **5**(12): p. e15187.
39. Bujak, M., et al., *Aging-related defects are associated with adverse cardiac remodeling in a mouse model of reperfused myocardial infarction.* J Am Coll Cardiol, 2008. **51**(14): p. 1384-92.
40. Shivakumar, K., et al., *Differential response of cardiac fibroblasts from young adult and senescent rats to ANG II.* Am J Physiol Heart Circ Physiol, 2003. **284**(4): p. H1454-9.
41. Heymes, C., et al., *Cardiac senescence is associated with enhanced expression of angiotensin II receptor subtypes.* Endocrinology, 1998. **139**(5): p. 2579-87.
42. Annoni, G., et al., *Age-dependent expression of fibrosis-related genes and collagen deposition in the rat myocardium.* Mech Ageing Dev, 1998. **101**(1-2): p. 57-72.
43. Khan, R. and R. Sheppard, *Fibrosis in heart disease: understanding the role of transforming growth factor-beta in cardiomyopathy, valvular disease and arrhythmia.* Immunology, 2006. **118**(1): p. 10-24.
44. Grainger, D.J., *TGF-beta and atherosclerosis in man.* Cardiovasc Res, 2007. **74**(2): p. 213-22.
45. Ruiz-Ortega, M., et al., *TGF-beta signaling in vascular fibrosis.* Cardiovasc Res, 2007. **74**(2): p. 196-206.
46. Ikedo, H., et al., *Smad protein and TGF-beta signaling in vascular smooth muscle cells.* Int J Mol Med, 2003. **11**(5): p. 645-50.
47. Cieslik, K.A., et al., *Immune-inflammatory dysregulation modulates the incidence of progressive fibrosis and diastolic stiffness in the aging heart.* J Mol Cell Cardiol, 2011. **50**(1): p. 248-56.
48. Chiao, Y.A., et al., *Matrix metalloproteinase-9 deletion attenuates myocardial fibrosis and diastolic dysfunction in ageing mice.* Cardiovasc Res, 2012. **96**(3): p. 444-55.
49. Ricard-Blum, S., *The collagen family.* Cold Spring Harb Perspect Biol, 2011. **3**(1): p. a004978.
50. Ghosh, A.K., *Factors involved in the regulation of type I collagen gene expression: implication in fibrosis.* Exp Biol Med (Maywood), 2002. **227**(5): p. 301-14.
51. Gelse, K., E. Poschl, and T. Aigner, *Collagens--structure, function, and biosynthesis.* Adv Drug Deliv Rev, 2003. **55**(12): p. 1531-46.
52. Baynes, J.W., *The role of AGEs in aging: causation or correlation.* Exp Gerontol, 2001. **36**(9): p. 1527-37.
53. Jensen, L.J., J. Ostergaard, and A. Flyvbjerg, *AGE-RAGE and AGE Cross-link interaction: important players in the pathogenesis of diabetic kidney disease.* Horm Metab Res, 2005. **37 Suppl 1**: p. 26-34.
54. Schmidt, A.M., et al., *The biology of the receptor for advanced glycation end products and its ligands.* Biochim Biophys Acta, 2000. **1498**(2-3): p. 99-111.

55. Reiser, K.M., *Influence of age and long-term dietary restriction on enzymatically mediated crosslinks and nonenzymatic glycation of collagen in mice.* J Gerontol, 1994. **49**(2): p. B71-9.
56. Lopez, B., et al., *Role of lysyl oxidase in myocardial fibrosis: from basic science to clinical aspects.* Am J Physiol Heart Circ Physiol, 2010. **299**(1): p. H1-9.
57. Chang, K., et al., *Increased collagen cross-linkages in experimental diabetes: reversal by beta-aminopropionitrile and D-penicillamine.* Diabetes, 1980. **29**(10): p. 778-81.
58. Boluyt, M.O., O.H. Bing, and E.G. Lakatta, *The ageing spontaneously hypertensive rat as a model of the transition from stable compensated hypertrophy to heart failure.* Eur Heart J, 1995. **16 Suppl N**: p. 19-30.
59. Yu, Q. and I. Stamenkovic, *Cell surface-localized matrix metalloproteinase-9 proteolytically activates TGF-beta and promotes tumor invasion and angiogenesis.* Genes Dev, 2000. **14**(2): p. 163-76.
60. Bergman, M.R., et al., *Cardiac matrix metalloproteinase-2 expression independently induces marked ventricular remodeling and systolic dysfunction.* Am J Physiol Heart Circ Physiol, 2007. **292**(4): p. H1847-60.
61. Matsusaka, H., et al., *Targeted deletion of matrix metalloproteinase 2 ameliorates myocardial remodeling in mice with chronic pressure overload.* Hypertension, 2006. **47**(4): p. 711-7.
62. Heymans, S., et al., *Loss or inhibition of uPA or MMP-9 attenuates LV remodeling and dysfunction after acute pressure overload in mice.* Am J Pathol, 2005. **166**(1): p. 15-25.
63. Okada, M., H. Yamawaki, and Y. Hara, *Angiotensin II enhances interleukin-1 beta-induced MMP-9 secretion in adult rat cardiac fibroblasts.* J Vet Med Sci, 2010. **72**(6): p. 735-9.
64. Li, H., et al., *MMP/TIMP expression in spontaneously hypertensive heart failure rats: the effect of ACE- and MMP-inhibition.* Cardiovasc Res, 2000. **46**(2): p. 298-306.
65. Sakata, Y., et al., *Activation of matrix metalloproteinases precedes left ventricular remodeling in hypertensive heart failure rats: its inhibition as a primary effect of Angiotensin-converting enzyme inhibitor.* Circulation, 2004. **109**(17): p. 2143-9.
66. Lopez, B., et al., *Association of plasma cardiotrophin-1 with stage C heart failure in hypertensive patients: potential diagnostic implications.* J Hypertens, 2009. **27**(2): p. 418-24.
67. Sivakumar, P., et al., *Upregulation of lysyl oxidase and MMPs during cardiac remodeling in human dilated cardiomyopathy.* Mol Cell Biochem, 2008. **307**(1-2): p. 159-67.
68. Hermida, N., et al., *A synthetic peptide from transforming growth factor-beta1 type III receptor prevents myocardial fibrosis in spontaneously hypertensive rats.* Cardiovasc Res, 2009. **81**(3): p. 601-9.
69. Bing, O.H., et al., *The effect of lathyrogen beta-amino proprionitrile (BAPN) on the mechanical properties of experimentally hypertrophied rat cardiac muscle.* Circ Res, 1978. **43**(4): p. 632-7.

70. Boak, A.M., et al., *Regulation of lysyl oxidase expression in lung fibroblasts by transforming growth factor-beta 1 and prostaglandin E2.* Am J Respir Cell Mol Biol, 1994. **11**(6): p. 751-5.
71. Mervaala, E., et al., *Blood pressure-independent effects in rats with human renin and angiotensinogen genes.* Hypertension, 2000. **35**(2): p. 587-94.
72. Mehta, P.K. and K.K. Griendling, *Angiotensin II cell signaling: physiological and pathological effects in the cardiovascular system.* Am J Physiol Cell Physiol, 2007. **292**(1): p. C82-97.
73. Carey, R.M. and H.M. Siragy, *Newly recognized components of the renin-angiotensin system: potential roles in cardiovascular and renal regulation.* Endocr Rev, 2003. **24**(3): p. 261-71.
74. Sakai, N., et al., *The renin-angiotensin system contributes to renal fibrosis through regulation of fibrocytes.* J Hypertens, 2008. **26**(4): p. 780-90.
75. Kai, H., et al., *Large blood pressure variability and hypertensive cardiac remodeling--role of cardiac inflammation.* Circ J, 2009. **73**(12): p. 2198-203.
76. Ishihata, A. and Y. Katano, *Role of angiotensin II and endothelin-1 receptors in aging-related functional changes in rat cardiovascular system.* Ann N Y Acad Sci, 2006. **1067**: p. 173-81.
77. Laplante, M.A. and J. de Champlain, *The interrelation of the angiotensin and endothelin systems on the modulation of NAD(P)H oxidase.* Can J Physiol Pharmacol, 2006. **84**(1): p. 21-8.
78. Billet, S., et al., *Gain-of-function mutant of angiotensin II receptor, type 1A, causes hypertension and cardiovascular fibrosis in mice.* J Clin Invest, 2007. **117**(7): p. 1914-25.
79. Rosin, N.L., et al., *Myocardial migration by fibroblast progenitor cells is blood pressure dependent in a model of angII myocardial fibrosis.* Hypertens Res, 2010.
80. Bedard, K. and K.H. Krause, *The NOX family of ROS-generating NADPH oxidases: physiology and pathophysiology.* Physiol Rev, 2007. **87**(1): p. 245-313.
81. Chen, W. and N.G. Frangogiannis, *The role of inflammatory and fibrogenic pathways in heart failure associated with aging.* Heart Fail Rev, 2010. **15**(5): p. 415-22.
82. Dai, D.F. and P.S. Rabinovitch, *Cardiac aging in mice and humans: the role of mitochondrial oxidative stress.* Trends Cardiovasc Med, 2009. **19**(7): p. 213-20.
83. Hein, L., et al., *Behavioural and cardiovascular effects of disrupting the angiotensin II type-2 receptor in mice.* Nature, 1995. **377**(6551): p. 744-7.
84. Rompe, F., et al., *Direct angiotensin II type 2 receptor stimulation acts anti-inflammatory through epoxyeicosatrienoic acid and inhibition of nuclear factor kappaB.* Hypertension, 2010. **55**(4): p. 924-31.
85. Probstfield, J.L. and K.D. O'Brien, *Progression of cardiovascular damage: the role of renin-angiotensin system blockade.* Am J Cardiol, 2010. **105**(1 Suppl): p. 10A-20A.
86. Sun, Y., *Myocardial repair/remodelling following infarction: roles of local factors.* Cardiovasc Res, 2009. **81**(3): p. 482-90.
87. Sopel, M.J., et al., *Myocardial fibrosis in response to Angiotensin II is preceded by the recruitment of mesenchymal progenitor cells.* Lab Invest.

88. Sugiyama, F., K. Yagami, and B. Paigen, *Mouse models of blood pressure regulation and hypertension.* Curr Hypertens Rep, 2001. **3**(1): p. 41-8.
89. Yancy, C.W., et al., *2013 ACCF/AHA guideline for the management of heart failure: a report of the American College of Cardiology Foundation/American Heart Association Task Force on Practice Guidelines.* J Am Coll Cardiol, 2013. **62**(16): p. e147-239.
90. Ferrari, R., et al., *Mechanisms of remodelling: a question of life (stem cell production) and death (myocyte apoptosis).* Circ J, 2009. **73**(11): p. 1973-82.
91. Boyle, A.J., et al., *Cardiomyopathy of aging in the mammalian heart is characterized by myocardial hypertrophy, fibrosis and a predisposition towards cardiomyocyte apoptosis and autophagy.* Exp Gerontol, 2011. **46**(7): p. 549-59.
92. Zolk, O., et al., *Chronic cardiotrophin-1 stimulation impairs contractile function in reconstituted heart tissue.* Am J Physiol Endocrinol Metab, 2005. **288**(6): p. E1214-21.
93. Swynghedauw, B., *Molecular mechanisms of myocardial remodeling.* Physiol Rev, 1999. **79**(1): p. 215-62.
94. Gonzalez, A., et al., *Biochemical markers of myocardial remodelling in hypertensive heart disease.* Cardiovasc Res, 2009. **81**(3): p. 509-18.
95. Chu, P.Y., et al., *Bone marrow-derived cells contribute to fibrosis in the chronically failing heart.* Am J Pathol, 2010. **176**(4): p. 1735-42.
96. Haudek, S.B., et al., *Monocytic fibroblast precursors mediate fibrosis in angiotensin-II-induced cardiac hypertrophy.* J Mol Cell Cardiol, 2010. **49**(3): p. 499-507.
97. Abe, R., et al., *Peripheral blood fibrocytes: differentiation pathway and migration to wound sites.* J Immunol, 2001. **166**(12): p. 7556-62.
98. Pilling, D., et al., *Identification of markers that distinguish monocyte-derived fibrocytes from monocytes, macrophages, and fibroblasts.* PLoS One, 2009. **4**(10): p. e7475.
99. Kisseleva, T., et al., *Bone marrow-derived fibrocytes participate in pathogenesis of liver fibrosis.* J Hepatol, 2006. **45**(3): p. 429-38.
100. Andersson-Sjoland, A., et al., *Fibrocytes are a potential source of lung fibroblasts in idiopathic pulmonary fibrosis.* Int J Biochem Cell Biol, 2008. **40**(10): p. 2129-40.
101. Wang, J.F., et al., *Fibrocytes from burn patients regulate the activities of fibroblasts.* Wound Repair Regen, 2007. **15**(1): p. 113-21.
102. Roderfeld, M., et al., *Bone marrow transplantation demonstrates medullar origin of CD34+ fibrocytes and ameliorates hepatic fibrosis in Abcb4-/- mice.* Hepatology, 2010. **51**(1): p. 267-76.
103. Bellini, A. and S. Mattoli, *The role of the fibrocyte, a bone marrow-derived mesenchymal progenitor, in reactive and reparative fibroses.* Lab Invest, 2007. **87**(9): p. 858-70.
104. Moore, B.B., et al., *CCR2-mediated recruitment of fibrocytes to the alveolar space after fibrotic injury.* Am J Pathol, 2005. **166**(3): p. 675-84.
105. Phillips, R.J., et al., *Circulating fibrocytes traffic to the lungs in response to CXCL12 and mediate fibrosis.* J Clin Invest, 2004. **114**(3): p. 438-46.

106. Falkenham, A., et al., *Early fibroblast progenitor cell migration to the AngII-exposed myocardium is not CXCL12 or CCL2 dependent as previously thought.* Am J Pathol, 2013. **183**(2): p. 459-69.
107. Rosenkranz, S., *TGF-beta1 and angiotensin networking in cardiac remodeling.* Cardiovasc Res, 2004. **63**(3): p. 423-32.
108. Xu, Q., et al., *In vitro models of TGF-beta-induced fibrosis suitable for high-throughput screening of antifibrotic agents.* Am J Physiol Renal Physiol, 2007. **293**(2): p. F631-40.
109. Campbell, S.E. and L.C. Katwa, *Angiotensin II stimulated expression of transforming growth factor-beta1 in cardiac fibroblasts and myofibroblasts.* J Mol Cell Cardiol, 1997. **29**(7): p. 1947-58.
110. Ruiz-Ortega, M., et al., *Molecular mechanisms of angiotensin II-induced vascular injury.* Curr Hypertens Rep, 2003. **5**(1): p. 73-9.
111. Rodriguez-Vita, J., et al., *Angiotensin II activates the Smad pathway in vascular smooth muscle cells by a transforming growth factor-beta-independent mechanism.* Circulation, 2005. **111**(19): p. 2509-17.
112. Ahmed, M.S., et al., *Connective tissue growth factor--a novel mediator of angiotensin II-stimulated cardiac fibroblast activation in heart failure in rats.* J Mol Cell Cardiol, 2004. **36**(3): p. 393-404.
113. Grotendorst, G.R., H. Okochi, and N. Hayashi, *A novel transforming growth factor beta response element controls the expression of the connective tissue growth factor gene.* Cell Growth Differ, 1996. **7**(4): p. 469-80.
114. Ruperez, M., et al., *Connective tissue growth factor is a mediator of angiotensin II-induced fibrosis.* Circulation, 2003. **108**(12): p. 1499-505.
115. Wang, X., et al., *Regulation of pro-inflammatory and pro-fibrotic factors by CCN2/CTGF in H9c2 cardiomyocytes.* J Cell Commun Signal. **4**(1): p. 15-23.
116. Matsui, Y. and J. Sadoshima, *Rapid upregulation of CTGF in cardiac myocytes by hypertrophic stimuli: implication for cardiac fibrosis and hypertrophy.* J Mol Cell Cardiol, 2004. **37**(2): p. 477-81.
117. Perbal, B., *CCN proteins: multifunctional signalling regulators.* Lancet, 2004. **363**(9402): p. 62-4.
118. Holmes, A., et al., *CTGF and SMADs, maintenance of scleroderma phenotype is independent of SMAD signaling.* J Biol Chem, 2001. **276**(14): p. 10594-601.
119. Endo, J., et al., *Bone marrow derived cells are involved in the pathogenesis of cardiac hypertrophy in response to pressure overload.* Circulation, 2007. **116**(10): p. 1176-84.
120. Kanematsu, Y., et al., *Pharmacologically induced thoracic and abdominal aortic aneurysms in mice.* Hypertension, 2010. **55**(5): p. 1267-74.
121. Inaba, S., et al., *Temporary treatment with AT1 receptor blocker, valsartan, from early stage of hypertension prevented vascular remodeling.* Am J Hypertens, 2011. **24**(5): p. 550-6.
122. Li, C., R. Salisbury, and D. Ely, *Hydralazine reverses stress-induced elevations in blood pressure, angiotensin II, testosterone, and coronary pathology in a social colony model.* ISRN Pathology, 2011. **2011**.

123. Teichholz, L.E., et al., *Problems in echocardiographic volume determinations: echocardiographic-angiographic correlations in the presence of absence of asynergy.* Am J Cardiol, 1976. **37**(1): p. 7-11.
124. Wang, G.W. and Y.J. Kang, *Inhibition of doxorubicin toxicity in cultured neonatal mouse cardiomyocytes with elevated metallothionein levels.* J Pharmacol Exp Ther, 1999. **288**(3): p. 938-44.
125. Marshall, R.P., R.J. McAnulty, and G.J. Laurent, *Angiotensin II is mitogenic for human lung fibroblasts via activation of the type 1 receptor.* Am J Respir Crit Care Med, 2000. **161**(6): p. 1999-2004.
126. Wolf, G., et al., *Angiotensin II-induced hypertrophy of cultured murine proximal tubular cells is mediated by endogenous transforming growth factor-beta.* J Clin Invest, 1993. **92**(3): p. 1366-72.
127. Lee, C.H., et al., *CTGF directs fibroblast differentiation from human mesenchymal stem/stromal cells and defines connective tissue healing in a rodent injury model.* J Clin Invest, 2010. **120**(9): p. 3340-9.
128. Garrett, Q., et al., *Involvement of CTGF in TGF-beta1-stimulation of myofibroblast differentiation and collagen matrix contraction in the presence of mechanical stress.* Invest Ophthalmol Vis Sci, 2004. **45**(4): p. 1109-16.
129. Li, W., et al., *Lysyl oxidase oxidizes basic fibroblast growth factor and inactivates its mitogenic potential.* J Cell Biochem, 2003. **88**(1): p. 152-64.
130. Rosin, N.L., et al., *Regulation and Role of Connective Tissue Growth Factor in AngII-Induced Myocardial Fibrosis.* Am J Pathol, 2013. **182**(3): p. 714-26.
131. Underwood, R.A., et al., *Color subtractive-computer-assisted image analysis for quantification of cutaneous nerves in a diabetic mouse model.* J Histochem Cytochem, 2001. **49**(10): p. 1285-91.
132. Pfaffl, M.W., *A new mathematical model for relative quantification in real-time RT-PCR.* Nucleic Acids Res, 2001. **29**(9): p. e45.
133. Brooks, W.W. and C.H. Conrad, *Myocardial fibrosis in transforming growth factor beta(1)heterozygous mice.* J Mol Cell Cardiol, 2000. **32**(2): p. 187-95.
134. Wang, X., et al., *Regulation of pro-inflammatory and pro-fibrotic factors by CCN2/CTGF in H9c2 cardiomyocytes.* J Cell Commun Signal, 2010. **4**(1): p. 15-23.
135. Weber, K.T., et al., *Collagen network of the myocardium: function, structural remodeling and regulatory mechanisms.* J Mol Cell Cardiol, 1994. **26**(3): p. 279-92.
136. Lindsey, M.L., et al., *Age-dependent changes in myocardial matrix metalloproteinase/tissue inhibitor of metalloproteinase profiles and fibroblast function.* Cardiovasc Res, 2005. **66**(2): p. 410-9.
137. Turner, N.A. and K.E. Porter, *Regulation of myocardial matrix metalloproteinase expression and activity by cardiac fibroblasts.* IUBMB Life, 2012. **64**(2): p. 143-50.
138. Koitabashi, N., et al., *Increased connective tissue growth factor relative to brain natriuretic peptide as a determinant of myocardial fibrosis.* Hypertension, 2007. **49**(5): p. 1120-7.
139. Trojanowska, M., *Role of PDGF in fibrotic diseases and systemic sclerosis.* Rheumatology (Oxford), 2008. **47 Suppl 5**: p. v2-4.

140. Detillieux, K.A., et al., *Biological activities of fibroblast growth factor-2 in the adult myocardium.* Cardiovasc Res, 2003. **57**(1): p. 8-19.
141. Lucero, H.A. and H.M. Kagan, *Lysyl oxidase: an oxidative enzyme and effector of cell function.* Cell Mol Life Sci, 2006. **63**(19-20): p. 2304-16.
142. Fischer, M., et al., *Prevalence of left ventricular diastolic dysfunction in the community. Results from a Doppler echocardiographic-based survey of a population sample.* Eur Heart J, 2003. **24**(4): p. 320-8.
143. Cieslik, K.A., J. Trial, and M.L. Entman, *Defective myofibroblast formation from mesenchymal stem cells in the aging murine heart rescue by activation of the AMPK pathway.* Am J Pathol, 2011. **179**(4): p. 1792-806.
144. Fox, J.G., *The Mouse in biomedical research*, in *American College of Laboratory Animal Medicine series*2007, Academic Press,: Amsterdam ; New York. p. 4 v. (ca. 1600 p.).
145. Domenighetti, A.A., et al., *Angiotensin II-mediated phenotypic cardiomyocyte remodeling leads to age-dependent cardiac dysfunction and failure.* Hypertension, 2005. **46**(2): p. 426-32.
146. Groban, L., et al., *Differential effects of late-life initiation of low-dose enalapril and losartan on diastolic function in senescent Fischer 344 x Brown Norway male rats.* Age (Dordr), 2012. **34**(4): p. 831-43.
147. Oxenham, H. and N. Sharpe, *Cardiovascular aging and heart failure.* Eur J Heart Fail, 2003. **5**(4): p. 427-34.
148. Cai, H., et al., *Investigation of thrombospondin-1 and transforming growth factor-beta expression in the heart of aging mice.* Exp Ther Med, 2012. **3**(3): p. 433-436.
149. Vater, C.A., E.D. Harris, Jr., and R.C. Siegel, *Native cross-links in collagen fibrils induce resistance to human synovial collagenase.* Biochem J, 1979. **181**(3): p. 639-45.
150. Tang, S.S., P.C. Trackman, and H.M. Kagan, *Reaction of aortic lysyl oxidase with beta-aminopropionitrile.* J Biol Chem, 1983. **258**(7): p. 4331-8.
151. Isoyama, S., et al., *Collagen deposition and the reversal of coronary reserve in cardiac hypertrophy.* Hypertension, 1992. **20**(4): p. 491-500.
152. Rucker, R.B., et al., *Copper, lysyl oxidase, and extracellular matrix protein cross-linking.* Am J Clin Nutr, 1998. **67**(5 Suppl): p. 996S-1002S.
153. Atsawasuwan, P., et al., *Lysyl oxidase binds transforming growth factor-beta and regulates its signaling via amine oxidase activity.* J Biol Chem, 2008. **283**(49): p. 34229-40.
154. Voloshenyuk, T.G., et al., *Induction of cardiac fibroblast lysyl oxidase by TGF-beta1 requires PI3K/Akt, Smad3, and MAPK signaling.* Cytokine, 2011. **55**(1): p. 90-7.
155. Ishiyama, Y., et al., *Upregulation of angiotensin-converting enzyme 2 after myocardial infarction by blockade of angiotensin II receptors.* Hypertension, 2004. **43**(5): p. 970-6.
156. de Resende, M.M., K. Kauser, and J.G. Mill, *Regulation of cardiac and renal mineralocorticoid receptor expression by captopril following myocardial infarction in rats.* Life Sci, 2006. **78**(26): p. 3066-73.

157. Zhao, Q., et al., *Essential role of vascular endothelial growth factor in angiotensin II-induced vascular inflammation and remodeling.* Hypertension, 2004. **44**(3): p. 264-70.
158. Brasier, A.R., A. Recinos, 3rd, and M.S. Eledrisi, *Vascular inflammation and the renin-angiotensin system.* Arterioscler Thromb Vasc Biol, 2002. **22**(8): p. 1257-66.
159. Schmieder, R.E., et al., *Renin-angiotensin system and cardiovascular risk.* Lancet, 2007. **369**(9568): p. 1208-19.
160. Liu, J., et al., *NAD(P)H oxidase mediates angiotensin II-induced vascular macrophage infiltration and medial hypertrophy.* Arterioscler Thromb Vasc Biol, 2003. **23**(5): p. 776-82.
161. Billet, S., et al., *Role of angiotensin II AT1 receptor activation in cardiovascular diseases.* Kidney Int, 2008. **74**(11): p. 1379-84.
162. Harada, K., et al., *Pressure overload induces cardiac hypertrophy in angiotensin II type 1A receptor knockout mice.* Circulation, 1998. **97**(19): p. 1952-9.
163. Li, H.L., et al., *Overexpression of myofibrillogenesis regulator-1 aggravates cardiac hypertrophy induced by angiotensin II in mice.* Hypertension, 2007. **49**(6): p. 1399-408.
164. Haudek, S.B., et al., *Bone marrow-derived fibroblast precursors mediate ischemic cardiomyopathy in mice.* Proc Natl Acad Sci U S A, 2006. **103**(48): p. 18284-9.
165. Haudek, S.B., et al., *Fc receptor engagement mediates differentiation of cardiac fibroblast precursor cells.* Proc Natl Acad Sci U S A, 2008. **105**(29): p. 10179-84.
166. Castanio AP, L.S., Surowy T, Nowlin BT, Turlapati SA, Patel T, Singh A, Li S, Lupher ML, Duffield JS, *Serum amyloid P inhibits fibrosis through FCgR-dependen monocyte-macrophage regulation in vivo.* Science Translational Medicine, 2009. **1**(5): p. 1-11.
167. Marvar, P.J., et al., *Central and peripheral mechanisms of T-lymphocyte activation and vascular inflammation produced by angiotensin II-induced hypertension.* Circ Res. **107**(2): p. 263-70.
168. Qi, G., et al., *Angiotensin II Infusion-Induced Inflammation, Monocytic Fibroblast Precursor Infiltration, and Cardiac Fibrosis are Pressure Dependent.* Cardiovasc Toxicol.
169. Haudek, S.B., et al., *Monocytic fibroblast precursors mediate fibrosis in angiotensin-II-induced cardiac hypertrophy.* J Mol Cell Cardiol.
170. He, Z., et al., *Differential regulation of angiotensin II-induced expression of connective tissue growth factor by protein kinase C isoforms in the myocardium.* J Biol Chem, 2005. **280**(16): p. 15719-26.
171. Chen, M.M., et al., *CTGF expression is induced by TGF- beta in cardiac fibroblasts and cardiac myocytes: a potential role in heart fibrosis.* J Mol Cell Cardiol, 2000. **32**(10): p. 1805-19.
172. Frenette, P.S. and D.D. Wagner, *Adhesion molecules--Part II: Blood vessels and blood cells.* N.Engl.J.Med., 1996. **335**(1): p. 43-45.
173. Frenette, P.S. and D.D. Wagner, *Adhesion molecules--Part 1.* N.Engl.J.Med., 1996. **334**(23): p. 1526-1529.
174. Sallusto, F. and C.R. Mackay, *Chemoattractants and their receptors in homeostasis and inflammation.* Curr.Opin.Immunol., 2004. **16**(6): p. 724-731.

175. Olson, T.S. and K. Ley, *Chemokines and chemokine receptors in leukocyte trafficking.* Am.J.Physiol Regul.Integr.Comp Physiol, 2002. **283**(1): p. R7-28.
176. Luster, A.D., *Chemokines--chemotactic cytokines that mediate inflammation.* N Engl J Med, 1998. **338**(7): p. 436-45.
177. Keeley, E.C., B. Mehrad, and R.M. Strieter, *The role of circulating mesenchymal progenitor cells (fibrocytes) in the pathogenesis of fibrotic disorders.* Thromb Haemost, 2009. **101**(4): p. 613-8.
178. Sakai, N., et al., *Secondary lymphoid tissue chemokine (SLC/CCL21)/CCR7 signaling regulates fibrocytes in renal fibrosis.* Proc Natl Acad Sci U S A, 2006. **103**(38): p. 14098-103.
179. Chen, J., et al., *Hypertension does not account for the accelerated atherosclerosis and development of aneurysms in male apolipoprotein e/endothelial nitric oxide synthase double knockout mice.* Circulation, 2001. **104**(20): p. 2391-4.
180. Paradis, P., et al., *Overexpression of angiotensin II type I receptor in cardiomyocytes induces cardiac hypertrophy and remodeling.* Proc Natl Acad Sci U S A, 2000. **97**(2): p. 931-6.
181. Watanabe, D., et al., *Renoprotective effects of an angiotensin II receptor blocker in experimental model rats with hypertension and metabolic disorders.* Hypertens Res, 2009. **32**(9): p. 807-15.
182. Shibata, S., et al., *Podocyte as the target for aldosterone: roles of oxidative stress and Sgk1.* Hypertension, 2007. **49**(2): p. 355-64.
183. Cheng, X.W., et al., *Mechanism of diastolic stiffening of the failing myocardium and its prevention by angiotensin receptor and calcium channel blockers.* J Cardiovasc Pharmacol, 2009. **54**(1): p. 47-56.
184. Nagata, K., et al., *Mineralocorticoid receptor antagonism attenuates cardiac hypertrophy and failure in low-aldosterone hypertensive rats.* Hypertension, 2006. **47**(4): p. 656-64.
185. Habibi, J., et al., *Mineralocorticoid Receptor Blockade Improves Diastolic Function Independent of Blood Pressure Reduction in Transgenic Model of Raas Overexpression.* Am J Physiol Heart Circ Physiol.
186. Rey, S. and G.L. Semenza, *Hypoxia-inducible factor-1-dependent mechanisms of vascularization and vascular remodelling.* Cardiovasc Res. **86**(2): p. 236-42.
187. Knowles, H.J., et al., *Novel mechanism of action for hydralazine: induction of hypoxia-inducible factor-1alpha, vascular endothelial growth factor, and angiogenesis by inhibition of prolyl hydroxylases.* Circ Res, 2004. **95**(2): p. 162-9.
188. Lin, M., et al., *Vasodilator therapy in chronic asymptomatic aortic regurgitation: enalapril versus hydralazine therapy.* J Am Coll Cardiol, 1994. **24**(4): p. 1046-53.
189. Schmieder, R.E., et al., *Update on reversal of left ventricular hypertrophy in essential hypertension (a meta-analysis of all randomized double-blind studies until December 1996).* Nephrol Dial Transplant, 1998. **13**(3): p. 564-9.
190. Greenberg, B., et al., *Long-term vasodilator therapy of chronic aortic insufficiency. A randomized double-blinded, placebo-controlled clinical trial.* Circulation, 1988. **78**(1): p. 92-103.
191. Yang, F., et al., *Angiotensin II induces connective tissue growth factor and collagen I expression via transforming growth factor-beta-dependent and -*

independent Smad pathways: the role of Smad3. Hypertension, 2009. **54**(4): p. 877-84.
192. Huang, X.R., et al., *Smad3 mediates cardiac inflammation and fibrosis in angiotensin II-induced hypertensive cardiac remodeling.* Hypertension, 2010. **55**(5): p. 1165-71.
193. Sonnylal, S., et al., *Selective expression of connective tissue growth factor in fibroblasts in vivo promotes systemic tissue fibrosis.* Arthritis Rheum, 2010. **62**(5): p. 1523-32.
194. Shi-Wen, X., A. Leask, and D. Abraham, *Regulation and function of connective tissue growth factor/CCN2 in tissue repair, scarring and fibrosis.* Cytokine Growth Factor Rev, 2008. **19**(2): p. 133-44.
195. Daniels, A., et al., *Connective tissue growth factor and cardiac fibrosis.* Acta Physiol (Oxf), 2009. **195**(3): p. 321-38.
196. Sopel, M., et al., *Fibroblast progenitor cells are recruited into the myocardium prior to the development of myocardial fibrosis.* Int J Exp Pathol, 2011.
197. Shimo, T., et al., *Connective tissue growth factor induces the proliferation, migration, and tube formation of vascular endothelial cells in vitro, and angiogenesis in vivo.* J Biochem, 1999. **126**(1): p. 137-45.
198. Chen, P.S., et al., *CTGF enhances the motility of breast cancer cells via an integrin-alphavbeta3-ERK1/2-dependent S100A4-upregulated pathway.* J Cell Sci, 2007. **120**(Pt 12): p. 2053-65.
199. Aguiar, D.P., et al., *CTGF/CCN2 has a chemoattractive function but a weak adhesive property to embryonic carcinoma cells.* Biochem Biophys Res Commun, 2011. **413**(4): p. 582-7.
200. Sopel M, R.N., Lee TDG, Legare JF, *Myocardial Fibrosis in Response to Angiotensin II is Preceded by the Recruitment of Mesenchymal Progenitor Cells.* Laboratory Investigations, 2010.
201. Suzuki, J., et al., *Rat angiotensin II (type 1A) receptor mRNA regulation and subtype expression in myocardial growth and hypertrophy.* Circ Res, 1993. **73**(3): p. 439-47.
202. Igarashi, A., et al., *Regulation of connective tissue growth factor gene expression in human skin fibroblasts and during wound repair.* Mol Biol Cell, 1993. **4**(6): p. 637-45.
203. Bradham, D.M., et al., *Connective tissue growth factor: a cysteine-rich mitogen secreted by human vascular endothelial cells is related to the SRC-induced immediate early gene product CEF-10.* J Cell Biol, 1991. **114**(6): p. 1285-94.
204. Hao, J., et al., *Interaction between angiotensin II and Smad proteins in fibroblasts in failing heart and in vitro.* Am J Physiol Heart Circ Physiol, 2000. **279**(6): p. H3020-30.
205. Shi, Y. and J. Massague, *Mechanisms of TGF-beta signaling from cell membrane to the nucleus.* Cell, 2003. **113**(6): p. 685-700.
206. Koitabashi, N., et al., *Pivotal role of cardiomyocyte TGF-beta signaling in the murine pathological response to sustained pressure overload.* J Clin Invest, 2011. **121**(6): p. 2301-12.
207. Wang, Q., et al., *Cooperative interaction of CTGF and TGF-beta in animal models of fibrotic disease.* Fibrogenesis Tissue Repair, 2011. **4**(1): p. 4.

208. Grotendorst, G.R. and M.R. Duncan, *Individual domains of connective tissue growth factor regulate fibroblast proliferation and myofibroblast differentiation.* FASEB J, 2005. **19**(7): p. 729-38.
209. Zhang, W. and H.T. Liu, *MAPK signal pathways in the regulation of cell proliferation in mammalian cells.* Cell Res, 2002. **12**(1): p. 9-18.
210. Sanchez-Lopez, E., et al., *CTGF promotes inflammatory cell infiltration of the renal interstitium by activating NF-kappaB.* J Am Soc Nephrol, 2009. **20**(7): p. 1513-26.
211. Reunanen, N., et al., *Activation of extracellular signal-regulated kinase 1/2 inhibits type I collagen expression by human skin fibroblasts.* J Biol Chem, 2000. **275**(44): p. 34634-9.
212. Ivkovic, S., et al., *Connective tissue growth factor coordinates chondrogenesis and angiogenesis during skeletal development.* Development, 2003. **130**(12): p. 2779-91.
213. Ikawa, Y., et al., *Neutralizing monoclonal antibody to human connective tissue growth factor ameliorates transforming growth factor-beta-induced mouse fibrosis.* J Cell Physiol, 2008. **216**(3): p. 680-7.
214. Wang, X., et al., *A novel single-chain-Fv antibody against connective tissue growth factor attenuates bleomycin-induced pulmonary fibrosis in mice.* Respirology, 2011. **16**(3): p. 500-7.
215. Yokoi, H., et al., *Reduction in connective tissue growth factor by antisense treatment ameliorates renal tubulointerstitial fibrosis.* J Am Soc Nephrol, 2004. **15**(6): p. 1430-40.
216. Adler, S.G., et al., *Phase 1 study of anti-CTGF monoclonal antibody in patients with diabetes and microalbuminuria.* Clin J Am Soc Nephrol, 2010. **5**(8): p. 1420-8.
217. Brigstock, D.R., *Strategies for blocking the fibrogenic actions of connective tissue growth factor (CCN2): From pharmacological inhibition in vitro to targeted siRNA therapy in vivo.* J Cell Commun Signal, 2009. **3**(1): p. 5-18.
218. Warnecke, C., et al., *Adenovirus-mediated overexpression and stimulation of the human angiotensin II type 2 receptor in porcine cardiac fibroblasts does not modulate proliferation, collagen I mRNA expression and ERK1/ERK2 activity, but inhibits protein tyrosine phosphatases.* J Mol Med (Berl), 2001. **79**(9): p. 510-21.
219. Ainscough, J.F., et al., *Angiotensin II type-1 receptor activation in the adult heart causes blood pressure-independent hypertrophy and cardiac dysfunction.* Cardiovasc Res, 2009. **81**(3): p. 592-600.
220. Dostal, D.E., et al., *Molecular mechanisms of angiotensin II in modulating cardiac function: intracardiac effects and signal transduction pathways.* J Mol Cell Cardiol, 1997. **29**(11): p. 2893-902.
221. Dobaczewski, M., W. Chen, and N.G. Frangogiannis, *Transforming growth factor (TGF)-beta signaling in cardiac remodeling.* J Mol Cell Cardiol, 2010. **51**(4): p. 600-6.
222. Groban, L., *Diastolic dysfunction in the older heart.* J Cardiothorac Vasc Anesth, 2005. **19**(2): p. 228-36.

223. Adiarto, S., et al., *ET-1 from endothelial cells is required for complete angiotensin II-induced cardiac fibrosis and hypertrophy.* Life Sci, 2012.
224. Iglarz, M. and M. Clozel, *At the heart of tissue: endothelin system and end-organ damage.* Clin Sci (Lond), 2010. **119**(11): p. 453-63.
225. Freed, D.H., et al., *Emerging evidence for the role of cardiotrophin-1 in cardiac repair in the infarcted heart.* Cardiovasc Res, 2005. **65**(4): p. 782-92.
226. Bang, L., et al., *Hydralazine-induced vasodilation involves opening of high conductance Ca2+-activated K+ channels.* Eur J Pharmacol, 1998. **361**(1): p. 43-9.
227. Leiro, J.M., et al., *Antioxidant activity and inhibitory effects of hydralazine on inducible NOS/COX-2 gene and protein expression in rat peritoneal macrophages.* Int Immunopharmacol, 2004. **4**(2): p. 163-77.
228. Fogari, R., et al., *Effects of lisinopril vs hydralazine on left ventricular hypertrophy and ambulatory blood pressure monitoring in essential hypertension.* Eur Heart J, 1995. **16**(8): p. 1120-5.
229. Brilla, C.G., R.C. Funck, and H. Rupp, *Lisinopril-mediated regression of myocardial fibrosis in patients with hypertensive heart disease.* Circulation, 2000. **102**(12): p. 1388-93.
230. Lopez, B., et al., *Usefulness of serum carboxy-terminal propeptide of procollagen type I in assessment of the cardioreparative ability of antihypertensive treatment in hypertensive patients.* Circulation, 2001. **104**(3): p. 286-91.
231. Ohmura, H., et al., *Cardiomyocyte-specific transgenic expression of lysyl oxidase-like protein-1 induces cardiac hypertrophy in mice.* Hypertens Res, 2012. **35**(11): p. 1063-8.
232. Pez, F., et al., *The HIF-1-inducible lysyl oxidase activates HIF-1 via the Akt pathway in a positive regulation loop and synergizes with HIF-1 in promoting tumor cell growth.* Cancer Res, 2011. **71**(5): p. 1647-57.
233. Basu, R.K., et al., *Interdependence of HIF-1alpha and TGF-beta/Smad3 signaling in normoxic and hypoxic renal epithelial cell collagen expression.* Am J Physiol Renal Physiol, 2011. **300**(4): p. F898-905.
234. Serini, G. and G. Gabbiani, *Mechanisms of myofibroblast activity and phenotypic modulation.* Exp Cell Res, 1999. **250**(2): p. 273-83.
235. Zeisberg, E.M. and R. Kalluri, *Origins of cardiac fibroblasts.* Circ Res, 2010. **107**(11): p. 1304-12.
236. Kuznetsov, V., et al., *Beta 2-adrenergic receptor actions in neonatal and adult rat ventricular myocytes.* Circ Res, 1995. **76**(1): p. 40-52.
237. de Jong, S., et al., *Direct detection of myocardial fibrosis by MRI.* J Mol Cell Cardiol, 2011. **51**(6): p. 974-9.
238. Liu, C.Y., et al., *Evaluation of age-related interstitial myocardial fibrosis with cardiac magnetic resonance contrast-enhanced T1 mapping: MESA (Multi-Ethnic Study of Atherosclerosis).* J Am Coll Cardiol, 2013. **62**(14): p. 1280-7.
239. Lucchesini, F., et al., *Synthesis of 2,6-disubstituted benzylamine derivatives as reversible selective inhibitors of copper amine oxidases.* Bioorg Med Chem, 2014. **22**(5): p. 1558-67.

APPENDIX A: COPYRIGHT PERMISSION

Chapter 4: Manuscript 2

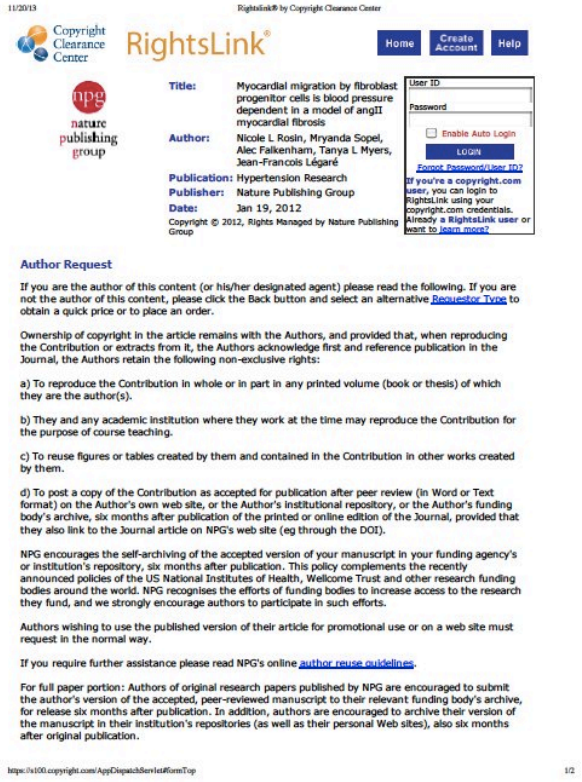

11/20/13 RightsLink® by Copyright Clearance Center

Copyright Clearance Center RightsLink® Home Create Account Help

nature publishing group

Title:	Myocardial migration by fibroblast progenitor cells is blood pressure dependent in a model of angII myocardial fibrosis
Author:	Nicole L Rosin, Mryanda Sopel, Alec Falkenham, Tanya L Myers, Jean-Francois Légaré
Publication:	Hypertension Research
Publisher:	Nature Publishing Group
Date:	Jan 19, 2012

Copyright © 2012, Rights Managed by Nature Publishing Group

User ID
Password
Enable Auto Login
LOGIN
Forgot Password/User ID?
If you're a copyright.com user, you can login to RightsLink using your copyright.com credentials. Already a RightsLink user or want to learn more?

Author Request

If you are the author of this content (or his/her designated agent) please read the following. If you are not the author of this content, please click the Back button and select an alternative Requestor Type to obtain a quick price or to place an order.

Ownership of copyright in the article remains with the Authors, and provided that, when reproducing the Contribution or extracts from it, the Authors acknowledge first and reference publication in the Journal, the Authors retain the following non-exclusive rights:

a) To reproduce the Contribution in whole or in part in any printed volume (book or thesis) of which they are the author(s).

b) They and any academic institution where they work at the time may reproduce the Contribution for the purpose of course teaching.

c) To reuse figures or tables created by them and contained in the Contribution in other works created by them.

d) To post a copy of the Contribution as accepted for publication after peer review (in Word or Text format) on the Author's own web site, or the Author's institutional repository, or the Author's funding body's archive, six months after publication of the printed or online edition of the Journal, provided that they also link to the Journal article on NPG's web site (eg through the DOI).

NPG encourages the self-archiving of the accepted version of your manuscript in your funding agency's or institution's repository, six months after publication. This policy complements the recently announced policies of the US National Institutes of Health, Wellcome Trust and other research funding bodies around the world. NPG recognises the efforts of funding bodies to increase access to the research they fund, and we strongly encourage authors to participate in such efforts.

Authors wishing to use the published version of their article for promotional use or on a web site must request in the normal way.

If you require further assistance please read NPG's online author reuse guidelines.

For full paper portion: Authors of original research papers published by NPG are encouraged to submit the author's version of the accepted, peer-reviewed manuscript to their relevant funding body's archive, for release six months after publication. In addition, authors are encouraged to archive their version of the manuscript in their institution's repositories (as well as their personal Web sites), also six months after original publication.

https://s100.copyright.com/AppDispatchServlet#FormTop 1/2

Chapter 5: Manuscript 3

ELSEVIER LICENSE
TERMS AND CONDITIONS

Nov 20, 2013

This is a License Agreement between Nicole L Rosin ("You") and Elsevier ("Elsevier") provided by Copyright Clearance Center ("CCC"). The license consists of your order details, the terms and conditions provided by Elsevier, and the payment terms and conditions.

All payments must be made in full to CCC. For payment instructions, please see information listed at the bottom of this form.

Supplier	Elsevier Limited The Boulevard,Langford Lane Kidlington,Oxford,OX5 1GB,UK
Registered Company Number	1982084
Customer name	Nicole L Rosin
Customer address	5850 College Street Halifax, NS B3H4R2
License number	3273231038214
License date	Nov 20, 2013
Licensed content publisher	Elsevier
Licensed content publication	The American Journal of Pathology
Licensed content title	Regulation and Role of Connective Tissue Growth Factor in AngII-Induced Myocardial Fibrosis
Licensed content author	Nicole L. Rosin,Alec Falkenham,Mryanda J. Sopel,Timothy D.G. Lee,Jean-Francois Légaré
Licensed content date	March 2013
Licensed content volume number	182
Licensed content issue number	3
Number of pages	13
Start Page	714
End Page	726
Type of Use	reuse in a thesis/dissertation
Portion	full article
Format	both print and electronic
Are you the author of this Elsevier article?	Yes
Will you be translating?	No

Title of your thesis/dissertation	Mechanisms of myocardial fibrosis development
Expected completion date	Mar 2014
Estimated size (number of pages)	300
Elsevier VAT number	GB 494 6272 12
Permissions price	0.00 USD
VAT/Local Sales Tax	0.00 USD / 0.00 GBP
Total	0.00 USD
Terms and Conditions	

INTRODUCTION

1. The publisher for this copyrighted material is Elsevier. By clicking "accept" in connection with completing this licensing transaction, you agree that the following terms and conditions apply to this transaction (along with the Billing and Payment terms and conditions established by Copyright Clearance Center, Inc. ("CCC"), at the time that you opened your Rightslink account and that are available at any time at http://myaccount.copyright.com).

GENERAL TERMS

2. Elsevier hereby grants you permission to reproduce the aforementioned material subject to the terms and conditions indicated.

3. Acknowledgement: If any part of the material to be used (for example, figures) has appeared in our publication with credit or acknowledgement to another source, permission must also be sought from that source. If such permission is not obtained then that material may not be included in your publication/copies. Suitable acknowledgement to the source must be made, either as a footnote or in a reference list at the end of your publication, as follows:

"Reprinted from Publication title, Vol /edition number, Author(s), Title of article / title of chapter, Pages No., Copyright (Year), with permission from Elsevier [OR APPLICABLE SOCIETY COPYRIGHT OWNER]." Also Lancet special credit - "Reprinted from The Lancet, Vol. number, Author(s), Title of article, Pages No., Copyright (Year), with permission from Elsevier."

4. Reproduction of this material is confined to the purpose and/or media for which permission is hereby given.

5. Altering/Modifying Material: Not Permitted. However figures and illustrations may be altered/adapted minimally to serve your work. Any other abbreviations, additions, deletions and/or any other alterations shall be made only with prior written authorization of Elsevier Ltd. (Please contact Elsevier at permissions@elsevier.com)

6. If the permission fee for the requested use of our material is waived in this instance, please be advised that your future requests for Elsevier materials may attract a fee.

7. Reservation of Rights: Publisher reserves all rights not specifically granted in the combination of (i) the license details provided by you and accepted in the course of this licensing transaction, (ii) these terms and conditions and (iii) CCC's Billing and Payment terms

and conditions.

8. License Contingent Upon Payment: While you may exercise the rights licensed immediately upon issuance of the license at the end of the licensing process for the transaction, provided that you have disclosed complete and accurate details of your proposed use, no license is finally effective unless and until full payment is received from you (either by publisher or by CCC) as provided in CCC's Billing and Payment terms and conditions. If full payment is not received on a timely basis, then any license preliminarily granted shall be deemed automatically revoked and shall be void as if never granted. Further, in the event that you breach any of these terms and conditions or any of CCC's Billing and Payment terms and conditions, the license is automatically revoked and shall be void as if never granted. Use of materials as described in a revoked license, as well as any use of the materials beyond the scope of an unrevoked license, may constitute copyright infringement and publisher reserves the right to take any and all action to protect its copyright in the materials.

9. Warranties: Publisher makes no representations or warranties with respect to the licensed material.

10. Indemnity: You hereby indemnify and agree to hold harmless publisher and CCC, and their respective officers, directors, employees and agents, from and against any and all claims arising out of your use of the licensed material other than as specifically authorized pursuant to this license.

11. No Transfer of License: This license is personal to you and may not be sublicensed, assigned, or transferred by you to any other person without publisher's written permission.

12. No Amendment Except in Writing: This license may not be amended except in a writing signed by both parties (or, in the case of publisher, by CCC on publisher's behalf).

13. Objection to Contrary Terms: Publisher hereby objects to any terms contained in any purchase order, acknowledgment, check endorsement or other writing prepared by you, which terms are inconsistent with these terms and conditions or CCC's Billing and Payment terms and conditions. These terms and conditions, together with CCC's Billing and Payment terms and conditions (which are incorporated herein), comprise the entire agreement between you and publisher (and CCC) concerning this licensing transaction. In the event of any conflict between your obligations established by these terms and conditions and those established by CCC's Billing and Payment terms and conditions, these terms and conditions shall control.

14. Revocation: Elsevier or Copyright Clearance Center may deny the permissions described in this License at their sole discretion, for any reason or no reason, with a full refund payable to you. Notice of such denial will be made using the contact information provided by you. Failure to receive such notice will not alter or invalidate the denial. In no event will Elsevier or Copyright Clearance Center be responsible or liable for any costs, expenses or damage incurred by you as a result of a denial of your permission request, other than a refund of the amount(s) paid by you to Elsevier and/or Copyright Clearance Center for denied permissions.

LIMITED LICENSE

The following terms and conditions apply only to specific license types:

15. **Translation**: This permission is granted for non-exclusive world **English** rights only unless your license was granted for translation rights. If you licensed translation rights you

may only translate this content into the languages you requested. A professional translator must perform all translations and reproduce the content word for word preserving the integrity of the article. If this license is to re-use 1 or 2 figures then permission is granted for non-exclusive world rights in all languages.

16. **Website**: The following terms and conditions apply to electronic reserve and author websites:
Electronic reserve: If licensed material is to be posted to website, the web site is to be password-protected and made available only to bona fide students registered on a relevant course if:
This license was made in connection with a course,
This permission is granted for 1 year only. You may obtain a license for future website posting,
All content posted to the web site must maintain the copyright information line on the bottom of each image,
A hyper-text must be included to the Homepage of the journal from which you are licensing at http://www.sciencedirect.com/science/journal/xxxxx or the Elsevier homepage for books at http://www.elsevier.com , and
Central Storage: This license does not include permission for a scanned version of the material to be stored in a central repository such as that provided by Heron/XanEdu.

17. **Author website** for journals with the following additional clauses:

All content posted to the web site must maintain the copyright information line on the bottom of each image, and the permission granted is limited to the personal version of your paper. You are not allowed to download and post the published electronic version of your article (whether PDF or HTML, proof or final version), nor may you scan the printed edition to create an electronic version. A hyper-text must be included to the Homepage of the journal from which you are licensing at http://www.sciencedirect.com/science/journal/xxxxx . As part of our normal production process, you will receive an e-mail notice when your article appears on Elsevier's online service ScienceDirect (www.sciencedirect.com). That e-mail will include the article's Digital Object Identifier (DOI). This number provides the electronic link to the published article and should be included in the posting of your personal version. We ask that you wait until you receive this e-mail and have the DOI to do any posting.

Central Storage: This license does not include permission for a scanned version of the material to be stored in a central repository such as that provided by Heron/XanEdu.

18. **Author website** for books with the following additional clauses:
Authors are permitted to place a brief summary of their work online only.
A hyper-text must be included to the Elsevier homepage at http://www.elsevier.com . All content posted to the web site must maintain the copyright information line on the bottom of each image. You are not allowed to download and post the published electronic version of your chapter, nor may you scan the printed edition to create an electronic version.

Central Storage: This license does not include permission for a scanned version of the material to be stored in a central repository such as that provided by Heron/XanEdu.

19. **Website** (regular and for author): A hyper-text must be included to the Homepage of the journal from which you are licensing at http://www.sciencedirect.com/science/journal/xxxxx. or for books to the Elsevier homepage at http://www.elsevier.com

20. **Thesis/Dissertation**: If your license is for use in a thesis/dissertation your thesis may be submitted to your institution in either print or electronic form. Should your thesis be published commercially, please reapply for permission. These requirements include permission for the Library and Archives of Canada to supply single copies, on demand, of the complete thesis and include permission for UMI to supply single copies, on demand, of the complete thesis. Should your thesis be published commercially, please reapply for permission.

21. **Other Conditions**:

v1.6

If you would like to pay for this license now, please remit this license along with your payment made payable to "COPYRIGHT CLEARANCE CENTER" otherwise you will be invoiced within 48 hours of the license date. Payment should be in the form of a check or money order referencing your account number and this invoice number RLNK501164141.
Once you receive your invoice for this order, you may pay your invoice by credit card. Please follow instructions provided at that time.

Make Payment To:
Copyright Clearance Center
Dept 001
P.O. Box 843006
Boston, MA 02284-3006

For suggestions or comments regarding this order, contact RightsLink Customer Support: customercare@copyright.com or +1-877-622-5543 (toll free in the US) or +1-978-646-2777.

Gratis licenses (referencing $0 in the Total field) are free. Please retain this printable license for your reference. No payment is required.